

© Copyright by Sanam Soomro 2018
All Rights Reserved

THE SCREENING AND APPLICATION OF BIOMARKERS IN AUTOIMMUNE DISEASE

A Dissertation

Presented to

the Faculty of the Department of Biomedical Engineering

University of Houston

In Partial Fulfillment

of the Requirements for the Degree

Doctor of Philosophy

in Biomedical Engineering

by

Sanam Soomro

December 2018

THE SCREENING AND APPLICATION OF BIOMARKERS IN AUTOIMMUNE DISEASE

Sanam Soomro

Approved:

Chair of the Committee
Chandra Mohan, Hugh Roy and Lillie
Cranz Cullen Endowed Professor,
Department of Biomedical Engineering

Committee Members:

Richard Willson, Huffington-
Woestemeyer Professor,
Department of Chemical and
Biomolecular Engineering

Sergey Shevkoplyas, Professor,
Department of Biomedical Engineering

Tianfu Wu, Assistant Professor,
Department of Biomedical Engineering

Yong Du, Research Assistant Professor,
Department of Biomedical Engineering

Suresh K. Khator, Associate Dean,
Cullen College of Engineering

Metin Akay, John S Dunn Endowed
Chair Professor, Department of
Biomedical Engineering

Acknowledgments

I would like to thank Dr. Chandra Mohan, my advisor and mentor, for accepting my young and naïve mind and allowing me to grow and learn so much about science, research, and life. I would like to thank and acknowledge my committee for their time and guidance as I complete this chapter of my career. Dr. Willson for allowing me to push my own domain of expertise, for taking me into his lab, and the guidance on the lateral flow assay project. Dr. Wu and Dr. Shevkoplyas for inviting me into the fields of proteomics and diagnostics when I was just an undergraduate. Dr. Du for reminding me there is always more to learn and do.

I would also like to thank my lab members and peers without whom my graduate school journey would have been much more difficult. Kamala for never repeating the same mistake twice. I would like to thank the faculty and staff in the Biomedical Engineering Department, the professors for exciting me with their passion of science, all of my advisors for the academic and emotional support, and the staff for facilitating my research.

I would like to acknowledge all the clinicians, staff, and students who have moved this research forward. Prior to this work, stool extraction optimization was conducted by Bindiya Marakkath and Marwa Kharboutli. I would like to thank the staff at Somalogic and RayBiotech for answering my endless questions. I would also like to thank our clinical collaborators for access to human patient samples without which our research would be impossible: Dr. Saxena at UTSW, Dr. Petri at JHMI, and Dr. Kugathasan at Emory. While processing the antibody array and ELISA validation,

the following people were mentored and have contributed to this work: Marwa Kharboutli, Vatsala Mundra, Ferial Koutani, Briony Strachan, and Malukah Al-Shaikh. Thank you to all my mentees for allowing me to pass on my knowledge and passions. ELISA validation of disease-specific biomarkers in the urine normalization study was conducted by Samantha Stanley. Studies on lateral flow were greatly supported by Dr. Willson's lab especially with the guidance and mentorship of Katerina Kourentzi, Heather Goux, and Joao Trabuco. Thank you.

Finally and most importantly, I would like to thank my parents, siblings, friends, and teachers. My parents for their sacrifices in hopes of making our futures brighter, for emphasizing the importance of work ethic and the pursuit of knowledge, and for their everlasting prayers, love, and support. My siblings and friends for reminding me there is much more to life than pipetting small volumes, for reconnecting me to the real world when I was lost in my own, and for being my greatest fans even when I couldn't see it. I would also like to acknowledge all of my and everyone's teachers, from elementary school to university, for their unrecognized effort in inspiring the young minds that grow to change the world.

To all whose paths I have had the honor to cross, thank you.

THE SCREENING AND APPLICATION OF BIOMARKERS IN AUTOIMMUNE DISEASE

An Abstract

of a

Dissertation

Presented to

the Faculty of the Department of Biomedical Engineering

University of Houston

In Partial Fulfillment

of the Requirements for the Degree

Doctor of Philosophy

in Biomedical Engineering

by

Sanam Soomro

December 2018

Abstract

This research portrays three aspects of the biomarker development pipeline: screening for stool biomarkers for pediatric inflammatory bowel disease (pIBD), validation of urine normalizer proteins, and translation of lupus nephritis (LN) urine biomarkers to phosphor-based lateral flow assays (LFAs).

As the diagnosis of pIBD is invasive and painful for children, two high-throughput technologies utilizing aptamers and antibodies have been used to screen over 1000 human proteins for noninvasive stool biomarkers for the two types of pIBD: Crohn's disease (CD) and ulcerative colitis (UC). The screens have uncovered 119 proteins elevated in both CD and UC stool, 19 proteins elevated in CD stool, 124 proteins elevated in UC stool, and 58 proteins dysregulated between CD and UC stool. ELISA validation of 23 proteins has uncovered 9 biomarkers for IBD, 1 biomarker for CD, 9 biomarkers for UC, and 10 biomarkers that distinguish UC from CD. Many hits have been implicated in the intestinal mucosa of pIBD patients and in inflammatory and other immunologic disease pathways. These biomarkers can aid in pIBD diagnosis and help elucidate the mechanisms of this complicated disease.

To increase the sensitivity of urine biomarkers in diagnostics, most quantitative biomarkers are normalized to creatinine to account for urine production. Creatinine is a small metabolite and antibodies to creatinine are difficult to develop, limiting the applications of quantitative urine diagnostics. An aptamer screen of 1000 proteins and ELISA validation has identified HVEM for the normalization of ALCAM and other urine biomarkers for LN.

To translate urine protein biomarkers for LN diagnostics to the point-of-care, sensitive and quantitative phosphor LFAs for the detection of ALCAM, an LN biomarker, and HVEM, a urine normalizer, have been created and optimized showing a limit of detection of 125 pg/mL in buffer. As this is the first application of nanophosphors in urine, the feasibility of nanophosphor use in urine has been evaluated and optimized showing detection limits around 5 ng/ml in urine. Although the current limit for the assay in urine is above the clinical range of ALCAM and HVEM, this work has created a foundation for the application of nanophosphors for the detection of urinary ALCAM and HVEM.

Table of Contents

Acknowledgments	v
Abstract	viii
Table of Contents	x
List of Figures	xii
List of Tables	xvii
Introduction	1
Autoimmune Disease	2
Biomarkers in Human Disease	2
Omics Technologies	3
The Protein Biomarker Pipeline	4
Biomarker identification.....	5
Biomarker validation.....	6
Assay development and validation.....	6
Clinical testing and utility.....	7
Chapter 1: Stool Protein Biomarkers of Pediatric IBD	8
Introduction	8
Inflammatory bowel disease	8
Stool biomarkers for IBD	10
SOMAscan aptamer-based screen.....	11
RayBiotech L1000 antibody array.....	12
Methods	13
Stool processing.....	13
SOMAscan assay	14
RayBiotech antibody array	17
ELISA validation	20
Results and Discussion	22
Stool feasibility of SOMAscan assay.....	22
Screening of pediatric IBD stool by an aptamer-based assay.....	23
Quality control of extraction and processing using antibody array.....	34
Screening of pediatric IBD stool by antibody array	37
Validation of biomarkers for pediatric IBD stool by ELISA	50
Conclusion	74
Chapter 2: Alternate markers to creatinine for urine normalization	77
Introduction	77
Methods	78
Human urine samples	78
Aptamer-based screen	79
Statistical analysis.....	80
ELISA validation	80
Results	81
Screening results.....	81
ELISA validation results	83
Testing the ability of urine HVEM to normalize urine biomarker levels.....	85
Discussion	86

Conclusion	89
Chapter 3: Lateral Flow Assay for Active LN Diagnosis	90
Introduction	90
Urine biomarkers for LN	92
Lateral flow assay	93
Persistently luminescent nanophosphors.....	95
Methods	97
Preparation of phosphor-labeled nanoparticles	98
Preparation of lateral flow membrane strips	101
Other reagents and materials	101
Lateral flow assay, image acquisition, and analysis	102
Results and Discussion	103
Buffer screen	103
Membrane selection.....	106
PLNP loading mass	108
Standard curve in buffer	110
Human urine feasibility.....	114
Human urine dilution	115
Standard curve in synthetic urine.....	121
Conclusion	124
Summary of Work	125
References	127
Appendix A: Normalization and Descriptive Statistics of ELISA Validation of Stool Biomarkers	164

List of Figures

Figure 1: The biomarker discovery pipeline.....	5
Figure 2: Crohn's disease and ulcerative colitis are two types of inflammatory bowel disease.....	9
Figure 3: A summary of the SOMAscan assay capable of detecting over 1100 human proteins.....	14
Figure 4: Summary of the processing of the RayBiotech L1000 antibody arrays on stool extract.....	18
Figure 5: The aptamer-based screen showed up-regulation of 80 proteins that were elevated in IBD patients versus healthy controls (A). 48 proteins showed significant elevation (FC >2, P < 0.05) in both CD versus HC and UC versus HC comparisons (B).....	24
Figure 6: IPA of the 48 elevated proteins in both Crohn's disease and ulcerative colitis patients' stool versus healthy controls showed involvement of three main pathways.....	25
Figure 7: The 48 elevated proteins in both Crohn's disease and ulcerative colitis patients' stool versus healthy controls were separated into five group by unsupervised hierarchical clustering.....	26
Figure 8: A summary of the 48 proteins elevated in both CD and UC patients' stool when compared to HC. Proteins are listed with the IPA network, hierarchical cluster, and elevation in a gene mucosa array. A total of 18 molecules were selected for validation by ELISA.....	27
Figure 9: The aptamer-based screen showed up-regulation of 50 proteins with FC > 1.25, P < 0.05 that were elevated in CD patients versus HC (A). 2 proteins showed a significant elevation in CD versus HC but not UC versus HC comparisons (B).....	28
Figure 10: IPA of the 2 elevated proteins in Crohn's disease patients' stool versus healthy control but not ulcerative colitis versus healthy controls showed involvement of three main pathways related to DNA replication, recombination, and repair, cell cycle, cell morphology.....	29
Figure 11: A summary of the 2 proteins elevated in only CD and not UC patients' stool when compared to HC. Proteins are listed with the IPA network, hierarchical cluster, and elevation in a gene mucosa array. One of the two molecules was selected for validation by ELISA.....	29
Figure 12: The aptamer-based screen showed up regulation of 120 proteins with FC > 1.25, P < 0.05 that were elevated in UC vs HC (A) and 33 proteins that were elevated in the stools of UC vs CD. 20 proteins showed significant elevation (FC >2, P < 0.05) in UC vs CD and vs HC (B).....	30
Figure 13: IPA of the 20 elevated proteins in UC patients' stool versus CD and HC but not CD versus HC showed an involvement of two main pathways.....	31
Figure 14: The 20 elevated proteins in elevated in ulcerative colitis patients when compared to Crohn's disease and healthy controls while not being elevated in Crohn's disease stool when compared to healthy controls were separated into five group by unsupervised hierarchical clustering.....	32

Figure 15: A summary of the 20 proteins elevated in ulcerative colitis patients when compared to CD and HC while not being elevated in CD vs HC. Seven molecules were selected for validation by ELISA.....	33
Figure 16: The effect of protein extraction on the antibody array.	34
Figure 17: The effect of the dialysis and biotinylation steps on the antibody array..	35
Figure 18: The effect of hybridization on the antibody array.....	35
Figure 19: Combinatorial effects on the antibody array.	36
Figure 20: Sample 14 was used to normalize three independent runs of samples....	37
Figure 21: The antibody array-based screen of 1000 human proteins in pediatric and healthy control stool extract showed up-regulation of 71 proteins with $FC > 2$, $P < 0.05$ that were elevated in IBD patients versus healthy controls (A) visualized on a heatmap (B).	38
Figure 22: IPA of the 71 proteins elevated in IBD stools when compared to healthy controls showed these top three networks.....	39
Figure 23: Unsupervised hierarchical clustering of the 71 proteins elevated in IBD stools versus healthy controls.	40
Figure 24: Of the 71 proteins elevated in IBD vs HC on the antibody array, the 17 visualized proteins had an average RFU > 200 and 13 were chosen for ELISA validation.	41
Figure 25: The antibody array-based screen of 1000 human proteins in pediatric and healthy control stool extract showed up-regulation of 17 proteins with $FC > 2$, $P < 0.05$ that were elevated in Crohn's disease patients versus healthy controls (A) visualized on a heatmap (B).	42
Figure 26: IPA of the 17 proteins elevated in Crohn's disease stools when compared to healthy controls.	42
Figure 27: Unsupervised hierarchical clustering of the 16 proteins elevated in Crohn's disease stools versus healthy controls.....	43
Figure 28: Of the 17 proteins elevated in CD vs HC on the antibody array, BDNF was the only protein with an average RFU > 200 and was chosen for ELISA validation.	43
Figure 29: The antibody array-based screen of 1000 human proteins in pediatric and healthy control stool extract showed up-regulation of 104 proteins with $FC > 2$, $P < 0.05$ that were elevated in ulcerative colitis patients versus healthy controls (A) visualized on a heatmap (B).	44
Figure 30 IPA of the 104 proteins elevated in ulcerative colitis stools when compared to healthy controls.	44
Figure 31: Unsupervised hierarchical clustering of the 104 protein elevated in ulcerative colitis stools versus healthy controls.....	45
Figure 32: Of the 104 proteins elevated in UC vs HC on the antibody array, the 21 proteins visualized had an average RFU > 200 and 12 were chosen for ELISA validation.	46
Figure 33: The antibody array-based screen of 1000 proteins in pediatric and healthy control stool showed up-regulation of 38 proteins with $FC > 2$, $P < 0.05$ that were dysregulated between ulcerative colitis patients versus Crohn's disease patients (A) visualized on a heatmap (B).	47

Figure 34: IPA of the 38 dysregulated proteins between Crohn's disease and ulcerative colitis stool.....	47
Figure 35: Unsupervised hierarchical clustering of the 38 proteins dysregulated in Crohn's disease and ulcerative colitis stools.	48
Figure 36: Of the 38 dysregulated proteins between UC and CD on the antibody array, the 12 visualized proteins had average RFU > 200 and 7 were chosen for ELISA validation.....	49
Figure 37: Of the 23 molecules validated by ELISA, 9 molecules were found to be elevated in both CD and UC vs HC. Of these, 3 were also significantly different between CD and UC stools. Descriptive statistics can be found in Appendix A. $P \leq 0.05$, $**P \leq 0.01$, $***P \leq 0.001$, $****P \leq 0.0001$	51
Figure 38: ROC analysis of the nine biomarkers for IBD.....	53
Figure 39: Of the 23 molecules validated by ELISA, one molecule was found to be elevated in CD vs HC. Additional descriptive statistics can be found in Appendix A. $*P \leq 0.05$, (A). ROC curve analysis of alkaline phosphatase (B).....	59
Figure 40: Of the 23 molecules validated by ELISA, 8 molecules were found to be elevated in UC vs HC. Of these, 7 were also significantly different between CD and UC stools. Additional descriptive statistics can be found in Appendix A. $P \leq 0.05$, $**P \leq 0.01$, $***P \leq 0.001$, $****P \leq 0.0001$	61
Figure 41: ROC analysis of biomarkers of UC.....	62
Figure 42: ROC analysis of the ten molecules distinguishing UC from CD.	68
Figure 43: Of the 23 proteins validated by ELISA, five proteins did not reach statistical significance.....	69
Figure 44: Of the 18 proteins validated from the aptamer screen, 14 had positive correlation to ELISA.	71
Figure 45: Of the 15 proteins validated by ELISA from the antibody array, 15 proteins had significant positive correlations between the two protein detection platforms (Spearman $r > 0.5$, $P < 0.05$).	73
Figure 46: A volcano plot visualizing the Pearson correlation of 1129 proteins with creatinine in the human urine of 23 healthy and SLE subjects	82
Figure 47: The screening identified five proteins that best positively correlate with creatinine and do not differ between subject groups.....	83
Figure 48: ELISA validation of the top five proteins in an independent cohort show positive correlation of HVEM and RELT to creatinine whereas Dectin-1 did not positively correlate in the validation set.....	84
Figure 49: HVEM, the most promising biomarker for urine biomarker normalization, shows positive correlation in both Caucasian and African American subjects..	85
Figure 50: Normalization of ALCAM, a proposed biomarker for LN, with urinary creatinine and urinary HVEM shows comparable diagnostic ability. Bars show mean \pm standard error of the mean. One sample was removed from the plots, as the HVEM concentration was too low to be detected by ELISA.	86
Figure 51: Histograms showing the concentrations of ALCAM and HVEM in human urine from subjects assayed in Chapter 2. ALCAM and HVEM have ranges of 0-32 ng/mL and 0-40 ng/mL, respectively in human urine.	92
Figure 52: Illustration of the lateral flow assay format.	94

Figure 53: Lateral flow assay format for the detection of ALCAM and HVEM in urine using persistently luminescent nanophosphors.....	97
Figure 54: A buffer screen for the ALCAM lateral flow assay showed a buffer composed of 10mM HEPES pH 7.95, 0.5% PVP40, 100mM NaCl, 1% BSA, 0.4% PEG to have the strongest signal intensity.	104
Figure 55: A buffer screen for the HVEM lateral flow assay showed a buffer composed of PBS pH 7.25, 2% Tween 20, 25mM NaCl, 0.5% non-fat dry milk to have the strongest signal intensity.	105
Figure 56: A nitrocellulose membrane screen for the ALCAM lateral flow assay showed GE FF80HP to have the strongest signal intensity.....	107
Figure 57: A nitrocellulose membrane screen for the HVEM lateral flow assay showed GE FF80HP to have the strongest signal intensity.....	107
Figure 58: Phosphor loading testing for the ALCAM LFA showed 3 ug/strip was sufficient for a positive signal.	109
Figure 59: Phosphor loading testing for the HVEM LFA showed 1 ug/strip was sufficient for a positive signal.	110
Figure 60: A standard curve for ALCAM in buffer was assayed in two runs (A). For the test and control line peak areas (B), replicates are averaged together while for the standard curve (C) replicates are plotted with mean and standard deviation. Standard deviations smaller than the size of the point are not visualized.	111
Figure 61: A standard curve for HVEM in buffer (A). For the test and control line peak areas (B), replicates are averaged together while for the standard curve (C) replicates are plotted with mean and standard deviation. Standard deviations smaller than the size of the point are not visualized.....	113
Figure 62: The buffer component of the ALCAM and HVEM lateral flow assays was replaced with undiluted human urine spiked with ALCAM and HVEM showing aggregation of PLNPs at the membrane sample pad interface and prevention of sample flow through the membrane.....	115
Figure 63: Human urine spiked with ALCAM was diluted with buffer and water to ascertain whether human urine inherently caused aggregation or if a buffer was required to facilitate sample flow and antigen binding.	116
Figure 64: Human urine spiked with HVEM was diluted with buffer and water to ascertain whether human urine inherently caused aggregation or if a buffer was required to facilitate sample flow and antigen binding.	117
Figure 65: Human urine spiked with ALCAM was further diluted with buffer to see the minimal amount of buffer needed for sample flow and antigen binding..	118
Figure 66: Human urine spiked with HVEM was further diluted with buffer To see the minimal amount of buffer needed for sample flow and antigen binding..	119
Figure 67: Synthetic urine spiked with ALCAM was diluted with buffer to see the minimal amount of buffer needed for sample flow and antigen binding and to quantitate non-specific background signal.....	120
Figure 68: Synthetic urine spiked with HVEM was diluted with buffer to see the minimal amount of buffer needed for sample flow and antigen binding and to quantitate non-specific background signal.....	121

Figure 69: A standard curve of ALCAM spiked in synthetic urine showed a positive correlation of signal intensity with ALCAM concentration. 122

Figure 70: A standard curve of HVEM spiked in synthetic urine showed a positive correlation of signal intensity with HVEM concentration. 123

List of Tables

Table 1: Demographic characteristics of the cohort used for the SOMAscan aptamer-based screening assay.	16
Table 2: Demographics information for the cohort use for the RayBiotech antibody-array based proteomic screen.	19
Table 3: Sample 14 was used to assess quality control of the antibody array processing of stool extract.....	19
Table 4: Summary of the ELISA kits used for the validation of stool biomarkers for pediatric IBD.....	21
Table 5: Demographics of the cohort used for ELISA validation of stool biomarkers for pediatric IBD.....	22
Table 6: Summary of the proteins elevated in both CD and UC in the ELISA validation. *P ≤ 0.05, **P ≤ 0.01, ***P ≤ 0.001, ****P ≤ 0.0001.	52
Table 7: Summary of the proteins elevated in CD vs HC in the ELISA validation. *P ≤ 0.05.	59
Table 8: Summary of the proteins elevated in UC vs HC in the ELISA validation. *P ≤ 0.05, **P ≤ 0.01, ***P ≤ 0.001, ****P ≤ 0.0001, >>FC could not be calculated as mean of healthy population was 0.	61
Table 9: Demographic and clinical characteristic of validation study cohort. Means are expressed with standard deviation.	79
Table 10: Proteins positively correlated to urinary creatinine that are not significantly different between patient groups.	82
Table 18: Descriptive statistics of ELISA validation of stool biomarkers for IBD. Concentrations have been normalized by the ratio of stool weight to volume of protein extract. Concentrations are in pg/ml unless otherwise noted: †[mg/mg], ∇ [ng/mg], § [ug/mg], ‡ [nIU/mg]	164
Table 19: Descriptive statistics of ELISA validation of stool biomarkers for IBD in protein extract. Concentrations are in ng/ml unless otherwise noted: ‡[mIU/ml], ∇ [pg/ml], §[ug/ml].....	165

Introduction

Autoimmune diseases are a class of disorders where a malfunction of the immune system instigates the targeted attack of healthy proteins, cells, and tissues of the body. This attack on the self can result in non-specific, painful symptoms and may result in tissue damage and organ failure when the disease is not diagnosed at an early stage. Many autoimmune diseases have cycles of flares and remissions when symptoms might get worse and then better. The need for early diagnosis and disease course monitoring leads autoimmune disease perfectly to the application of biomarkers.

As defined by the National Cancer Institute, biomarkers are “biological molecule found in blood, other body fluids, or tissues that is a sign of a normal or abnormal process, or of a condition or disease” [1]. Autoimmune disease’s nonspecific symptoms, cycles of flares and remissions, and end stage organ damage support for the use of noninvasive biomarkers to diagnose the disease earlier and less painfully without the use of a biopsy. Biomarkers can also track and predict active flares allowing for preemptive intervention for the management of flares preventing further organ damage.

This work aims to demonstrate the diagnostic biomarker identification pipeline where novel stool biomarkers for pediatric inflammatory bowel disease are identified through innovative high-throughput screening technologies, urine normalizer proteins are validated patient cohorts using established molecular

detection technologies, and lupus nephritis urine biomarkers are translated to a point-of-care device for use by clinicians and patients.

Autoimmune Disease

The class of autoimmune diseases consists of a multitude of different disorders. Depending on the target of the immune system attack and organ involvement, different autoimmune disease will have different manifestations and outcomes. Despite the variety of autoimmune diseases, the underlying phenomena common to this class is the disruption of self-tolerance or the loss of the ability to differentiate healthy tissue or antigens of the self from diseased or foreign antigens. Whereas in a normal immune response, foreign antigens are recognized by the immune system and antibodies are produced allowing for the targeted removal of foreign invaders, in autoimmune disease, the immune system forms autoantibodies or antibodies that are specific to antigens in its own body. These antibodies facilitate the attack on self-antigens resulting in inflammation and tissue damage. This loss of self-tolerance has been attributed to many genetic, immunologic, and environmental factors, [2] where a perfect combination of factors compounds to the triggering of an autoimmune response. As the exact mechanism disease initiation of many autoimmune diseases is not yet elucidated, understanding of pathogenesis for many diseases is still ongoing.

Biomarkers in Human Disease

Biomarkers are measurable characteristics that reflect a particular physiological state. Traditionally these characteristics have included physiological measurements including body temperature and blood pressure, but the definition of

a biomarker has evolved to refer to a biological molecule or signature. These biomarkers may refer to DNA, RNA, proteins, or metabolites. Their applications to human disease can bring great insight in terms of diagnostic, prognostic, and therapeutic applications.

Omics Technologies

The discovery of new biomarkers for human conditions has traditionally been biased in terms of searching for molecules that fit into existing knowledge about the disease and the human body. Although this has historically successfully uncovered biomarkers, unbiased searches for biomarkers will not only uncover novel biomarkers for clinical applications, but these biomarkers can also help elucidate disease pathogenesis and further expand our understanding of the human body and its mechanisms. Omics refers to the study of genomics, transcriptomics, proteomics, and metabolomics. In other terms the large-scale studying of the genes, RNA, proteins, and metabolites. Omics methods and technologies allow scientists to gain a broader, unbiased perspective of what is happening in a disease. With the development of high throughput technologies like next-generation DNA sequencing and antibody arrays, scientists can now study whole genomes and proteomes compared to one gene or protein at a time. These technologies have revolutionized biomarker research expanding the possible candidates for biomarkers of human disease.

Proteomics, the large-scale detection of proteins, has an advantage of over genomics in that proteomics can capture an immediate picture of what is happening in the body at a current state. All biological functions rely on proteins, whether they

relate to enzymatic activity, cellular signaling, immune cell trafficking, or structural components of the cell and tissues. These functions rely on the time course of proteins ranging from a few minutes to days. The manifestation of diseases also is a result of these biological functions going awry. As a result, protein biomarkers can give immediate insight into what is happening in the current state of the body.

Disease-specific protein biomarkers can then be identified with the comparison of a healthy proteome with the proteome from a diseased individual. The study of the diseased proteome in noninvasive body fluids is of even more relevance as noninvasive fluids such as blood, urine, stool, saliva, and sweat allow for the simple, painless, and continuous sampling of a patient. Body fluids that come in direct contact with the organ in which a disease occurs will offer great insight into the current state of the disease. For example, for diseases affecting the intestines, stool is an ideal body fluid of interest as the stool directly passes through the intestine. In terms of disease manifestations of the kidney, urine may be a more suitable noninvasive body fluid of interest.

The Protein Biomarker Pipeline

The discovery of new biomarkers has five main stages as illustrated in Figure 1: biomarkers identification, biomarker validation, assay development and validation, clinical testing, and the final creation of diagnostic products.



Figure 1: The biomarker discovery pipeline.

As mentioned previously, this work focuses on the first three stages of the biomarker pipeline: biomarkers identification, biomarker validation, and assay development.

Biomarker identification

In the biomarker identification stage, proteins are screened ideally using an unbiased, high throughput technology allowing for the simultaneous detection of candidate proteins. Currently, proteomic technologies include multiplexed ELISAs with the detection of up to ten proteins simultaneously [3] to more high-throughput technologies including an aptamer-based screen by Somalogic [4] and antibody arrays [5] capable of detecting over 1000 proteins simultaneously. The experimental design of the screen will dictate the purpose of the candidate biomarkers selected. By including samples from healthy and diseased individuals, one would detect diagnostic biomarkers. Prognostic biomarkers would be identified by the inclusion of longitudinal samples and therapeutic biomarkers may be identified by the use of patient samples with different therapeutic responses. As these technologies are far more complex than the traditional protein detection technologies, the limiting factor in the biomarker identification screens are related to cost often resulting in the use of fewer samples. The collection of biomarker screening data is often multidimensional and with the use of exploratory data analytic techniques, candidate biomarkers can be identified for further validation.

Biomarker validation

During the biomarker validation stage, candidate biomarkers from the screening phase are proven to be relevant in larger cohorts of subjects. Whereas a screening study may contain 20 subjects, validation studies can have closer to 200 subjects. This allows for the determination of an effect of compounding variables including age, sex, and other disease manifestations. Traditional molecular biology techniques such as ELISA are often used at this stage, as it is easier to run a larger number of samples at a lower cost. Biomarker qualification also occurs at this stage where the sensitivity and specificity of the biomarker's ability to distinguish diseased individuals from healthy subjects are analyzed [6]. The probability of false positive and false negatives is also examined to understand the clinical utility of this biomarker.

Assay development and validation

Once biomarkers are thoroughly validated in large, independent cohorts, assays specific for the biomolecule can be developed determined on the biomarker purpose. Protein biomarkers used in the clinical setting may have assays developed that can be commercialized for large high-throughput machines in a hospital lab whereas a biomarker that is useful for a patient at home or a doctor at a smaller clinic relies on rapid diagnostics at the point-of-care (POC). These point-of-care assays must be sensitive enough to be able to detect the biomolecule by the end user but also safe and stable enough to sell to the public. Similar to biomarker validation, these assays must also be validated in large cohorts of patients to make understand their specifications and diagnostic accuracy [6], [7].

Clinical testing and utility

Once novel assays and diagnostic methods are developed, they must undergo clinical testing and validation in order to be sold to the end user. In the United States, the Federal Drug Administration regulates the approval of diagnostic point-of-care devices as well as home-grown assays developed by labs to make sure they are safe and reliable for the end user [8]. Diagnostic laboratories are also controlled by Clinical Laboratory Improvement Amendments guidelines in agreement with state-specific regulations. After FDA regulations have been met, a well-validated diagnostic device may be rendered useless if it does not fit into the existing health care system. Insurance reimbursement and doctor and patient compliance are important for diagnostic devices to be successful at the point-of-care.

This work focuses on the first three stages of the biomarker pipeline: biomarker identification, biomarker validation, and assay development. Chapter 1 shows the application of two high-throughput proteomic screening platforms, the aptamer screen and the antibody array, to uncover noninvasive stool biomarkers of pediatric inflammatory bowel disease. These biomarker candidates are also validated in a small cohort of patients to establish their clinical significance and the verification of the screening platforms. In Chapter 2 of this work, a urine normalizer protein is identified and validated for the normalization of urine biomarkers at the point-of-care. In Chapter 3, phosphor-based lateral flow assays for the detection of a urine biomarker of lupus nephritis flares and a urine normalizer protein has been established and optimized for use in urine. As a whole, this work pushes the discovery and application of biomarkers in noninvasive body fluids for chronic autoimmune diseases.

Chapter 1: Stool Protein Biomarkers of Pediatric IBD

Introduction

Inflammatory bowel disease (IBD) is an autoimmune disease that involves immune mediated chronic inflammation to parts of the digestive tract. The disease has two subtypes, Crohn's disease and ulcerative colitis, which manifest differently alluding to different underlying pathogenesis. As IBD often presents in childhood and is diagnostically confirmed using endoscopic procedure, a need for noninvasive biomarkers to assist in IBD diagnosis is warranted as endoscopic procedures in children can be more difficult and painful. This study utilizes two proteomic screening platforms, Somalogic's SOMAscan aptamer assay and RayBiotech's L1000 glass slide antibody array, to discover novel diagnostic stool biomarkers for IBD. Candidate biomarkers have been validated by ELISA in a pilot cohort of samples to characterize their clinical utility and establish the efficacy of these high-throughput screening platforms for use in stool.

Inflammatory bowel disease

Inflammatory bowel disease involves chronic inflammation of all or part of the digestive track with immune-mediated mechanisms. Its prevalence occurs among 1.6 million Americans, including as many as 80,000 children [9]. With over 20% of cases being diagnosed before the age of 17, IBD is one of the most common chronic diseases affecting children and adolescents [10].

The cause of IBD is still being studied, but as with other autoimmune diseases, a combination of genetics, environmental factors, and the immune system may initiate the inflammation. Some evidence has shown that foreign antigens may cause an initial trigger of the inflammation after which the body is unable to return

to its uninfamed state. This chronic inflammation is the cause of many of the symptoms related to IBD including severe diarrhea, pain, fatigue, and weight loss. As most autoimmune diseases, IBD's symptoms occur in series of flares and remissions.

The disease has two types: ulcerative colitis and Crohn's disease as illustrated in Figure 2 [11].

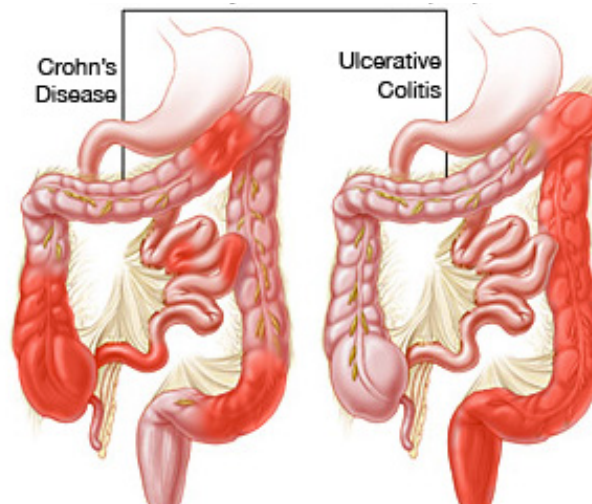


Figure 2: Crohn's disease and ulcerative colitis are two types of inflammatory bowel disease. Crohn's disease involves deep inflammation of one or more layers of the intestinal tract in discontinuous areas in the lining of the digestive tract. Ulcerative colitis involves inflammation and ulcers in the innermost lining of the colon and rectum.

Current treatment for IBD involves the control of this intestinal inflammation allowing for a relief of symptoms, prevention of flares, and achievement of mucosal healing and remission. These treatments rely on medicine or nutritional therapy but are used mostly for disease management, as there is no current cure for IBD.

Diagnosis of IBD occurs by endoscopic procedures with confirmation with mucosal biopsy histology. Serological blood testing as aided in the diagnosis of IBD with current testing focusing on the detection of autoantibodies [12]. Serum C-

reactive protein (CRP) is also often useful in distinguishing IBD from the non-immune mediated acute disease of irritable bowel syndrome where high CRP levels are predictive of IBD, while low CRP indicates the absence of IBD [13]. As serological blood testing has been promising in terms of stratification of IBD, stool becomes an interesting additional body fluid to investigate, as stool is closer to the site of disease and inflammation than blood.

Stool biomarkers for IBD

Current research in stool biomarkers for inflammatory bowel disease has uncovered many potential biomarker candidates [14]–[19]. Many stool biomarkers identified thus far are not specific for IBD itself but are related to intestinal inflammation. The two most promising stool markers for IBD are calprotectin and lactoferrin.

The S100A8/S100A9 complex also known as calprotectin has been thoroughly investigated to aid in stool diagnostics of IBD [20]–[22]. Intestinal calprotectin is shown to indicate neutrophil migration to the intestines. Interestingly, fecal calprotectin can differentiate IBD from IBS and is often used for differential diagnosis. Increased stool calprotectin levels are indicative of a higher likelihood of IBD [13] and have been implicated in pediatric IBD as well [23]. The use of calprotectin in IBD diagnosis and management has also seen promise [24], [25] as a decrease in calprotectin levels after therapy can allude to mucosal healing [26]. Calprotectin is also seen to rise before disease relapse [27]. Unfortunately, calprotectin may be elevated in other intestinal diseases [28] including colorectal cancer [29] alluding to calprotectin being a marker of intestinal inflammation not

related to IBD. Calprotectin is also not able to distinguish between ulcerative colitis and Crohn's disease patients [24].

Lactoferrin another marker of neutrophil migration is seen to be elevated in the stools of patients with inflammatory bowel disease patients and can successfully rule out patients with IBS [30]. It is also seen to be a marker of mucosal healing as fecal lactoferrin levels are seen to decrease after therapy [31].

Other stool markers that have been implicated in IBD [32] include hemoglobin [33], MMP-9 [34]–[36], MPO [37], lipocalin-2 [38], [39], and elastase [40]–[42]. The source of these markers has been not been elucidated and can come from the molecules leaking from the blood into the intestines, release from the intestinal mucosa itself, or from the shedding of cells and tissue as a result of chronic inflammation. Biomarkers from inflammatory cells and the mucosal lining have the greatest potential as markers of IBD in terms of diagnosis as they are excreted or shed because of the disease itself. Even more promising is the incorporation of these markers into understanding the pathology of IBD allowing for the creation of better, targeted therapeutics. With the risk of performing repeated endoscopic procedures, especially in pediatric patients, novel stool biomarkers of pediatric inflammatory bowel disease are have been examined using two high-throughput technologies: the aptamer-based SOMAscan and an antibody-based glass slide array.

SOMAscan aptamer-based screen

The SOMAscan aptamer-based screen employs SOMAmers (slow off-rate modified aptamers) as protein binding reagents for the simultaneous detection of

over 1000 human proteins. At the time of this study, SOMAscan was capable of detecting 1120 human proteins but now has the capability of detecting over 5000 human proteins. The screen is highly sensitive with a large dynamic range capable of the detection of proteins from fM to uM concentrations by employing multiple dilutions of the sample. The modification of these aptamers allows for highly specific protein binding allowing the assay to be reproducible with a median %CV for over 95% of SOMAmers to be less than 10% in human plasma [4]. The screen can be adapted to numerous sample matrixes with studies published in human plasma, serum, CSF, urine, synovial fluid, bronchoalveolar and nasal lavage, cell culture supernatant, cell and tissue lysates. At the time, a review paper summarizing the application of the SOMAscan aptamer-based screen in human body fluids showed applications in Alzheimer's disease [43], [44], pulmonary tuberculosis [45], [46], Duchenne muscular dystrophy [47], lung cancer [48], [49], and mesothelioma [50]. Since, the screen has been employed in coronary heart disease [51], cancers, and other chronic diseases. The current study is the first use of the SOMAscan aptamer-based screen on stool samples.

RayBiotech L1000 antibody array

The RayBiotech L1000 antibody array is a glass slide based high-density array on which 1000 antibodies are printed. Biotinylated sample mix and streptavidin Cy-3 allow for the semi-quantitative detection of over 1000 human proteins. At the time when this study was conducted, the L1000 array was capable of detecting 1000 human protein but now has expanded to the detection of 2000 human proteins. The dynamic range of the screen is limited to the picogram to

nanogram range as the array is conventionally done at a single dilution [5]. The array has been used in a variety of human diseases and body fluids including hepatocellular carcinoma serum [52], colorectal cancer plasma [53], healthy aqueous humor [54], pancreatic cancer serum [55], heart failure serum [56], COPD plasma [57], rectal cancer serum [58], chronic ulcer patients' wound fluid [59], neurosyphilis CSF [60], psoriasis serum [61]. Although one study on colorectal cancer stool [62] did employ an antibody array, the study only screened for 507 proteins versus 1000 on the full array. This work is the first to screen for pediatric IBD stool markers using high-throughput antibody arrays.

Methods

Stool processing

Proteins from the stool were extracted using SB17 Extraction buffer (120mM NaCl, 5mM KCl, 5mM MgCl₂, 40mM HEPES pH 7.5, 0.05% Tween20) for the aptamer-based proteomic screen and Buhlmann extraction buffer (Buhlmann B-CAL-EX3) for the antibody-based proteomic screen and ELISA validations. The human stool was weighed precisely and added to extraction buffer at a ratio of 100 mg to 600 ul of extraction buffer. The sample mixture was vortexed for 1 minute alternating with a 5-minute ice bath until no fecal granules were visible. After thorough vortexing, the sample mixture was centrifuged for 5 minutes at 3,000 RPM at 4°C. The supernatant was collected and chilled on ice for 60 minutes followed by additional centrifugation for 30 minutes at 10,000 RPM, 4°C. The supernatant fraction was again collected and the volume was measured. Protein content was measured using the BCA assay

(Thermo Fisher Scientific PI23227). Stool extract was aliquoted and frozen at -80°C until further processing.

SOMAscan assay

Stool extract was diluted to 200 µg/mL with SB17 extraction buffer and sent to Somalogic Inc. (Boulder, CO, USA) for SOMAscan assay optimization and processed using the cell and tissue lysate assay protocol.

As illustrated in Figure 3, for the SOMAscan assay capable of detecting 1129 human proteins, 120 µL of stool extract at a total protein concentration of 20 µg/mL was combined with 1.2 µL 100x HALT protease inhibitor (Fisher Scientific P178440), and 2 µL of Z-block (a SOMAmer mimic to prevent non-specific binding). The sample mixture was incubated with aptamer-coated beads for 3.5 hours.

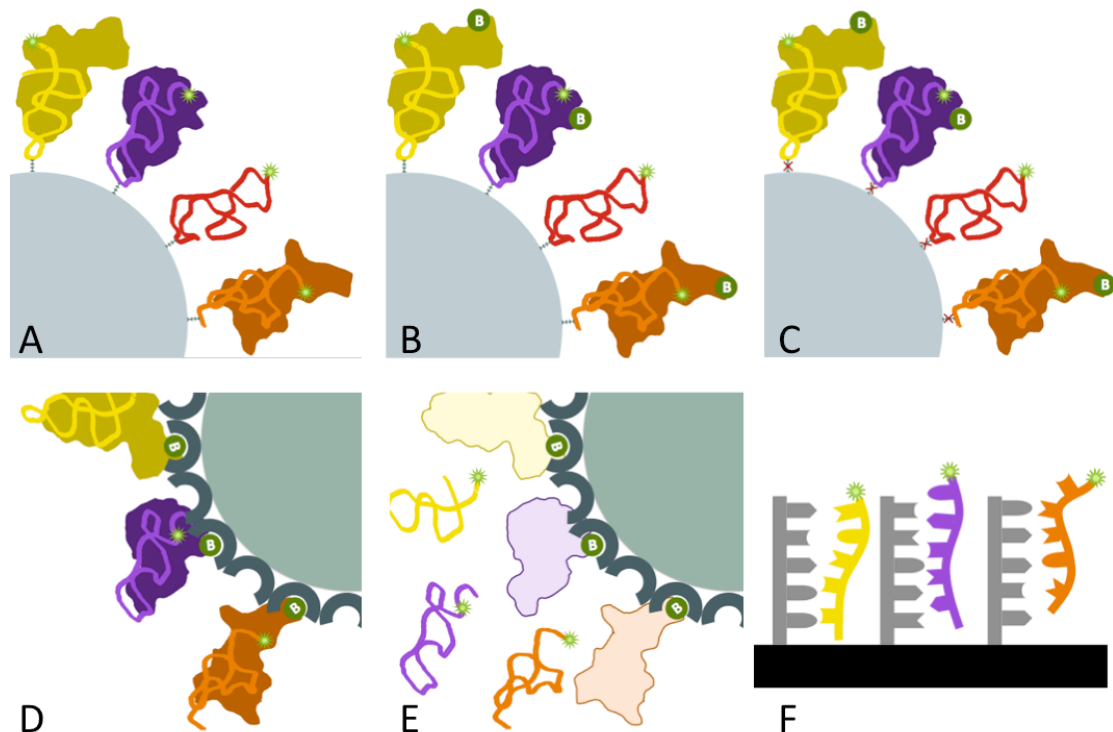


Figure 3: A summary of the SOMAscan assay capable of detecting over 1100 human proteins.

During incubation, proteins in the stool sample bound to their corresponding aptamers on the beads (Figure 3 A). After incubation, the sample was removed and

the aptamer-coated beads were washed to remove unbound proteins. Proteins from the sample that had bound to their cognate aptamers were biotinylated (Figure 3 B) and aptamer-protein complexes were photocleaved using a UV light from the beads (Figure 3 C) and bound to streptavidin-coated magnetic beads (Figure 3 D). This step removed any aptamers that did not bind to their corresponding protein. The protein-aptamer complexes were washed thoroughly using high volume and temperature controlled washes to minimize nonspecific interactions. The proteins were denatured and aptamers were eluted using a high salt buffer (Figure 3 E) and the aptamer oligos hybridized onto a custom Agilent DNA array overnight (Figure 3 F). The arrays were with Agilent buffers (Agilent 5188-5221) and scanned using a microarray scanner (Agilent G4900DA). Data was extracted using Agilent Feature extraction software. Along with the stool samples, eight controls were included to allow for quality control and normalization. A no protein buffer blank allowed for the assessment of background signal.

For initial feasibility studies, a pooled sample consisting of six human stool extract samples (two CD, two UC, and two HC) was used to perform a 16-point titration across the assay detecting 1129 human proteins.

For the proteomic screen, 24 human stool extract samples (eight CD, eight UC, and eight HC) were assayed for 1129 human proteins. The stool was collected at Emory University School of Medicine. This study was approved by the Institutional Review Boards of both Emory University and the University of Houston. Details of the subjects are listed in Table 1.

Table 1: Demographic characteristics of the cohort used for the SOMAscan aptamer-based screening assay.

Variable	Healthy Controls n=9	Crohn's Disease n=10	Ulcerative Colitis n=5
Sex			
Male	5	6	2
Female	4	4	3
Race			
Caucasian	6	2	7
African American	2	1	3
Other	1	2	0

Data analysis of the SOMAscan assay

For the data processing of the aptamer-based screen, data was normalized at Somalogic Inc. using hybridization and median normalization. Hybridization normalization accounts for variation in the microarray hybridization procedure by taking advantage of hybridization control sequences in the assay elution sample and hybridization probes on the microarray slide. These probes are normalized across all samples and controls run in the SOMAscan assay. Median normalization accounts for variation in the experimental procedure of the SOMAscan assay by taking advantage of the fact that all samples were assayed at the same concentration. After feature extraction, the median intensity of each sample is normalized across samples using a median scale factor.

For analysis of the aptamer-based screen, R Version 1.0.136 with the readxl [63], stats [64], and hmisc [65] packages were used to carry out data analysis. All data was log-normalized and fold change was defined as the ratio of the average intensity of a disease group to the average intensity of the control group. Mann-Whitney U-test was used to compare between groups to identify proteins that were

significantly different between the subject groups. Heatmaps were created using the PACKAGE and complete hierarchical clustering using Euclidian distance was used for clustering of proteins into five groups. Integrated Pathway Analysis (Qiagen) was used to identify established networks of interrelated proteins. Proteins were sorted by their cluster and established IPA network where proteins were selected from each individual cluster and network pair. Implications of the proteins in IBD literature and the elevation of the protein in a gene expression array on mucosal biopsies of overlapping subjects biased the selection of molecules, after which 26 proteins were selected for ELISA validation.

RayBiotech antibody array

For the RayBiotech L1000 antibody array detecting 1000 human proteins, antibody array processing kits were purchased from RayBiotech (AAH-BLG-1000-4). 80 uL of stool extract was dialyzed overnight in PBS pH 8.0. Protein concentration was measured via BCA assay and 30 ug of protein was biotinylated followed by another overnight dialysis in PBS pH 8.0. Dialyzed sample was measured and normalized across samples after which the biotinylated stool extract was diluted 1:10 and added to two blocked glass slides spotted with a total of 1000 antibodies in duplicate specific for 1000 unique human proteins (407 antibodies on the L407 slide and 503 antibodies on the L593 slide). After an overnight incubation with the dialyzed, biotinylated sample, slides were washed and incubated with streptavidin-Cy3. The glass slides were then thoroughly washed with wash buffer and dried in a ventilated hood after which they were scanned on a glass slide array

scanner (GenePix 4000B). Feature extraction was conducted using GenePix Pro Software. A summary of the antibody array processing is depicted in Figure 4.

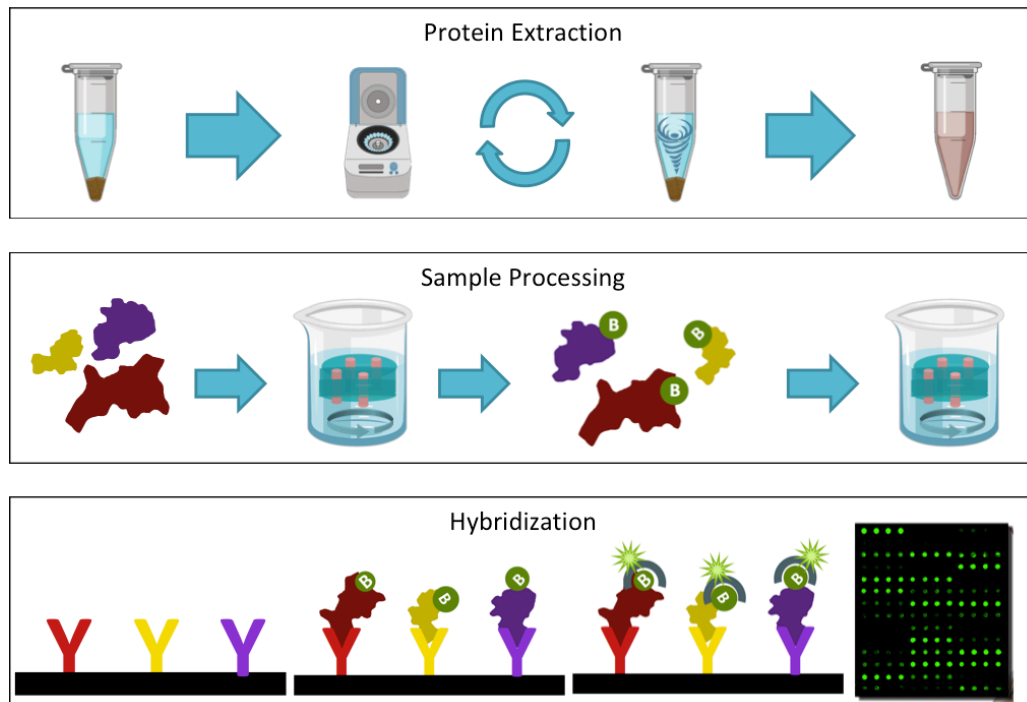


Figure 4: Summary of the processing of the RayBiotech L1000 antibody arrays on stool extract.

The antibody array screening was conducted on 31 pediatric stool samples (10 CD, 11 UC, 10 HC) in three separate runs. The stool was collected at Emory University School of Medicine. This study was approved by the Institutional Review Boards of both Emory University and the University of Houston. Demographics of the screening population are illustrated in Table 2.

Table 2: Demographics information for the cohort use for the RayBiotech antibody-array based proteomic screen.

Variable	Healthy Controls	Crohn's Disease	Ulcerative Colitis
	n=10	n=10	n=11
Sex			
Male	5	6	5
Female	5	4	6
Race			
Caucasian	6	7	7
African American	2	3	2
Other	2	0	2
Run			
Run A	5	5	0
Run B	3	3 (+1 repeat)	4
Run C	2	2 (+1 repeat)	7

One sample was repeated on all three runs to allow for normalization between runs and to assess variation in the stool processing, sample dialysis, and biotinylation, and antibody array processing illustrated in Table 3.

Table 3: Sample 14 was used to assess quality control of the antibody array processing of stool extract.

Sample	Run	Extraction	Processing	Hyb
14.1	A	1	A	A
14.2	B	1	B	B
14.3	B	1	A	B
14.4	B	2	B	B

Sample 14 was used from two different extraction dates, processed, and hybridized onto the antibody arrays on two different runs.

RayBiotech data analysis

After feature extraction using GenePix Pro software, data was imported into Microsoft Excel for normalization. Biotinylated IgG's at three concentrations printed

in duplicate at three locations on each array allowed for normalization of samples within the run. Buffer printed as negative controls allowed for the assessment of background signal. A repeat sample (Sample 14) was run on each run to allow for normalization between run.

For analysis of the antibody array screen, R Version 1.0.136 with the readxl [63], stats [64], and hmisc [65] packages were used to carry out data analysis. Fold change was defined as the ratio of the average intensity of a disease group to the average intensity of the control group. Mann-Whitney U-test was used to compare between groups to identify proteins that were significantly different between the subject groups. Integrated Pathway Analysis (Qiagen) was used to identify established networks of interrelated proteins. Heatmaps were created and complete hierarchical clustering using Euclidian distance was used for clustering of proteins into groups based on the number of IPA networks found. Both the heatmaps and hierarchical clustering was based on log-normalized data. Proteins were sorted by their cluster and established IPA network where proteins were selected from each individual cluster and network pair. Implications of the proteins in IBD literature and the elevation of the protein in a gene expression array on mucosal biopsies of overlapping subjects influenced the selection, after which 17 proteins were selected for ELISA validation.

ELISA validation

ELISA validation was carried out for 26 proteins selected from the aptamer-based screen and 17 proteins on antibody array. After initial testing for optimal sample dilution, 23 molecules could be detected in stool samples at a dilution of at

least 1:2. Vendor, catalog number, and stool sample dilution for these molecules are listed in Table 4.

Table 4: Summary of the ELISA kits used for the validation of stool biomarkers for pediatric IBD.

Molecule	Vendor	Catalog Number	Dilution Used
Albumin	RayBiotech	LH-Albumin-1	1:2
Alkaline phosphatase	RayBiotech	ELH-ALKP-1	1:10
Cystatin A	RayBiotech	ELH-CystatinA-1	1:20
D-Dimer	RayBiotech	ELH-DDIMER-1	1:20
Elastase	Abcam	ab119553	1:5
Ferritin	RayBiotech	ELH-Ferritin-1	1:5
Fibrinogen	Imm. Cons. Laboratory	E-80FIB	1:5
Fibronectin	RayBiotech	ELH-FN1-1	1:2
Haptoglobin	R&D Systems	DHAPG0	1:50
Hemoglobin	RayBiotech	ELH-Hgb-1	1:5
Kallistatin / SerpinA4	R&D Systems	DY1669	1:50
Galectin-3BP / LG3BP	R&D Systems	DY2226	1:15
Lipocalin-2	RayBiotech	ELH-Lipocalin2	1:100
MMP-8	R&D Systems	DY908	1:1000
MMP-9	RayBiotech	ELH-MMP9-1	1:100
Myeloperoxidase	R&D Systems	DY3174	1:4000
PGRP-S	R&D Systems	DY2590	1:100
Properdin	RayBiotech	ELH-PROPE-1	1:10
Proteinase 3	R&D Systems	DY6134-05	1:25000
Resistin	R&D Systems	DY1359	1:5
S100 A8/A9	Hycult Biotech	HK325-01	1:400
SAP	Abcam	ab137970	1:2
SSEA-1 / FUT4	Cloud-Clone Corp	SEB059Hu	1:10

Validation of these 23 molecules was carried out in a pilot cohort of 30 subjects' stool (15 CD, 5 UC, 10 HC) collected at Emory University Medical School. This study was approved by the Institutional Review Boards of both Emory University and the University of Houston. A summary of these subjects is listed in Table 5.

Table 5: Demographics of the cohort used for ELISA validation of stool biomarkers for pediatric IBD.

Variable	Healthy Controls	Crohn's Disease	Ulcerative Colitis
	n=10	n=15	n=5
Sex			
Male	5	11	2
Female	5	4	3
Race			
Caucasian	7	11	2
African American	2	4	1
Other	1	0	2

ELISA validation analysis

ELISAs were read and analyzed using a Biotek Plate reader and Gene5 Software. Validation data was normalized by the ratio of stool weight to volume of protein extract collected during the extraction process. Fold change and Mann-Whitney U-test was used to establish statistical significance of elevated markers using GraphPad Version 6.05.

Results and Discussion

Stool feasibility of SOMAscan assay

The titration of the pooled stool protein extract allowed for assessment of stool as a sample matrix for the SOMAscan assay and optimization of the stool extract dilution. With the combination of six independent samples from Crohn's disease, ulcerative colitis, and healthy controls, sample-to-sample variation was minimized in the optimization procedure. The pooled sample consisted of equal parts of two CD, two UC, and two HC samples and was assayed for 1129 proteins using the SOMAscan assay. The 16-point 2-fold titration consisted of stool protein extract at total protein concentrations ranging from 80 ug/mL to 2.4 mg/mL.

The most stringent criteria for sample feasibility by Somalogic states 25% of SOMAmers have linear titration behavior over four or more titrations points with less stringent criteria being 25% of SOMAmers have linear titration behavior over 3 or more titration points. Of the 1129 proteins assayed in the stool detected by the 1129 SOMAmers, 20% of the SOMAmers had a linear titration behavior over four or more titrations points and 35% of the SOMAmers had a linear titration behavior over three or more titrations points. Of these, 87% had linear coverage within one point at 20 ug/mL. As advised by Somalogic, 20 ug/mL was the total protein concentration of stool used for the SOMAscan screen on stool samples and the sample matrix was considered feasible for the assay.

Screening of pediatric IBD stool by an aptamer-based assay

For the aptamer-based screening for biomarkers of pediatric IBD in stool extract, 24 stool samples were assayed for 1129 proteins using Somalogic's SOMAscan assay at 20 ug/mL of total protein. After normalization to account for hybridization variation and median normalization to account for experimental variation between samples, all 24 stool samples passed Somalogic's quality control threshold of normalization ratios of 0.4 - 2.5 for each sample. All calibrators, controls, and blanks performed within thresholds optimized by Somalogic.

Of the 1129 proteins assayed by the aptamer-based screen, a large up-regulation of proteins was seen in IBD stools versus healthy controls, as seen in Figure 5 A.

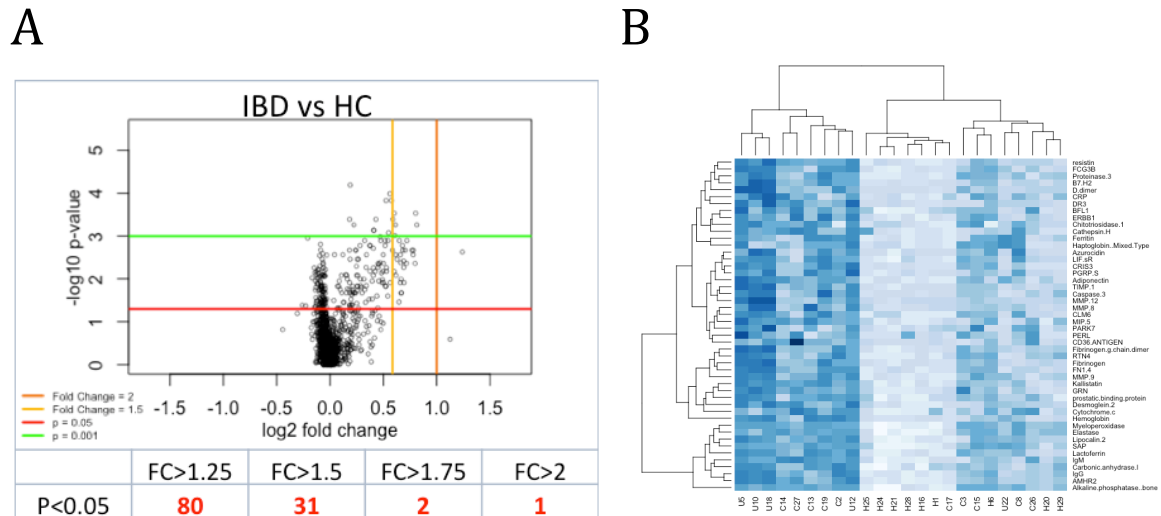


Figure 5: The aptamer-based screen showed up-regulation of 80 proteins that were elevated in IBD patients versus healthy controls (A). 48 proteins showed significant elevation (FC >2, P < 0.05) in both CD versus HC and UC versus HC comparisons (B).

Of proteins that were elevated in IBD vs HC, 80 proteins were found to be elevated at least 1.25-fold with a Mann-Whitney U-test P value < 0.05 in IBD samples versus healthy controls. Looking at more elevated proteins, 31 proteins were elevated at least 1.5-fold, 2 proteins were elevated 1.75-fold, and 1 protein was elevated at least 2-fold in both IBD populations versus healthy controls. To look molecules specific to both types of inflammatory bowel disease, the 48 molecules that were elevated in both CD vs HC and UC vs HC comparisons (FC > 1.25, P < 0.05) were selected for future analysis. These elevated proteins are also visualized by heatmap (Figure 5B) showing elevation in CD and UC samples compared to healthy controls.

Integrated pathway analysis has shown that these 48 proteins elevated in both CD vs HC and UC vs HC are interconnected according to literature in three main pathways: (1) developmental disorders, hematological diseases, hereditary disorders (Figure 6A), (2) cellular function and maintenance, cell-to-cell signaling

and interaction, inflammatory response (Figure 6B), and (3) cell death and survival, organismal injury and abnormalities, skeletal and muscular disorders (Figure 6C).

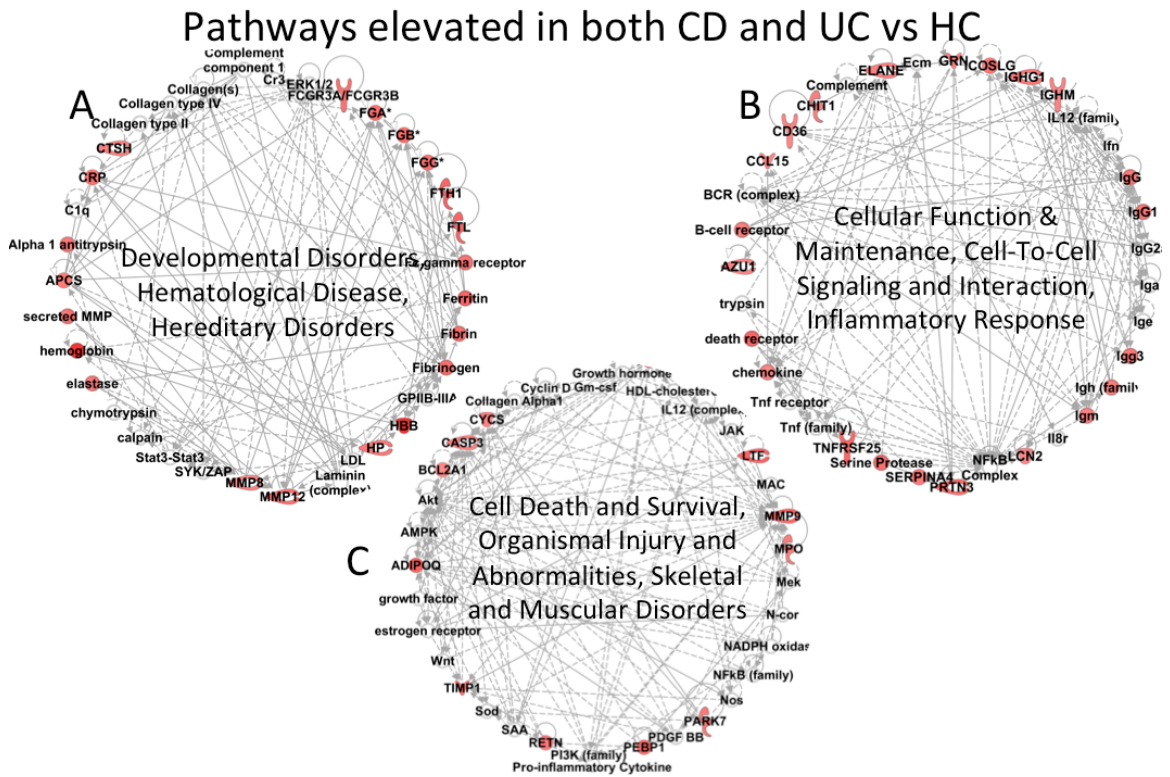


Figure 6: IPA of the 48 elevated proteins in both Crohn's disease and ulcerative colitis patients' stool versus healthy controls showed involvement of three main pathways.

To group these proteins based on similarity trends in the screening assay, hierarchical clustering was used to cluster the 48 elevated proteins ($FC > 1.25$, $P < 0.05$) in CD vs HC and UC vs HC into five groups as seen in Figure 7.

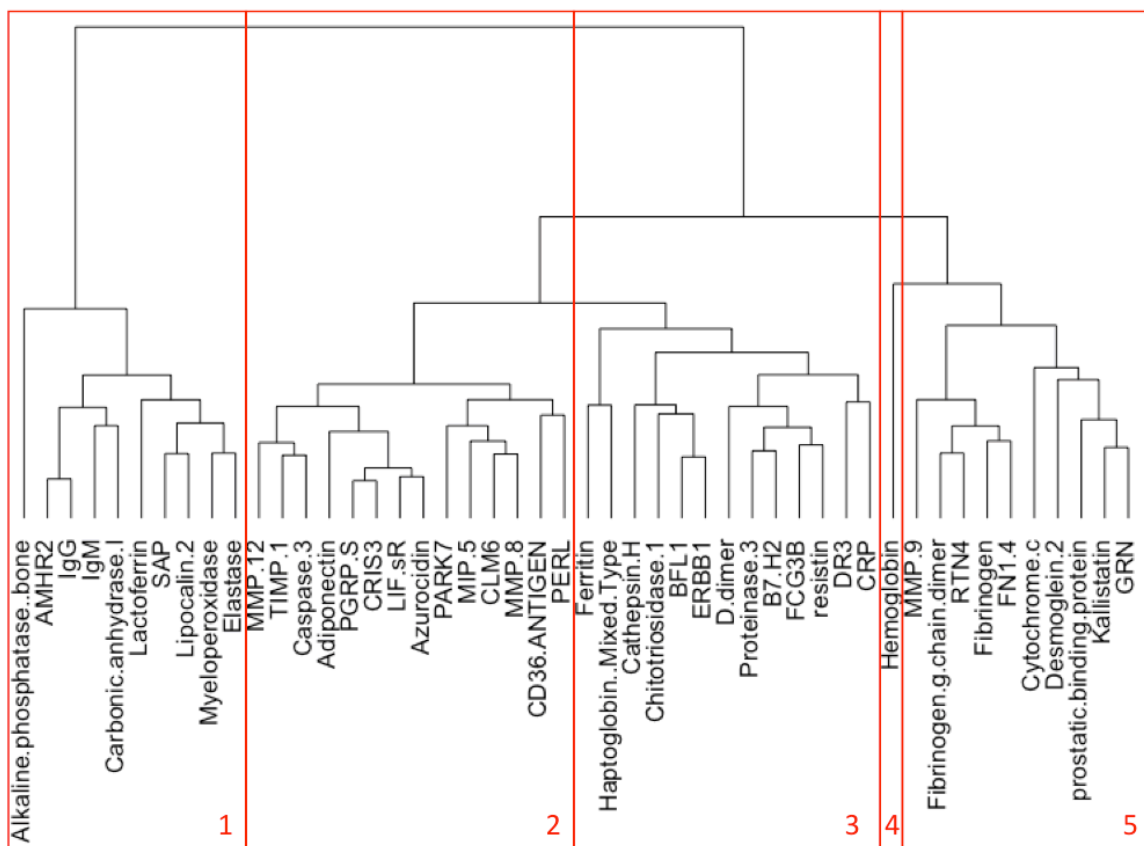


Figure 7: The 48 elevated proteins in both Crohn's disease and ulcerative colitis patients' stool versus healthy controls were separated into five group by unsupervised hierarchical clustering.

To choose molecules for further validation, at least one molecule was chosen from an each IPA network, hierarchical cluster pair with emphasis on molecules implicated in inflammatory bowel disease literature. A gene expression array on mucosal biopsies from a selection of patients in this cohort (conducted by Emory University) showed elevations in Lipocalin 2 also elevated in this screen. Figure 8 summarizes the 48 proteins elevated in the stool of both Crohn's disease and ulcerative colitis subjects when compared to healthy controls. Indication of their IPA network, hierarchical cluster, elevation in the gene expression array, and implication in literature is also listed.

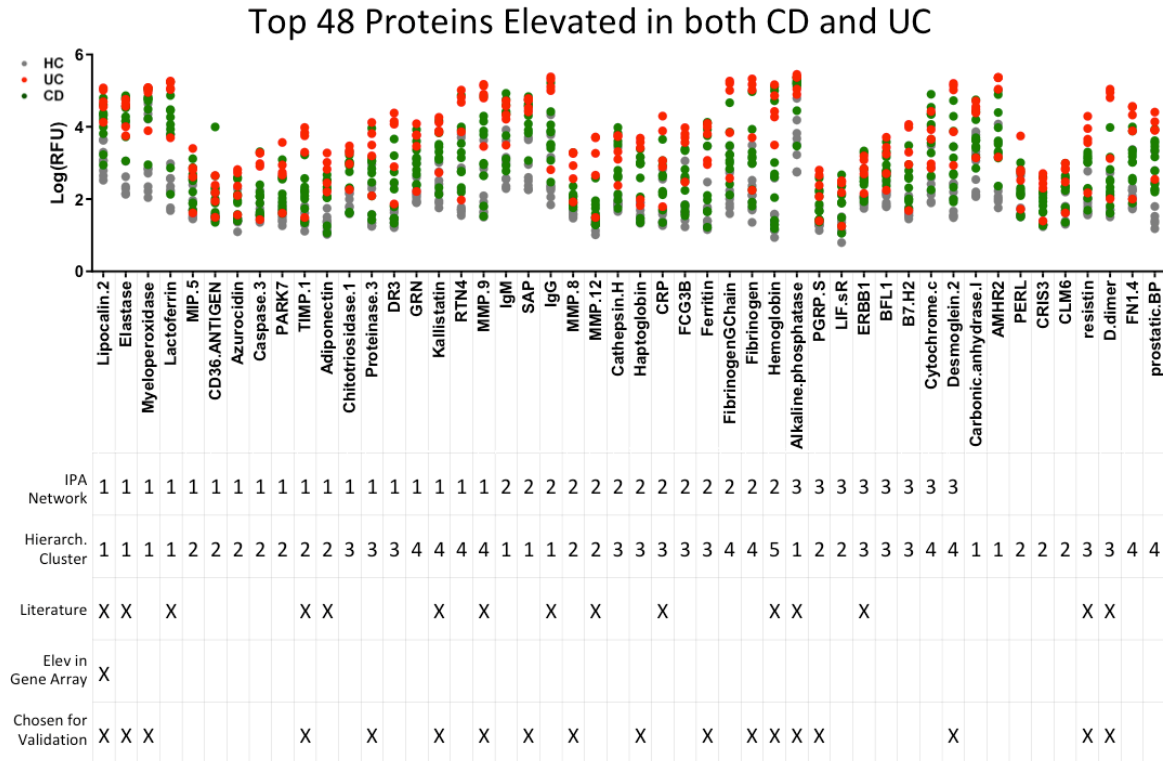


Figure 8: A summary of the 48 proteins elevated in both CD and UC patients' stool when compared to HC. Proteins are listed with the IPA network, hierarchical cluster, and elevation in a gene mucosa array. A total of 18 molecules were selected for validation by ELISA.

Using these criteria, 18 molecules were selected for validation by ELISA.

To look at diagnostic markers of Crohn's disease, the aptamer-based screen of 1129 proteins indicated 50 proteins elevated at least 1.25-fold, 7 proteins elevated at least 1.5-fold, and 1 protein elevated greater than 2-fold when comparing Crohn's disease stool to that of healthy controls as visualized in the volcano plot and heatmap in Figure 9.

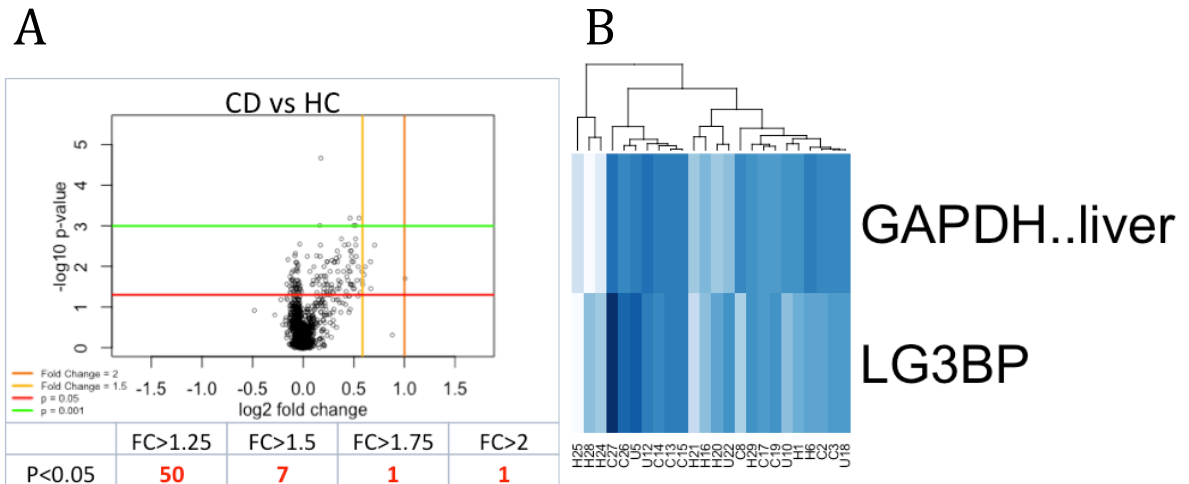


Figure 9: The aptamer-based screen showed up-regulation of 50 proteins with FC > 1.25, P < 0.05 that were elevated in CD patients versus HC (A). 2 proteins showed a significant elevation in CD versus HC but not UC versus HC comparisons (B).

After removing proteins that were also elevated in ulcerative colitis when compared to healthy controls, only two proteins were found to be elevated in the stool of Crohn's disease patients (FC > 1.25, P < 0.05): GAPDH and LG3BP. Integrated pathway analysis (Figure 10) revealed that these two proteins were connected in a pathway related to cell signaling, antimicrobial response, and inflammatory response.

Pathway elevated in CD vs HC

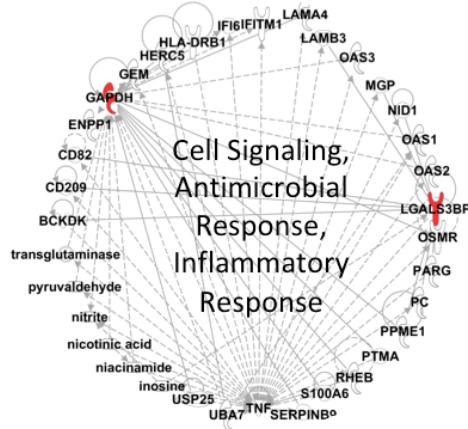


Figure 10: IPA of the 2 elevated proteins in Crohn's disease patients' stool versus healthy control but not ulcerative colitis versus healthy controls showed involvement of three main pathways related to DNA replication, recombination, and repair, cell cycle, cell morphology.

Because only two proteins were found to be elevated in the stool of only Crohn's disease patients', hierarchical clustering was not performed. A summary of these molecules is illustrated in Figure 11 where LG3BP was chosen for further validation.

Molecules Elevated in CD



Figure 11: A summary of the 2 proteins elevated in only CD and not UC patients' stool when compared to HC. Proteins are listed with the IPA network, hierarchical cluster, and elevation in a gene mucosa array. One of the two molecules was selected for validation by ELISA.

Looking at diagnostic markers of ulcerative colitis, the aptamer screen of

1129 human proteins revealed 120 proteins elevated in the stool of ulcerative colitis

patients with fold-change of at least 1.25 when compared to healthy controls as seen in Figure 12.

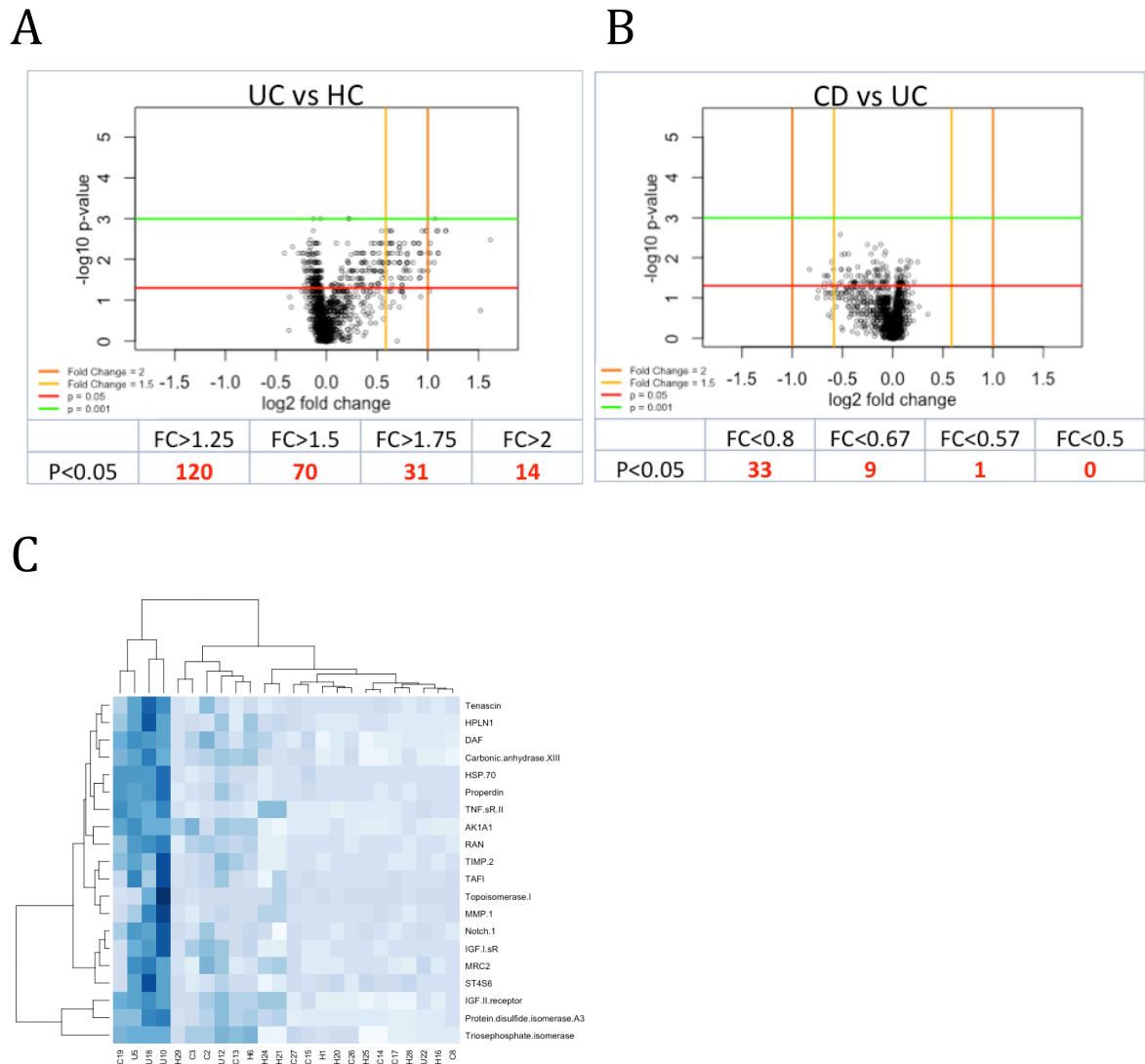


Figure 12: The aptamer-based screen showed up regulation of 120 proteins with FC > 1.25, P < 0.05 that were elevated in UC vs HC (A) and 33 proteins that were elevated in the stools of UC vs CD. 20 proteins showed significant elevation (FC >2, P < 0.05) in UC vs CD and vs HC (B).

Of these 120 proteins elevated in the stools of ulcerative colitis patients when compared to healthy controls (FC > 2, P < 0.05), 20 proteins were found to be also elevated in ulcerative colitis patients when compared to Crohn's disease while not being elevated in Crohn's disease stool when compared to healthy controls as visualized in Figure 12C.

Integrated Pathway Analysis showed these 20 proteins to be interrelated in literature with two biological pathways shown in Figure 13: (1) cellular movement, organismal injury and abnormalities, humoral immune response and (2) cancer, organismal injury and abnormalities, cellular development.

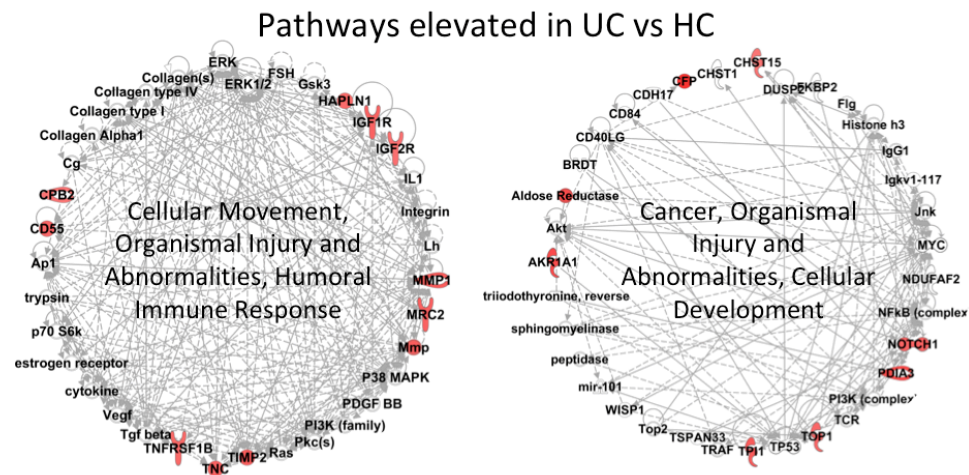


Figure 13: IPA of the 20 elevated proteins in UC patients' stool versus CD and HC but not CD versus HC showed an involvement of two main pathways.

Hierarchical clustering of these elevated proteins in ulcerative colitis is shown in Figure 14 where these 20 proteins have been clustered into five groups based on their similarity trends in the screening assay.

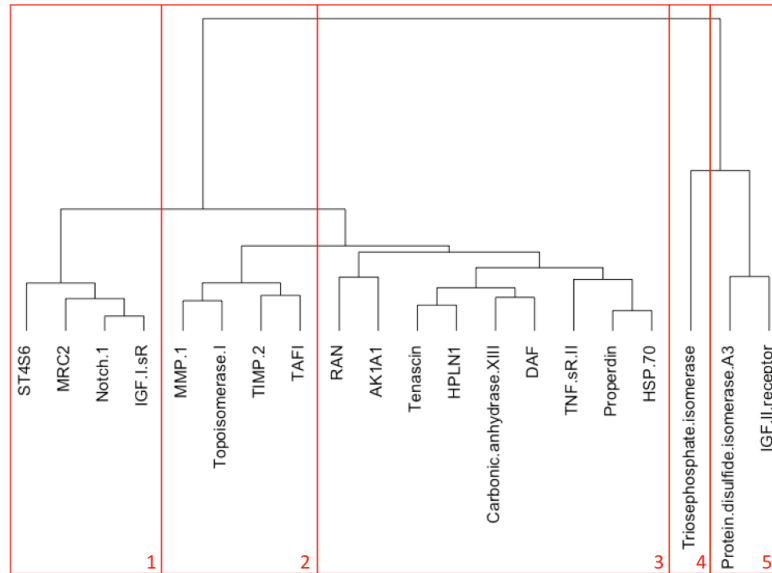


Figure 14: The 20 elevated proteins in elevated in ulcerative colitis patients when compared to Crohn's disease and healthy controls while not being elevated in Crohn's disease stool when compared to healthy controls were separated into five group by unsupervised hierarchical clustering.

Of these 20 proteins elevated in the stools of only ulcerative colitis patients when compared to healthy controls and Crohn's disease, DAF was also seen to be elevated in the gene expression arrays of mucosal biopsies (conducted at Emory University). Seven proteins were chosen for ELISA validation by choosing proteins from each individual IPA network, hierarchical cluster pair as summarized in Figure 15.

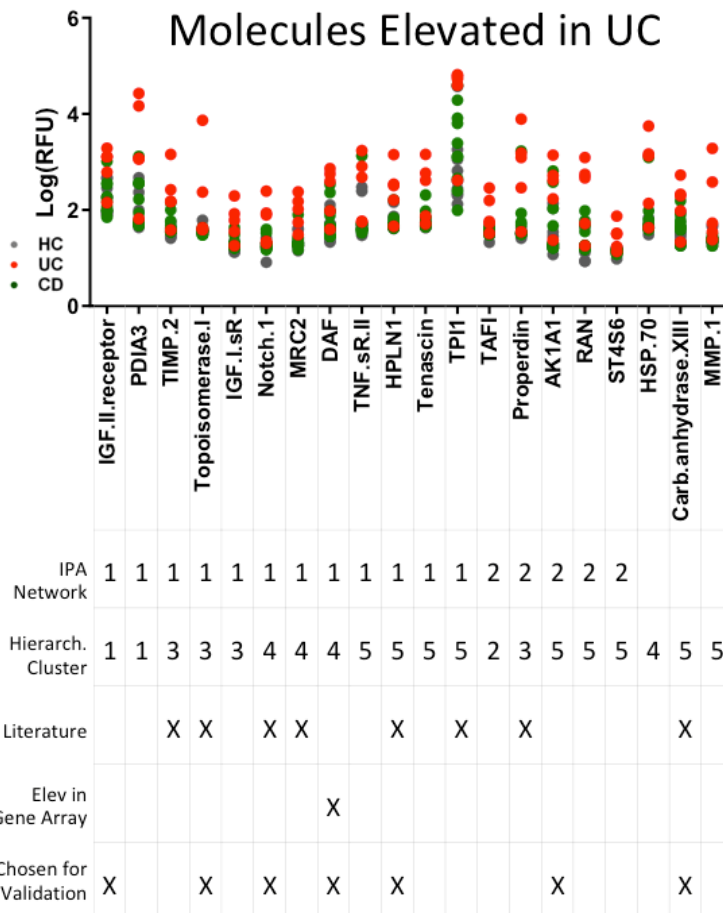


Figure 15: A summary of the 20 proteins elevated in ulcerative colitis patients when compared to CD and HC while not being elevated in CD vs HC. Seven molecules were selected for validation by ELISA.

In summary, the aptamer-based screen identified 48 proteins elevated in the stool of both Crohn’s disease and ulcerative colitis subjects versus healthy controls and 18 were chosen for ELISA validation. Two proteins were elevated in the stool of Crohn’s disease patients but not ulcerative colitis when compared to healthy controls and one were chosen for ELISA validation. 20 proteins were elevated in the stool of ulcerative colitis patients when compared to healthy controls and Crohn’s disease while not being elevated in Crohn’s disease versus healthy controls and 7 were chosen for ELISA validation. In total 26 proteins were chosen for ELISA validation.

Quality control of extraction and processing using antibody array

To assess variation in protein extraction, sample processing, and hybridization, one sample was selected for extraction, processing, and hybridization on different runs of the antibody array as illustrated in Figure 4 above.

To assess the effect of protein extraction, Sample 14.2 was compared to Sample 14.4 where stool from Subject 14 was extracted on two different dates, but processed and hybridized during the same antibody array run as seen in Figure 16.

Effect of Protein Extraction

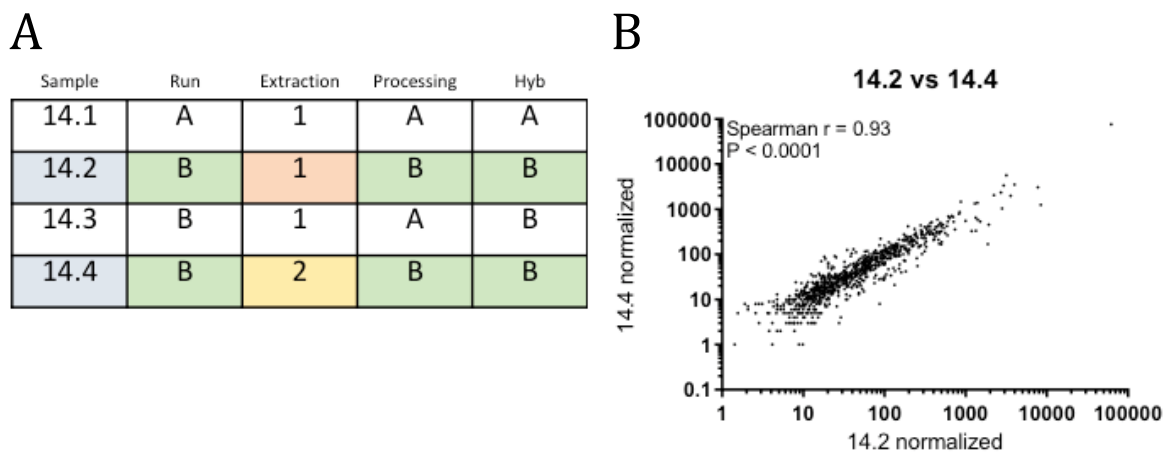


Figure 16: The effect of protein extraction on the antibody array.

Using Spearman correlation, Sample 14.2 was seen to correlate very well with Sample 14.4 with $r = 0.93$, $P < 0.0001$ showing that the current protein extraction procedure is quite reproducible between different days.

To assess the effect of sample processing in terms of the dialysis and biotinylation steps, Sample 14.2 was compared to Sample 14.3 in Figure 17 where one sample extract was dialyzed and biotinylated on two different dates and hybridized together in the same run.

Effect of Sample Processing

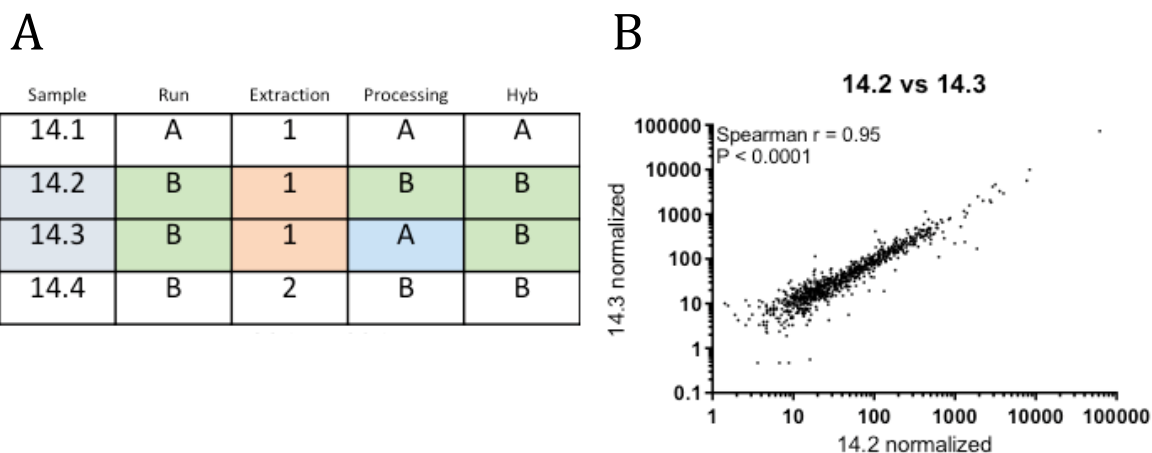


Figure 17: The effect of the dialysis and biotinylation steps on the antibody array.

Sample 14.2 was seen to again correlate very well to Sample 14.3 with a Spearman $r = 0.96$, $P < 0.0001$ showing that the dialysis and biotinylation procedures are also reproducible in the stool extract samples.

To assess the effect of hybridization, Figure 18 shows Sample 14.1 compared to Sample 14.3 where the one stool sample was protein extracted, processed, but hybridized to the antibody array during two different runs.

Effect of Hybridization

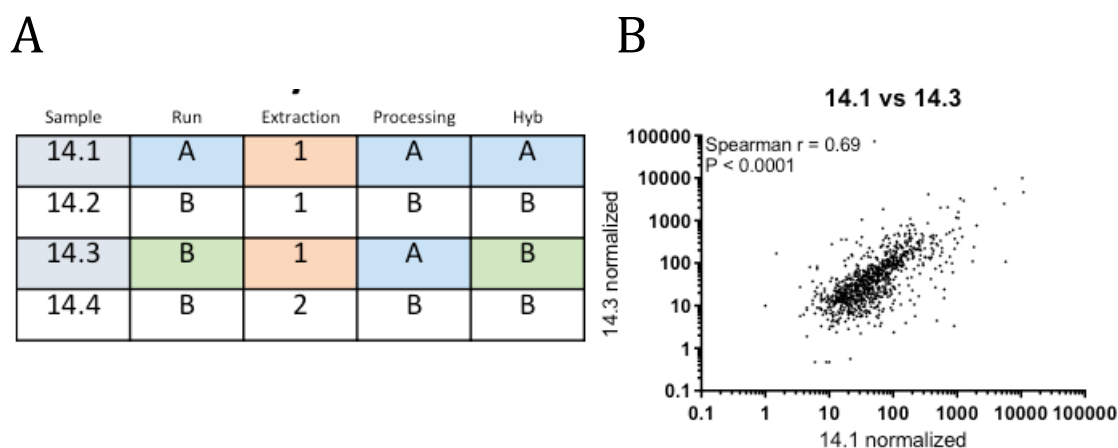


Figure 18: The effect of hybridization on the antibody array.

Although the correlation of these two samples was lower than that of comparing protein extraction and sample processing, the Spearman correlation between

Sample 14.1 and 14.3 was still positive with $r = 0.69$, $P < 0.0001$. These two samples were compared after normalization with positive controls within the run and before normalization between the runs.

Combinatorial effects of stool sample extraction, processing, and hybridization are shown in Figure 19.

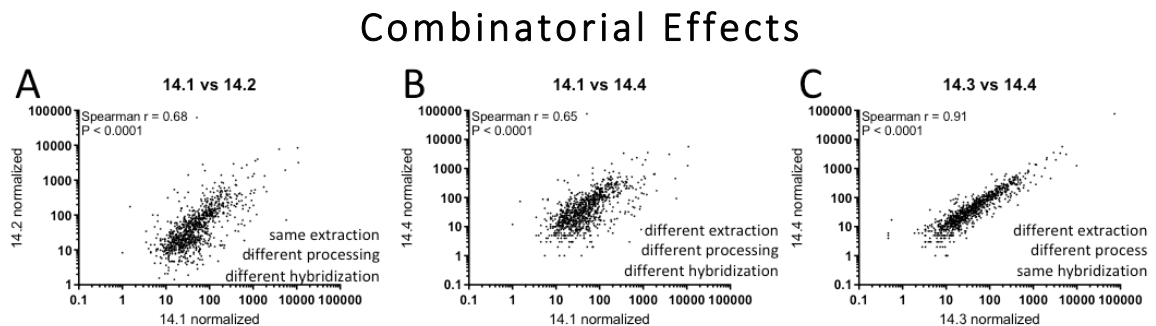


Figure 19: Combinatorial effects on the antibody array.

Comparison of Sample 14.1 with Sample 14.2 shows that the same protein extract with different sample processing and hybridization has a positive correlation of Spearman $r = 0.68$, $P < 0.001$ (Figure 19A). Comparison of Sample 14.1 with sample 14.4 shows the triple combinatory effect of different extraction, processing, and hybridization with a Spearman $r = 0.65$, $P < 0.0001$ (Figure 19B). Correlation of the samples is increased when samples are hybridized on the same run as illustrated by the comparison of Sample 14.3 with Sample 14.4 (Figure 19C) where a stool sample was extracted at two times, processed on different dates, but hybridized in the same run of antibody arrays. This assessment shows that the hybridization step may cause the most variation between samples while the other steps are quite reproducible. In an ideal scenario, all samples would be assayed together and hybridized at the same time, but due to the manual handling of the arrays during the slide hybridization and washing, samples are often separated into multiple runs.

Screening of pediatric IBD stool by antibody array

The screening of the 31 pediatric stools was completed on three runs with one overlapping sample used for normalization. Sample 14 was used as a normalizer between runs and correlations of Sample 14 on each run are shown in Figure 20.

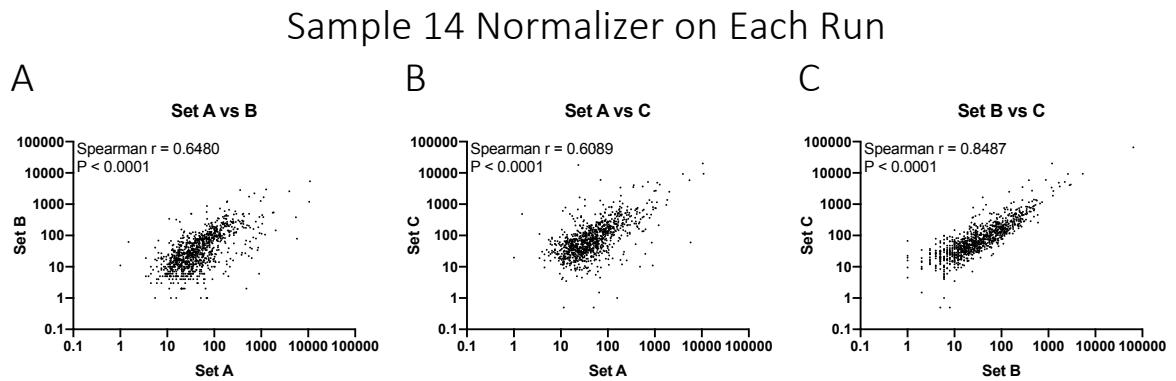


Figure 20: Sample 14 was used to normalize three independent runs of samples.

The variation of sample 14 between Set A and Set B and between Set A and C showed more variation with a decreased Spearman correlation of 0.65 and 0.60 respectively. Correlation of Sample 14 between Set B and C was more reproducible with a higher Spearman correlation of 0.85. To minimize the experimental variation between sets, all samples were normalized to Set A.

Among the 1000 proteins screened on the antibody array, 71 proteins were found to be elevated ($FC > 2$, $P < 0.05$) in the stools of IBD patients versus healthy controls as visualized in the volcano plot and heatmap in Figure 21.

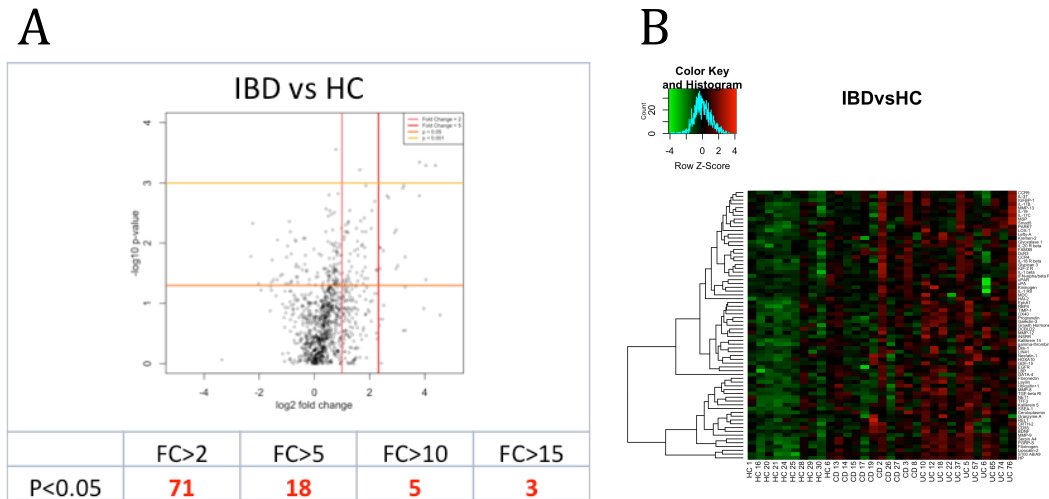


Figure 21: The antibody array-based screen of 1000 human proteins in pediatric and healthy control stool extract showed up-regulation of 71 proteins with FC > 2, P < 0.05 that were elevated in IBD patients versus healthy controls (A) visualized on a heatmap (B).

Among these elevated proteins 18 had FC > 5, 5 had FC > 10 and 3 proteins had FC > 15 in the stools of IBD patients when compared to healthy controls.

Integrated Pathway Analysis of these 71 elevated proteins found seven networks with the top three networks related to (1) cellular movement, immune cell trafficking, cell-to-cell signaling and interaction, (2) cellular movement, hematological system development and function, immune cell trafficking, and (3) organ morphology, organismal development, reproductive system development and function as shown in Figure 22.

Pathways Elevated in IBD vs HC

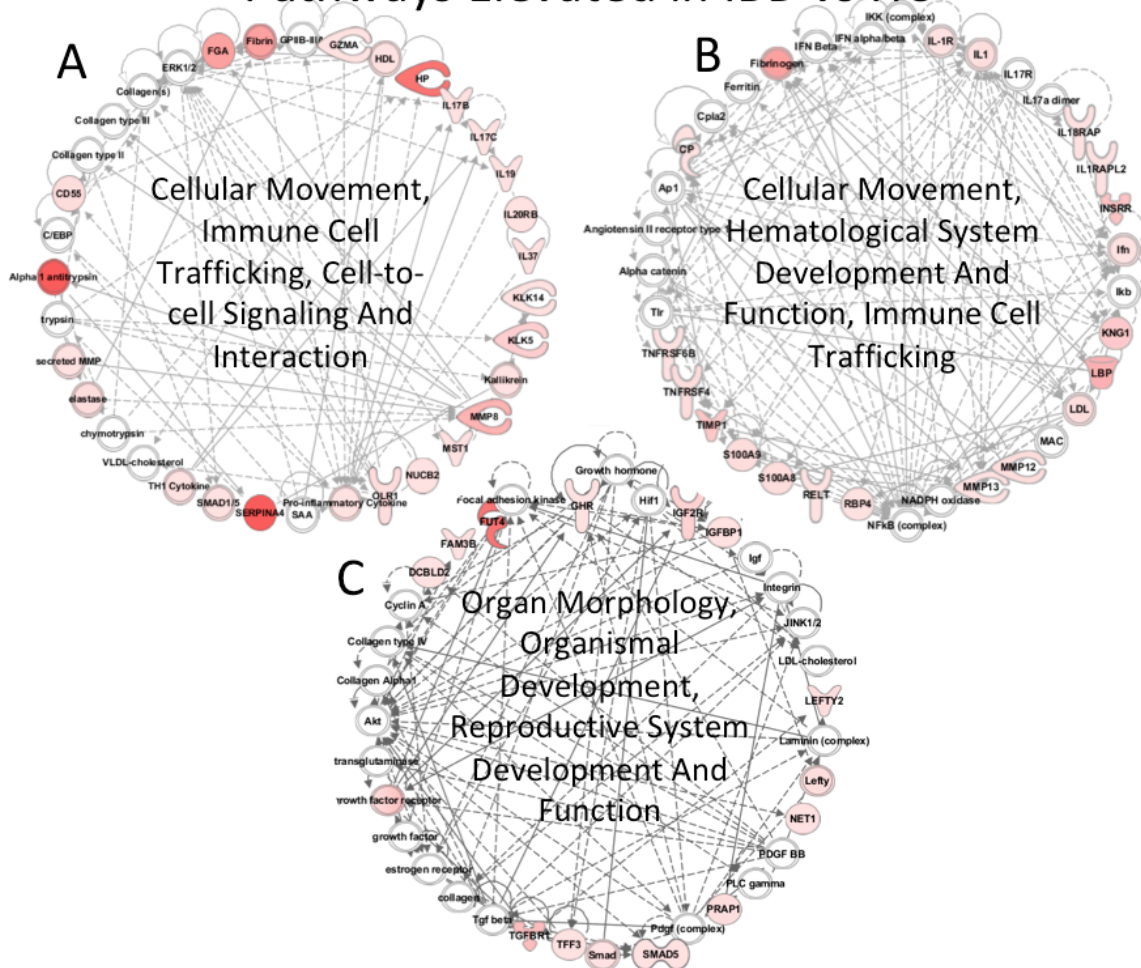


Figure 22: IPA of the 71 proteins elevated in IBD stools when compared to healthy controls showed these top three networks.

Hierarchical clustering of these 71 proteins elevated in the stool of IBD patients versus healthy controls is shown in Figure 23 where the proteins were clustered into seven groups based on the number of IPA networks found.

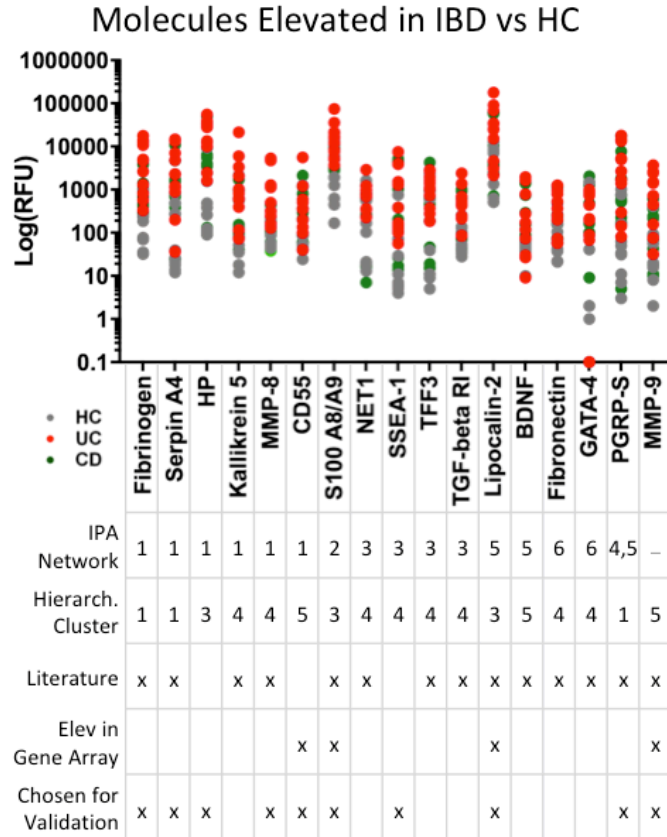


Figure 24: Of the 71 proteins elevated in IBD vs HC on the antibody array, the 17 visualized proteins had an average RFU > 200 and 13 were chosen for ELISA validation.

Thirteen proteins were chosen for ELISA validation by choosing proteins from each individual IPA network, hierarchical cluster pair with a bias on molecules that were detected on the gene mucosal array and those implicated in IBD literature.

When looking at molecules elevated in the stools of Crohn’s disease patients when compared to healthy controls 17 molecules were found to be elevated at least 17-fold and 3 molecules were elevated at least 5-fold as visualized in the volcano plot and heatmap in Figure 25.

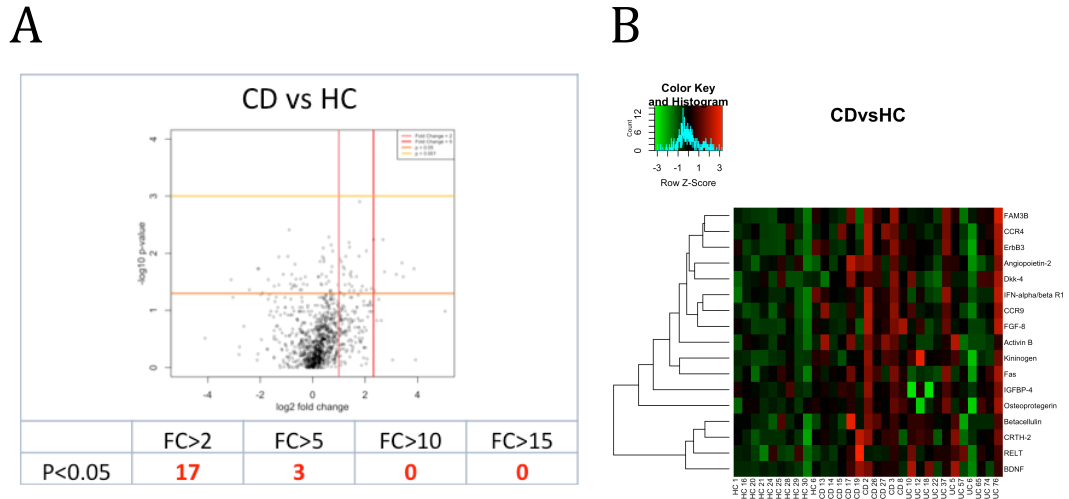


Figure 25: The antibody array-based screen of 1000 human proteins in pediatric and healthy control stool extract showed up-regulation of 17 proteins with FC > 2, P < 0.05 that were elevated in Crohn's disease patients versus healthy controls (A) visualized on a heatmap (B).

Integrated pathway analysis of these 17 proteins identified three pathways with Figure 26 showing top pathway being related to tissue development, cellular movement, and lipid metabolism.

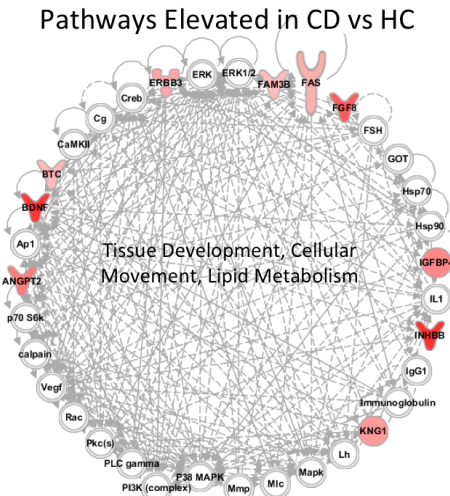


Figure 26: IPA of the 17 proteins elevated in Crohn's disease stools when compared to healthy controls.

Hierarchical clustering of these 17 molecules into three groups based on the number of found IPA networks is shown in Figure 27.

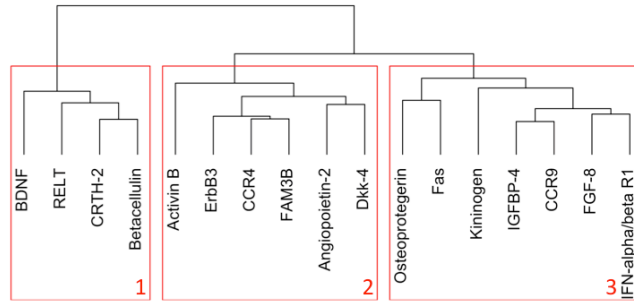


Figure 27: Unsupervised hierarchical clustering of the 16 proteins elevated in Crohn's disease stools versus healthy controls.

Of the 17 proteins elevated in the stools of Crohn's patients when compared to healthy controls, BDNF was chosen for ELISA validation as it was the only protein with an average RFU > 200 on the antibody array as visualized in Figure 28.

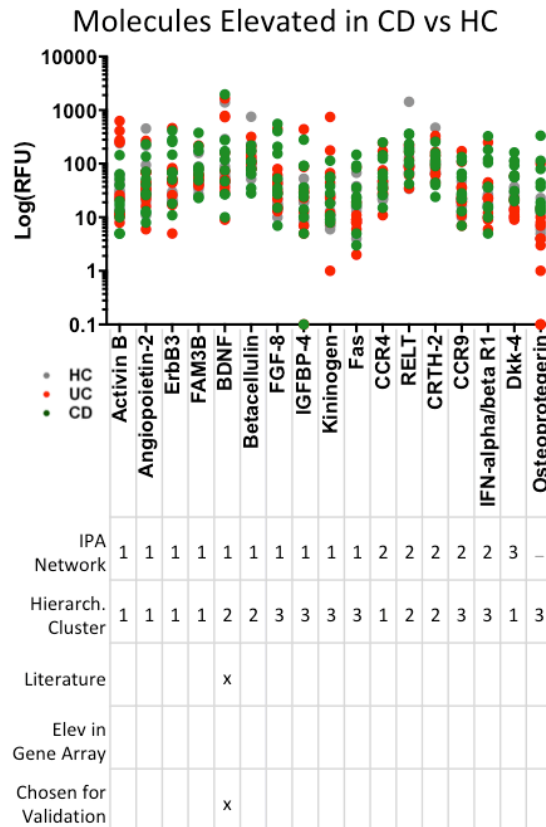


Figure 28: Of the 17 proteins elevated in CD vs HC on the antibody array, BDNF was the only protein with an average RFU >200 and was chosen for ELISA validation.

Of the 1000 proteins screened on the antibody array, 104 proteins were found to be elevated in the stools of ulcerative colitis patients versus healthy controls as seen in the volcano plot and heatmap in Figure 29.

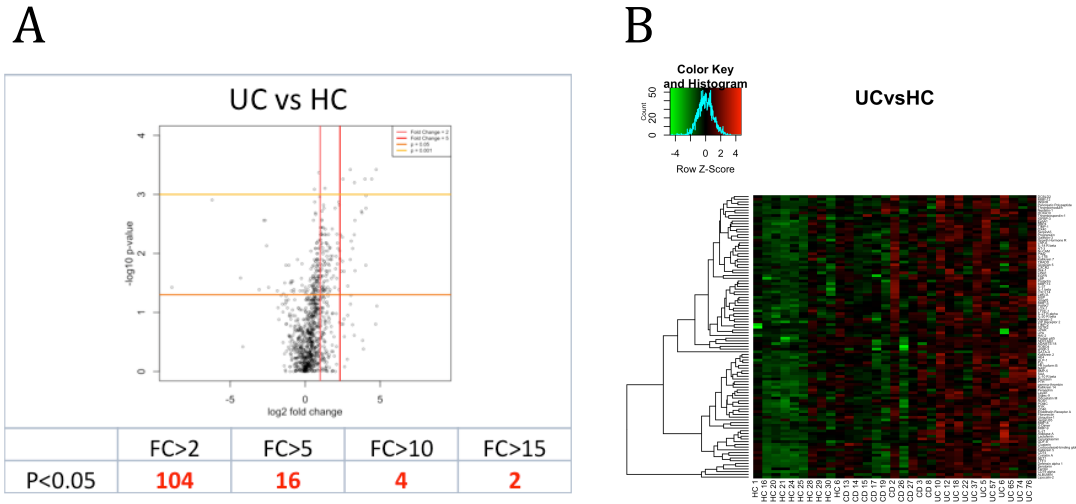


Figure 29: The antibody array-based screen of 1000 human proteins in pediatric and healthy control stool extract showed up-regulation of 104 proteins with FC > 2, P < 0.05 that were elevated in ulcerative colitis patients versus healthy controls (A) visualized on a heatmap (B).

Integrated Pathway Analysis of these 104 proteins elevated in ulcerative colitis showed nine networks. The top network related to post-translational modification, protein degradation, and protein synthesis is shown in Figure 30.

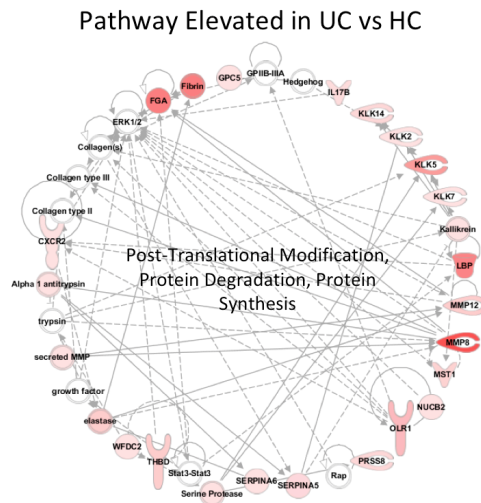


Figure 30 IPA of the 104 proteins elevated in ulcerative colitis stools when compared to healthy controls.

Hierarchical clustering of these 104 proteins into eight groups is shown in Figure 31.

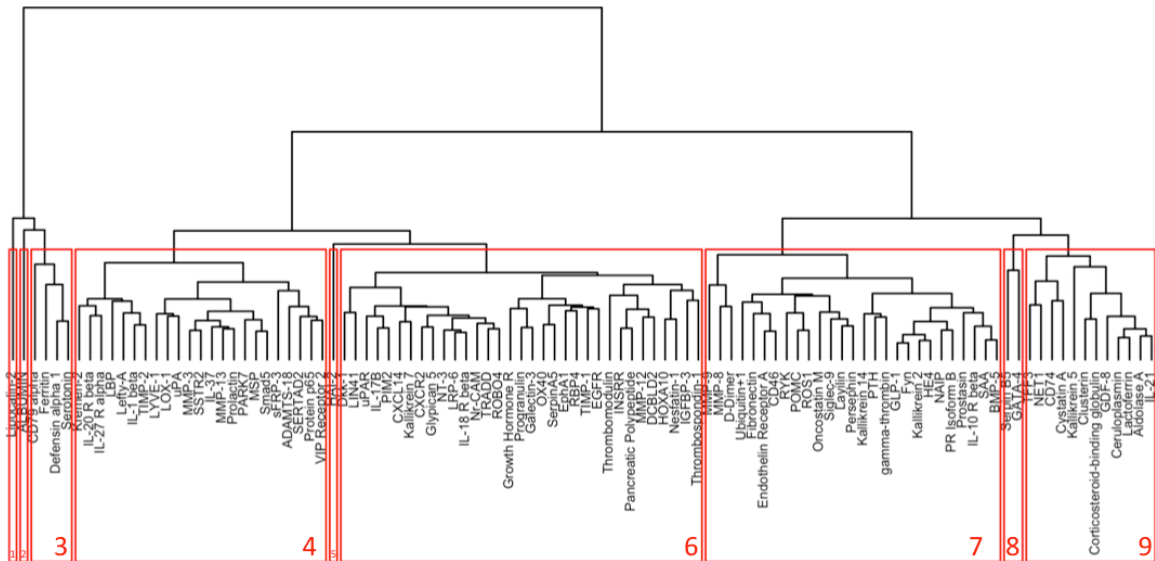


Figure 31: Unsupervised hierarchical clustering of the 104 protein elevated in ulcerative colitis stools versus healthy controls.

Of the 104 proteins elevated in the stools of ulcerative colitis patients when compared to healthy controls, Lipocalin-2, MMP-9, Thrombomodulin, Growth Hormone R, LTF, and uPA was also elevated on the gene mucosa array conducted at Emory University. Of the 104 proteins elevated in the stools of ulcerative colitis patients versus healthy controls, 21 had RFU values on the antibody array greater than 200 RFU. Of these 12 were chosen for ELISA validation as summarized in Figure 32.

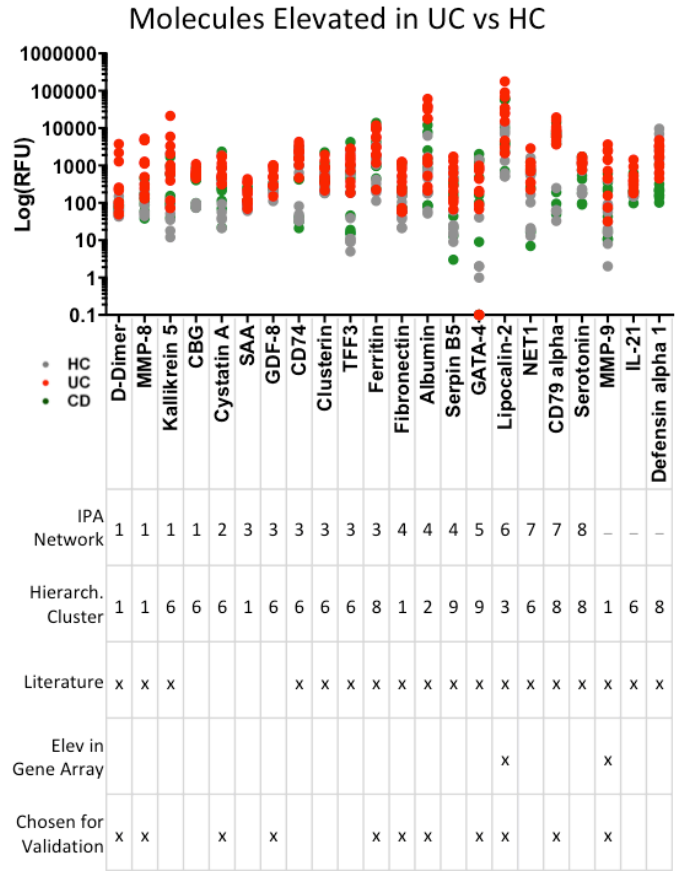


Figure 32: Of the 104 proteins elevated in UC vs HC on the antibody array, the 21 proteins visualized had an average RFU >200 and 12 were chosen for ELISA validation.

When looking at proteins that were dysregulated among ulcerative colitis and Crohn’s disease, 36 proteins were elevated in ulcerative colitis stool when compared to Crohn’s disease with FC >2, 8 with FC > 5 and 1 with FC >15 as seen in the volcano plot and heatmap in Figure 33.

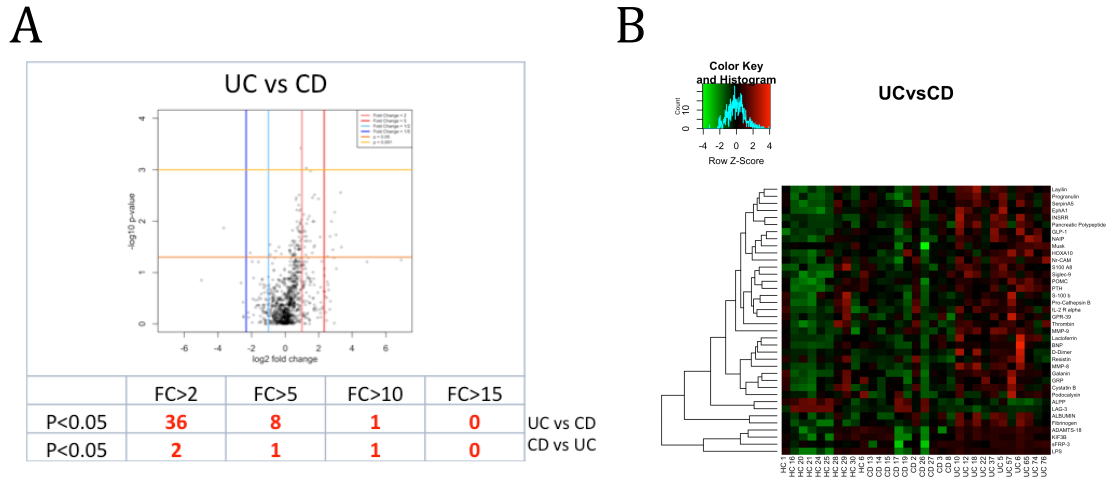


Figure 33: The antibody array-based screen of 1000 proteins in pediatric and healthy control stool showed up-regulation of 38 proteins with FC > 2, P < 0.05 that were dysregulated between ulcerative colitis patients versus Crohn's disease patients (A) visualized on a heatmap (B).

For proteins elevated in Crohn's disease when compared to ulcerative colitis, only two proteins were elevated with FC > 2.

Integrated Pathway analysis of these 38 total dysregulated proteins among ulcerative colitis and Crohn's disease showed five pathways and the pathway relating to cell-to-cell signaling and interaction, cellular movement, hematological system development and function as illustrated in Figure 34.

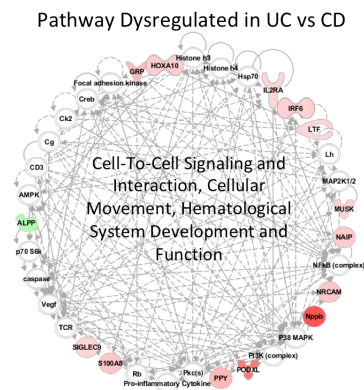


Figure 34: IPA of the 38 dysregulated proteins between Crohn's disease and ulcerative colitis stool. Hierarchical clustering of these 38 proteins into five groups is shown in

Figure 35.

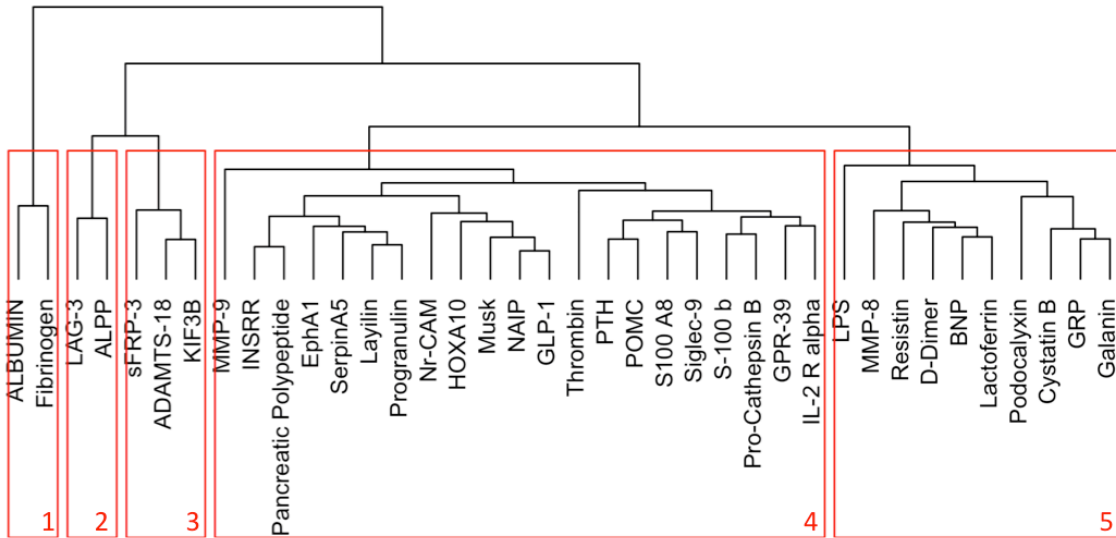


Figure 35: Unsupervised hierarchical clustering of the 38 proteins dysregulated in Crohn’s disease and ulcerative colitis stools.

Of the 38 proteins dysregulated in the stools of Crohn’s disease and ulcerative colitis patients, LTF, S100A8, and MMP-9 was also elevated on the gene mucosa array conducted at Emory University. Of the 38 proteins dysregulated in the stools of Crohn’s disease and ulcerative colitis patients, 12 had values on the antibody array greater than 200 RFU. Of these 7 were chosen for ELISA validation as summarized in Figure 36.

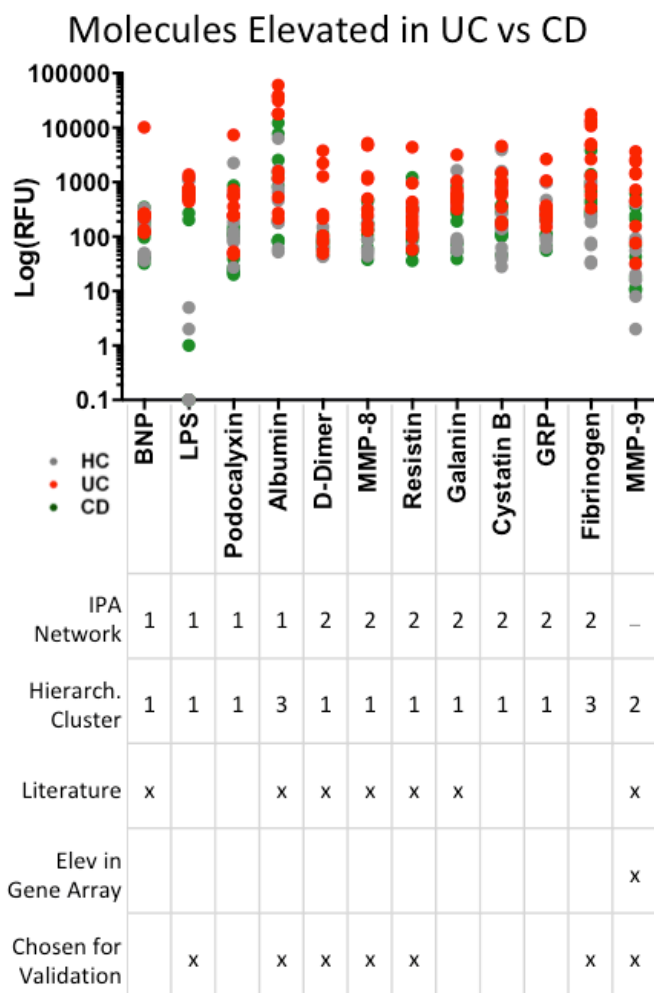


Figure 36: Of the 38 dysregulated proteins between UC and CD on the antibody array, the 12 visualized proteins had average RFU > 200 and 7 were chosen for ELISA validation.

In summary, the antibody-based screen of 1000 human proteins identified 71 proteins elevated in the stool of inflammatory bowel disease patients versus healthy controls and 13 were chosen for ELISA validation. 17 proteins were elevated in the stool of Crohn’s disease patients and one was chosen for ELISA validation. 104 proteins were elevated in the stool of ulcerative colitis patients when compared to healthy controls and 12 were chosen for ELISA validation. 38 proteins were dysregulated between Crohn’s disease and ulcerative colitis and 7 molecules were chosen for ELISA validation. In total 17 unique proteins were chosen from the antibody array for ELISA validation.

Validation of biomarkers for pediatric IBD stool by ELISA

Among the 26 molecules selected for validation from the aptamer-based screen and the 17 molecules selected from the antibody array, a total of 33 unique molecules were selected for ELISA validation from both screens. Of these 33 molecules, only 23 molecules could be detected in stool samples with a sample dilution of at least 1:2. ELISAs were not conducted on neat stool samples to prevent excessive interference of the stool and extraction buffer on the assay binding capabilities. With the SOMAscan's use of aptamers and final DNA hybridization, the detection limit and sensitivity is quite lower than detection by ELISA. Similarly, for the antibody array, the fluorescent detection mechanism is far more sensitive than the colorimetric reading of ELISA. For these reasons as well as the unconventional sample type of stool, not all ELISAs may be able to detect proteins in the stool that were detectable by the aptamer screen and antibody array.

These 23 molecules were assayed for on a pilot set of 30 stool samples from 15 Crohn's disease patients, 5 ulcerative colitis patients, and 10 healthy controls. All validation data was normalized by the ratio of stool weight to volume of protein extract collected during the extraction process. Descriptive statistics of this data as well as the effect of normalization by stool weight can be found in Appendix A.

Of the 23 molecules, nine were elevated in the stools of both patients with Crohn's disease and ulcerative colitis as visualized in Figure 37 and summarized in Table 6.

Biomarkers of IBD

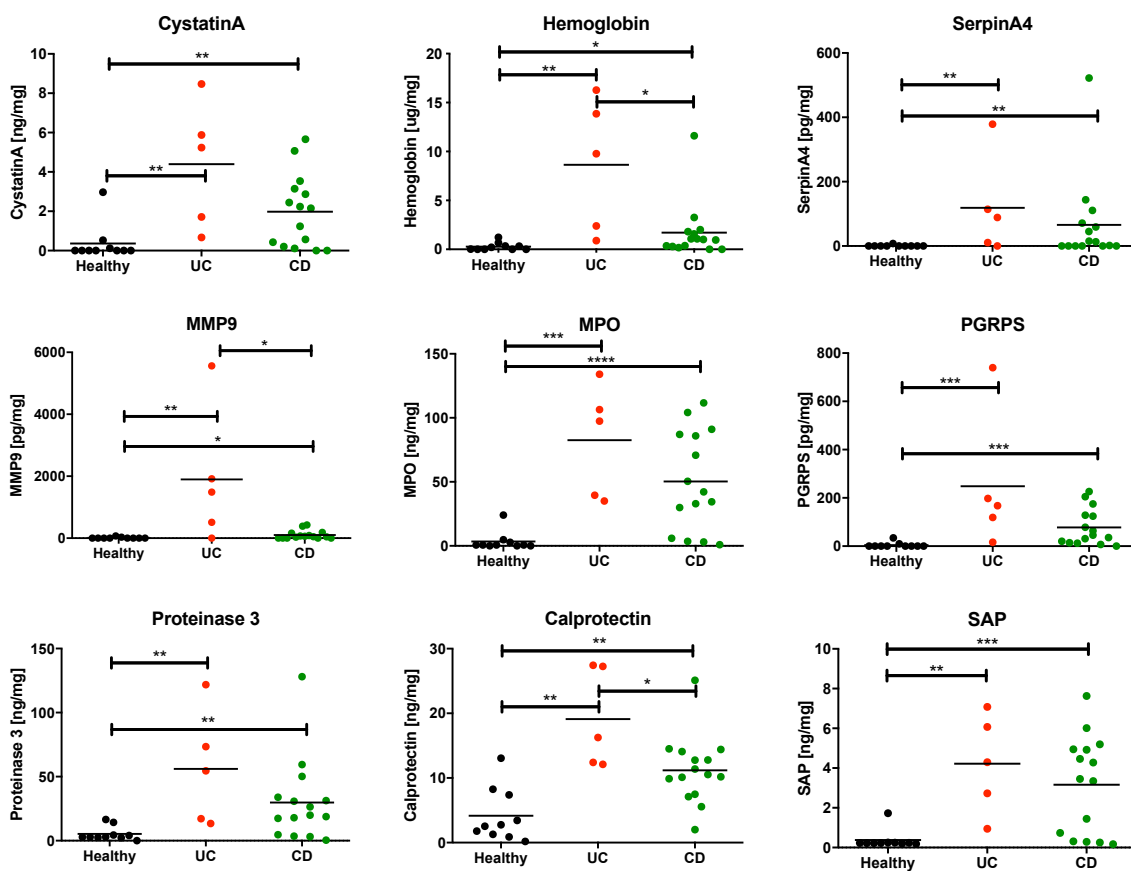


Figure 37: Of the 23 molecules validated by ELISA, 9 molecules were found to be elevated in both CD and UC vs HC. Of these, 3 were also significantly different between CD and UC stools. Descriptive statistics can be found in Appendix A. $P \leq 0.05$, $**P \leq 0.01$, $***P \leq 0.001$, $****P \leq 0.0001$

Table 6: Summary of the proteins elevated in both CD and UC in the ELISA validation. *P ≤ 0.05, **P ≤ 0.01, *P ≤ 0.001, ****P ≤ 0.0001.**

Protein	Fold Change		
	CDvsHC	UCvsHC	UCvsCD
Cystatin A	5.46**	12.13**	2.22
Hemoglobin	6.13*	31.00**	5.06*
SerpinA4	87.20**	157.68**	1.81
MMP-9	9.25*	174.10**	18.82*
MPO	14.61****	23.98***	1.64
PGRPS	17.78***	56.70***	3.19
Proteinase 3	5.63**	10.61**	1.88
Calprotectin	2.69**	4.59**	1.71*
SAP	8.42***	11.25**	1.34

Among these, three molecules, hemoglobin, MMP-9, and calprotectin, were also significantly elevated in the stools of ulcerative colitis patients when compared to Crohn's. None of these proteins were found to be elevated in Crohn's disease versus ulcerative colitis stool.

ROC analysis of these molecules to distinguish IBD from HC as seen in Figure 38 showed these nine molecules to have AUCs of greater than 0.79, with MPO having the highest distinguishing power with an AUC of 0.96.

Biomarkers of IBD

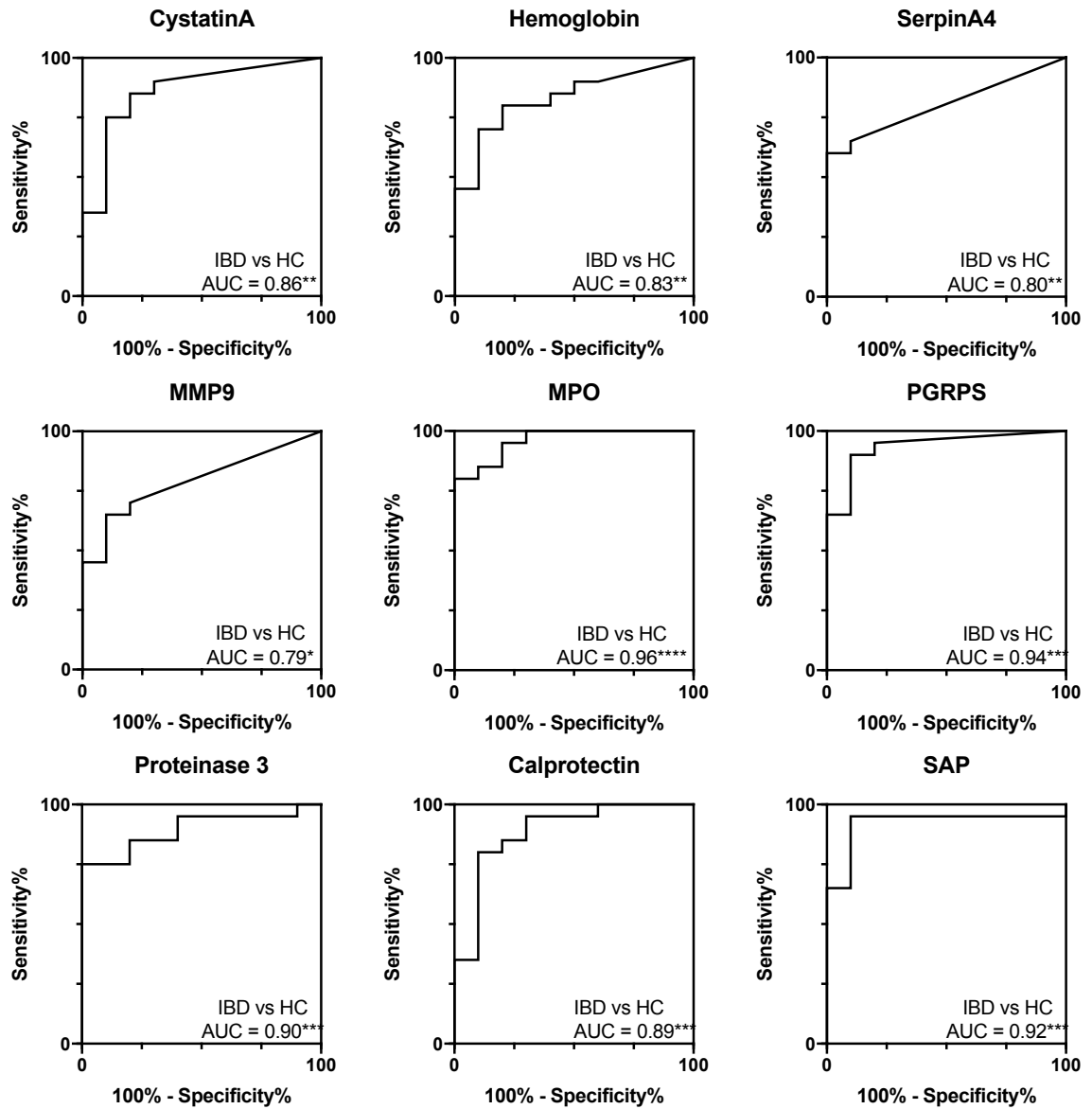


Figure 38: ROC analysis of the nine biomarkers for IBD.

Many of these molecules have been already implicated in IBD, but some have been the first finding of these molecules in pediatric IBD stool.

Cystatin A is an intracellular proteinase inhibitor and is involved in cell adhesion and plays a role in epidermal development and maintenance [66]. In this work, Cystatin A was found to be elevated more than 5-fold in CD stool and more

than 12-fold in UC stool when compared to HC stool. A DNA microarray on inflamed colonic tissue has found a 3-fold increase of Cystatin A in CD but not UC when compared to controls [67]. Although no additional literature could be found tying Cystatin A to IBD, expression of Cystatin A has is increased in psoriatic skin [68] and other inflammatory skin conditions [69]. While testing for Cystatin A in additional samples can help understand its capability in diagnosing pediatric IBD, implications of Cystatin A in the inflamed intestinal mucosa and other inflammatory skin conditions supports the relevance of Cystatin A in IBD.

Hemoglobin, the oxygen transport protein in red blood cells, has been found to be elevated in both CD and UC stools when compared to HC, 6 and 31-fold respectively, with an increase in UC stool when compared to CD stool by 5-fold. In literature, fecal hemoglobin has been used adjacent to fecal calprotectin in the prediction of active inflammation confirmed by colonoscopy [33]. Hemoglobin has also been studied as a prognostic biomarker for Crohn's disease where low blood hemoglobin was shown to be a predictor of a shorter time to occurrence of an initial complication or CD-related surgery [70]. As hemoglobin may be a product of inflammation and ulcers due to IBD, it may be a non-specific marker of IBD but a direct and obvious marker of uncontrolled intestinal inflammation and ulcers.

Serpin A4 or Kallistatin is another proteinase inhibitor specific for the inhibition of tissue kallikrein. In this work, Kallistatin was found to be elevated more than 85-fold in CD and 150-fold in UC when compared to HC stool. Although no implication of Kallistatin in IBD stool has been prior to this study, Kallistatin was found to be decreased in the plasma of patients with active IBD when compared to

normal controls and decreased in inflamed intestinal IBD tissue when compared to non-inflammatory controls [71]. Contrastingly, Kallistatin along with kallikrein was seen to have higher reactivity in interstitial space of IBD patients' intestinal biopsies versus controls and the increase of Kallistatin activity was correlated with the degree of tissue inflammation [72]. Although the concentration of Kallistatin shows to be decreased in inflamed IBD tissue, the increase of the molecule in the intestinal extracellular space may allow for the release of the molecule into the stool. As the molecule has been seen as a marker for intestinal inflammation, Kallistatin may be nonspecific for IBD and additional studies are warranted for the implication of Kallistatin in other gastrointestinal diseases.

MMP-9 is a matrix metalloproteinase that plays an important role in the breakdown of extracellular matrix in normal but also disease processes [66]. In this study, MMP-9 was seen to be elevated in the stools of both CD and UC patients, 9 and 174-fold, when compared to HC. Fecal MMP-9 was also seen to be elevated more than 18-fold in UC versus CD patients. MMP-9 has been seen to be elevated in the stool of UC patients with correlation to disease and endoscopic scores [34]. As studies have shown that fecal MMP-9 is a better biomarker for UC [35], [36], this study also shows an increase of MMP-9 in both CD and UC patients with greater elevation in UC patients. In addition to fecal MMP-9, mucosal and serum MMP-9 expression and protein levels have been seen to be significantly higher in UC patients compared to controls where these levels corresponded to the severity of the disease [73]. MMP-9 has also been implicated in leukocyte migration whereas in IBD, intestinal inflammation in both UC and CD is caused by increase leukocyte

recruitment from the circulation [74] and leukocyte trafficking has been researched as an interesting target for IBD therapy [75], [76]. Although MMP-9 has been implicated in many other inflammatory conditions [77]–[81], fecal MMP-9 has shown to be a specific marker for active inflammation, especially for ulcerative colitis.

Myeloperoxidase, or MPO, is a component of neutrophil granules in part of the host defense system that has been implicated in many cardiovascular, neurological, and inflammatory diseases [82]. In this study, MPO was elevated about 14-fold in CD and 24-fold in UC stool when compares to healthy controls. In literature, fecal MPO levels are increased in active IBD patients and correlated with laboratory parameters and endoscopic grades of inflammation [37]. These levels have also been seen to decrease with the alleviation of active disease. Anti-neutrophil cytoplasmic antibodies, a type of autoantibody implicated in IBD pathogenesis, have shown reactivity to MPO in 14% of UC patients in a small cohort [83]. MPO has also been used as an index of intestinal inflammation in DSS-induced models of IBD [84]. As MPO has already been implicated in the stool of active IBD patients, with the expansion of sample number, its use in the diagnosis of pediatric IBD can further be elucidated.

PGRPS, peptidoglycan recognition protein 1, plays a role in innate immunity by recognizing and acting on gram-positive bacteria. In this work, fecal PGRPS was increased in 17-fold in CD and 57-fold in UC when compared to HC. In normal humans, PGRPs protect the host from inflammation, tissue damage and colitis [85], but polymorphisms in peptidoglycan recognition protein genes have been

associated with CD and UC and may provide insight into the genetic mechanism of pathogenesis in IBD [86]. PGRPS has recently been implicated in lymphocyte migration [87], which is of previously stated relevance to IBD [74]–[76]. Although PGRPS has not been studied in intestinal mucosa and stool of IBD, its relevance to intestinal immunity and genetic susceptibility in IBD warrants further research for its pathological and diagnostic implication in IBD.

Proteinase 3 is a protease that degrades collagen and like MPO is a component of neutrophil granules [88]. In this work fecal proteinase 3 has been seen to be elevated 5-fold in CD and 10-fold in UC patients when compared to controls. Although expression of proteinase 3 has not been studied in IBD, the anti-neutrophil cytoplasmic antibodies indicative of IBD have also been shown to show reactivity to proteinase 3 [83] especially in active UC [89]. As the autoantibodies to proteinase 3 show diagnostic promise in UC diagnosis, evaluation of proteinase 3 as a marker itself holds potential.

Calprotectin, the complex of S100 calcium binding proteins A8/A9, is the current gold standard of fecal IBD diagnosis [22]. In this work, calprotectin is seen to be elevated almost 3-fold in CD and 5-fold in UC patients when compared to controls. In literature, fecal calprotectin is seen as an accurate marker of IBD in both children and adult patients [90], correlates with disease activity and mucosal healing [26], and may be helpful in predicting impending clinical relapse [91]. Although the literature has not seen a significant difference in fecal calprotectin levels between CD and UC, this work has seen a slight elevation of calprotectin in UC patients when compared to CD patients by 1.7-fold. Pathogenic relevance of

calprotectin is seen with the molecule by inflammatory neutrophils promoting apoptosis in the surrounding areas [92]. In a colitis-associated colon cancer mouse model, S100A8/A9 expression on cells is essential for the development of colon tumors [93]. Although calprotectin has been seen to be a very promising biomarker of IBD, it cannot distinguish between CD and UC. Elevation of this marker in this work shows the alignment of the current results with literature.

Serum amyloid P component, or SAP, is the serum form of the amyloid p component that forms amyloid deposits. This protein is implicated in amyloidosis diseases including Creutzfeldt–Jakob disease and Alzheimer’s disease [94] where it has also been targeted for therapy. In this work, SAP has been found to be elevated in both UC and CD patients 8 and 11-fold respectively. Although this form of amyloid has not extensively researched in IBD, amyloidosis can be a rare and deadly complication of IBD, especially in CD often resulting in renal failure [95]–[99]. Further research of the diagnostic capability of SAP is warranted especially as a prognostic predictor of amyloidosis complications.

One of the validated proteins, alkaline phosphatase, was elevated in stools of only Crohn’s disease patients when compared to healthy controls, but not in the stools of ulcerative colitis patients when compared to healthy controls as visualized in Figure 39A and Table 7.

Biomarker of CD

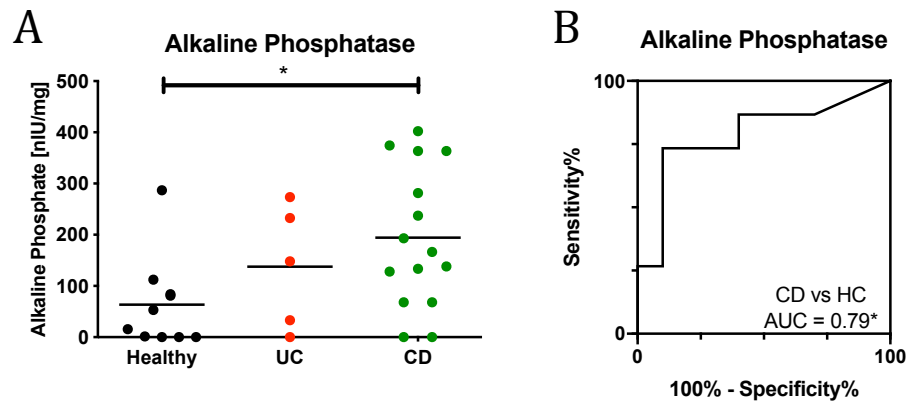


Figure 39: Of the 23 molecules validated by ELISA, one molecule was found to be elevated in CD vs HC. Additional descriptive statistics can be found in Appendix A. *P ≤ 0.05, (A). ROC curve analysis of alkaline phosphatase (B).

Table 7: Summary of the proteins elevated in CD vs HC in the ELISA validation. *P ≤ 0.05.

Protein	Fold Change		
	CDvsHC	UCvsHC	UCvsCD
Alkaline Phosphatase	3.06*	2.17	0.71

ROC analysis of alkaline phosphatase showed an AUC of 0.79 (Figure 39B) showing good diagnostic ability of alkaline phosphatase to differentiate CD from HC.

Alkaline phosphatase is an enzyme with four different isotypes: placental, germ cell, intestinal and tissue non-specific (liver, bone, kidney). Tissue non-specific alkaline phosphatase is a membrane-bound enzyme expressed throughout the body with high concentrations in blood. Intestinal alkaline phosphatase is involved in the gut mucosal defense system. In this work, tissue non-specific alkaline phosphatase has been found to be elevated 3-fold in the stools of CD patients when compared to HC and a statistically insignificant elevation in UC stools when compared to HC while intestinal alkaline phosphatase has not been assayed. In literature, an increase in tissue non-specific alkaline phosphatase expression was observed in the intestines of in experimental colitis animal models and treatment with the tissue

non-specific alkaline phosphatase inhibitor resulted in increased protection from colonic inflammation [100]. Oxidative stress may have a play in the pathological implication of tissue non-specific alkaline phosphatase as increased activity of alkaline phosphatase is seen in intestinal inflammation and the addition of oxidative stress causes a shift in the isotope of alkaline phosphatase from liver to either kidney or bone type [101]. Interestingly, the loss of intestinal alkaline phosphatase expression is associated with increased inflammation [102], [103] and the administration of intestinal alkaline phosphatase in the intestines reduces inflammation in DSS-colitis induced models of IBD [104], [105] and humans [106]. Although the exact pathological implication of tissue non-specific alkaline phosphatase has not been elucidated in literature, increased levels of the molecule in stool have a basis on intestinal inflammation as well as blood leakage from colonic ulcers. Expansion of sample number will allow for the distinguishing of alkaline phosphatase as a marker for CD or IBD in general as much concentrations of alkaline phosphatase are in similar ranges in CD and UC but are not statistically significant with the small sample number in UC.

For biomarkers of ulcerative colitis, eight molecules were elevated in the stools of ulcerative colitis patients when compared to healthy controls but not in the stools of Crohn's disease patients when compared to healthy controls as visualized and summarized in Figure 40 and Table 8.

Candidate Biomarkers of UC

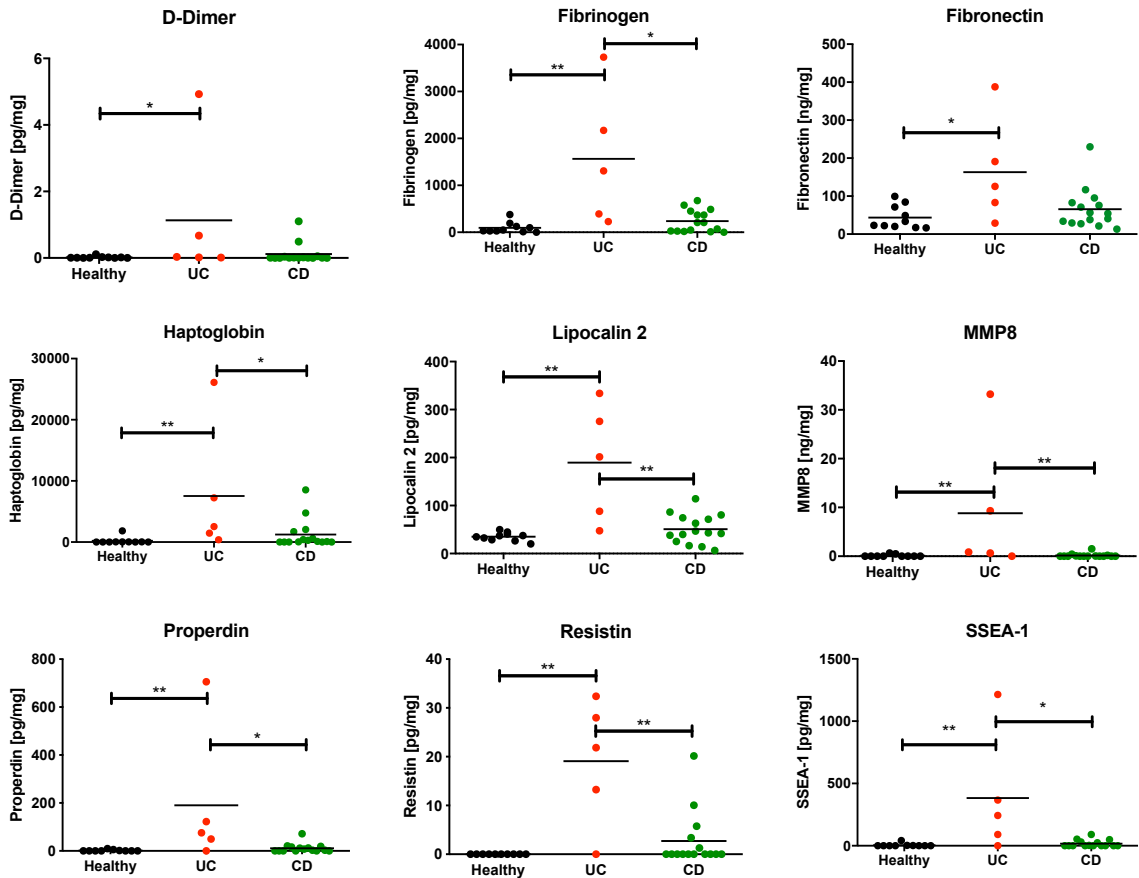


Figure 40: Of the 23 molecules validated by ELISA, 8 molecules were found to be elevated in UC vs HC. Of these, 7 were also significantly different between CD and UC stools. Additional descriptive statistics can be found in Appendix A. $P \leq 0.05$, $**P \leq 0.01$, $***P \leq 0.001$, $****P \leq 0.0001$

Table 8: Summary of the proteins elevated in UC vs HC in the ELISA validation. $*P \leq 0.05$, $**P \leq 0.01$, $***P \leq 0.001$, $****P \leq 0.0001$, $>>FC$ could not be calculated as mean of healthy population was 0.

Protein	Fold Change		
	CDvsHC	UCvsHC	UCvsCD
D-Dimer	5.99	57.85*	9.66
Fibrinogen	2.50	16.55**	6.62*
Fibronectin	1.50	3.74*	2.48
Haptoglobin	6.07	36.89**	6.08*
Lipocalin 2	1.44	5.37**	3.72**
MMP 8	1.34	78.25**	58.26**
Properdin	6.62	114.08**	17.24*
Resistin	>>	>>**	7.05**
SSEA-1	3.61	82.12**	22.75*

Among these, seven molecules (fibrinogen, haptoglobin, lipocalin 2, MMP-8, properdin, resistin, SSEA-1) were also elevated in the stools of ulcerative colitis patients when compared to Crohn's disease patients. ROC analysis of these molecules (Figure 41) showed all AUCs of greater than 0.84 with fibrinogen and lipocalin 2 showing the best diagnostic capability differentiating UC from HC with AUC of 0.98.

Candidate Biomarkers of UC

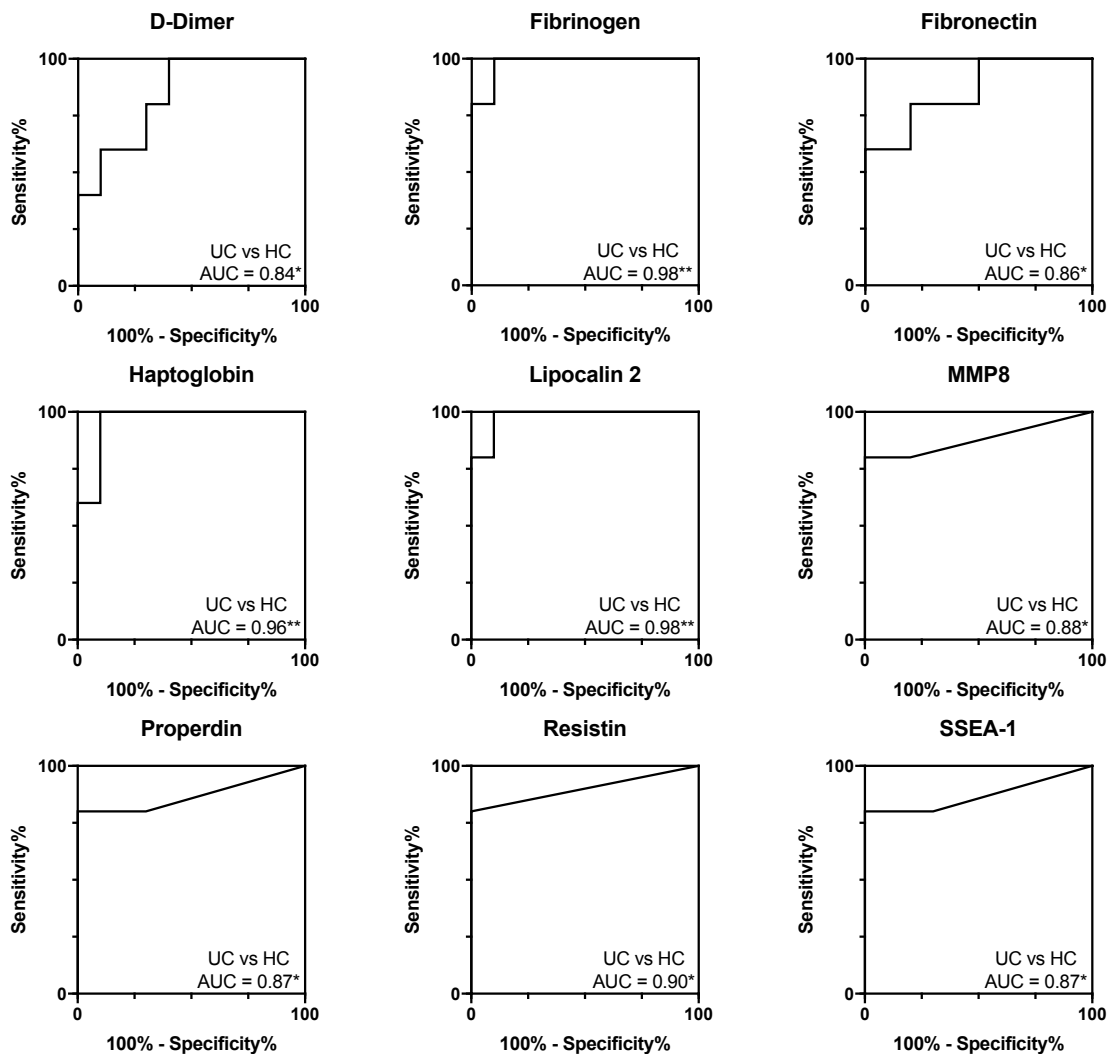


Figure 41: ROC analysis of biomarkers of UC.

Many of the molecules found in UC stool are part of blood clotting and degradation pathways that may be sourced from colonic ulcers or blood leakage into the stool.

D-dimer is a fibrin degradation product as remains as a result of blood clot degeneration. In this study, d-dimer was seen to be elevated in the stools of UC patients by more than 50-fold when compared to HC and elevation but not statistically significant in the stools of CD versus HC and UC versus CD. In IBD, some studies have shown blood d-dimer levels have been seen to be increased in ulcerative colitis patients when compared to CD, HC, and other gastrointestinal controls [107], while others have stated blood d-dimer levels to be insignificantly different between CD and UC [108]. In either case, high levels of d-dimer may have a link to the increased thromboembolic tendency seen in IBD [109]. Although this work is first to detect d-dimer in pediatric IBD stool, studies on the efficacy of d-dimer as a diagnostic biomarker for IBD as well as a prognostic indicator of thromboembolic complications are warranted.

Fibrinogen is a precursor molecule to the fibrin and thrombin that are the basis of blood clotting. Fibrinogen acts by occluding blood vessels and thereby stops excessive bleeding. In this work, fibrinogen was seen to be elevated 16-fold in UC patients when compared to HC and 6-fold when compared to CD patients. CD patients did show a slight 2-fold increase of fibrinogen in their stools when compared to HC, but the elevation was not statistically significant in this pilot sample cohort. In literature, fibrinogen was found to be elevated in the blood of IBD patients [110], [111] with correlations to clinical parameters in CD [112]. Although this is the primary study showing fibrinogen levels in IBD stools, research in fibrinogen as a blood-based biomarker for IBD warrants its additional research as a noninvasive stool marker.

Fibronectin is a part of the extracellular matrix that binds to receptor integrins and also has a soluble form, which is a major component of blood plasma [113]. In this work, stool fibronectin levels were seen to be increased more than 3-fold in UC patients when compared to healthy controls. A moderate but statistically insignificant elevation was seen in the stool of CD patients versus HC and UC versus CD patients. In literature, cytokines have been shown to affect various fibronectin isoforms modulating the migration of fibroblast cells in CD mucosa [114]. In addition fibronectin deposits are increased in the submucosa of IBD patients [115] with the effect of the extracellular matrix composition being altered in IBD [116]. Although additional studies are warranted for the specificity of fibronectin in UC and CD, fibronectin could be implicated in the immune cell recruitment and adhesion in the intestinal endothelium.

Haptoglobin is a protein that binds to free hemoglobin released from red blood cells allowing for the safe removal of hemoglobin from the body system. In this work, stool haptoglobin was increased in UC patients by more than 35-fold with moderate but insignificant increases in CD versus HC and UC versus CD. In literature polymorphisms in the HP1 and HP2 allele is seen to be more common in autoimmune diseases including CD and UC [117]–[120]. Although additional implications of the haptoglobin protein in IBD was not found and increases UC in this work may be the effect of an outlier in the small sample size, the inclusion of additional samples will better elucidate haptoglobin's diagnostic capability in IBD.

Lipocalin 2, also known as neutrophil gelatinase-associated lipocalin (NGAL), is an iron-binding protein involved in many processes including apoptosis, innate

immunity and renal development [121]. In this work lipocalin 2 was elevated more than 5-fold in UC when compared to HC and 3-fold when compared to CD. Fecal lipocalin has been studied in literature to be a noninvasive biomarker of intestinal inflammation in a DSS-induced colitis mouse model [38] and increases of lipocalin 2 have been seen in stool and rectal dialysate of patients with increasing UC activity [39]. Serum lipocalin-2 levels are also seen to be elevated IBD patients when compared to controls [122]. Whereas no difference was found between CD and UC patients, serum lipocalin 2 was able to distinguish active from inactive IBD [123], [124]. As lipocalin 2 has been implicated in other inflammatory immune diseases, its presence in literature corroborates this work's finding of elevated lipocalin 2 in UC stool.

MMP-8 is another matrix metalloproteinase that cleaves certain types of collagen in the extracellular matrix. In this work, MMP-8 was elevated in the stools of UC patients when compared to HC and CD patients by more than 78 and 58-fold. In literature, MMP-8 expression is seen to be elevated in the intestines of DSS-induced colitis mouse models [125] and IBD patients [126]. Serum levels of MMP-8 have also been seen to be increased in pediatric IBD patients but do not reflect disease activity during glucocorticoid treatment [127]. Genetic variants of MMP-8 have been associated with the susceptibility and outcome of UC [128]. Although intestinal and serum expression of MMP-8 has been studied in literature, this is the first study showing fecal levels of MMP-8 in UC patients. With the expansion of sample number and longitudinal studies, the diagnostic efficacy of MMP-8 can be

further elucidated as has been done with other matrix metallopeptidases in relation to IBD.

Properdin is a positive regulator of the alternate pathway of the complement system facilitating an immune response and tissue inflammation. In this work, stool properdin was elevated more than 114-fold in UC patients when compared to HC and more than 17-fold when compared to CD. Although levels of intestinal and fecal properdin have not been studied in IBD subjects, animal studies have shown properdin to have a protective effect in intestinal inflammation [129], [130]. IL10 knockout and IL-10/properdin double knockout mouse models of IBD have shown activation of the complement system in the IL10 knockout and the genetic suppression of properdin exacerbated the colonic injury [130]. Disruptions of the alternative pathway of the complement system have been seen in IBD with decreased levels of serum properdin in IBD patients [131]. As the implication of properdin and the alternative pathway of the complement system has been made in relation to IBD, further studies into the diagnostic capability of properdin by the expansion of sample numbers and the inclusion of patients with increasing disease activity continue to be warranted.

Resistin is a hormone that has been controversially implicated in insulin resistance and has also been connected to inflammation and energy homeostasis [132]–[134]. In this work, resistin was not detected in the stools of healthy patients and elevations of fecal resistin was seen in UC patients when compared to HC and CD. Some elevation of resistin was also seen in CD stools when compared to healthy controls, but the increase was not statistically significant. In literature, resistin was

increased in the serum of IBD patients [135]–[137], with the administration of therapy causing a reduction in serum resistin levels [138]. Although resistin has been implicated in IBD, this is the first study showing resistin elevation in IBD stools. Further expansion of sample number of IBD patients with varying disease activity will help elucidate resistin's ability as a biomarker for UC and IBD.

SSEA-1, or Fut4, is an enzyme involved in protein glycosylation. In this work, SSEA-1 was seen to be elevated more than 80 fold in the stool of UC patients when compared to HC and 22-fold when compared to CD stool. In literature, the expression of SSEA-1 was increased in UC peripheral blood mononuclear cells [139], [140]. Soluble levels of SSEA-1 have not been elucidated in IBD, though an increase in SSEA-1 is seen in colon cancer tissue causing the glycosylation of beta-haptoglobin [141]. Further research of SSEA-1 in IBD is warranted with expanded sample number and further investigation in the pathological relevance of SSEA-1 in IBD, especially UC.

Of these 19 candidate stool biomarkers for IBD, CD, and UC, 10 biomarkers also were significantly different between the stools of CD and UC populations. ROC analysis of these molecules in Figure 42 showed AUCs greater than 0.82 with the lipocalin 2 having the highest distinguishing power between UC and CD and AUC of 0.91.

Biomarkers Distinguishing UC from CD

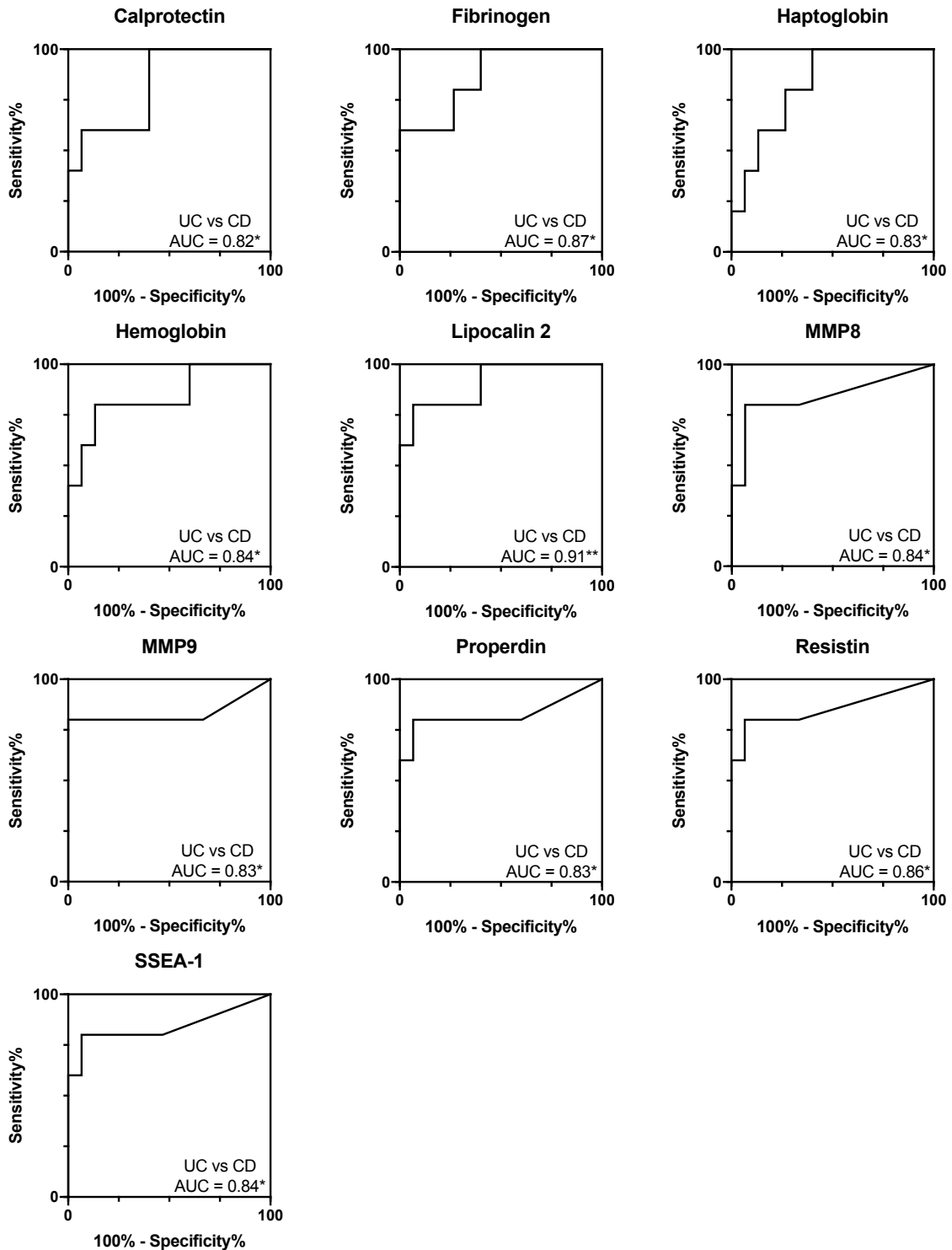


Figure 42: ROC analysis of the ten molecules distinguishing UC from CD.

Five proteins of the 23 molecules validated by ELISA did not reach statistical significance as visualized in Figure 43.

Additional ELISA Validated Proteins in IBD Stool

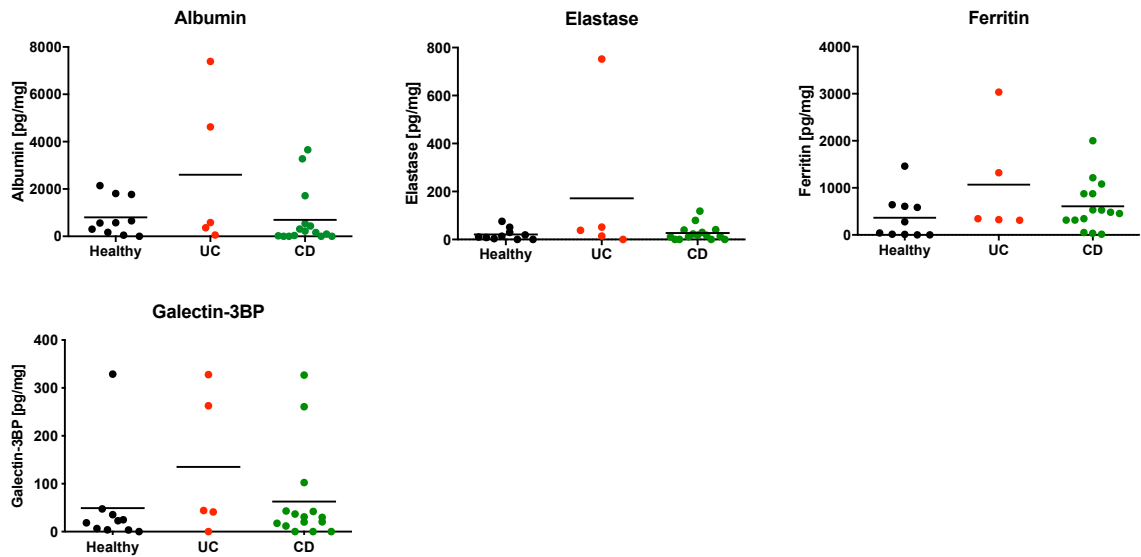


Figure 43: Of the 23 proteins validated by ELISA, five proteins did not reach statistical significance. Although D-Dimer was not statistically significant before stool weight and extract normalization, after normalization it was found to be elevated in ulcerative colitis patients stool when compared to healthy controls. Of these proteins that did not reach significance, all five molecules seem to be elevated in UC vs CD without statistical significance. With a small UC population of only five subjects in this study, expansion of sample number will better determine these marker's diagnostic abilities. Interestingly, some of these molecules have already been implicated in IBD.

Albumin is a globular protein that is a major component of blood that regulates osmotic pressure and binds many ions, hormones, and pharmaceuticals. In this work, albumin was increased in the stool of two UC patients. In literature, low blood albumin levels at diagnosis have been seen as a prognostic marker to predict the clinical course of UC [142]. In a piglet animal model of colitis, albumin synthesis was seen to be increased as a result of colonic inflammation while levels of albumin are decreased point to the loss of albumin during colitis [143].

Elastase is a protease that breaks down elastin, a component of connective tissue. In this study, elastase was increased in the stool of one UC patient. Interestingly fecal elastase levels were increased in a mouse model gut wall injury [40] and were able to distinguish IBD from IBS in human stool samples [41] with correlation of the levels of elastase to active disease [41], [42]. As the sample number of UC patients in this initial pilot cohort is small and the indication of clinical activity is not given, literature still provides hope in the use of elastase in the noninvasive diagnosis of IBD.

Ferritin is an intracellular protein used for the storage and controlled release of iron. In this study, stool ferritin levels were increased in one UC patient with an overlap of stool ferritin concentrations between UC, CD, and HC. Although implications of ferritin are not widely seen in the pathology of IBD, one study has shown serum ferritin levels to be indicative of iron-deficiency in chronic IBD [144].

Galectin-3BP is a binding protein that aids in modulating cell-cell and cell-matrix interactions. In this work, galectin-3BP was elevated in two UC, two CD, and one HC. Galectin-3BP has not been implicated in IBD literature.

Additional descriptive statistics of all validation data as well as the effect of normalization by stool weight can be found in Appendix A.

Correlation of SOMAscan validated proteins

For the 18 proteins validated from the aptamer-based SOMAscan screen, the relative fluorescence intensity of the SOMAscan signal was compared to their ELISA concentrations as seen in Figure 44.

ELISA Validation of SOMAscan Molecules

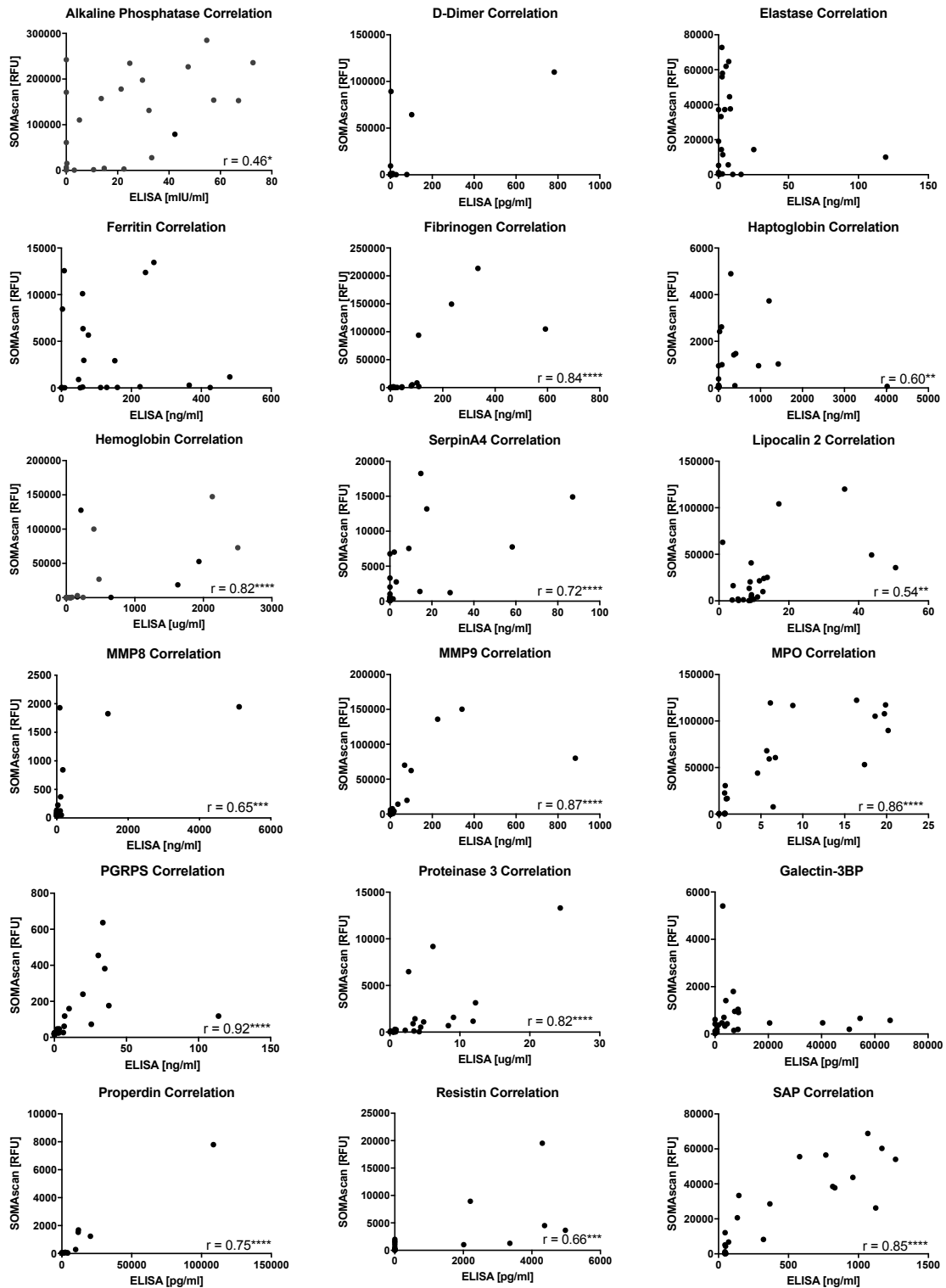


Figure 44: Of the 18 proteins validated from the aptamer screen, 14 had positive correlation to ELISA.

14 of the 18 proteins had a strong positive correlation between their screening fluorescence intensity to their ELISA concentrations (Spearman $R > 0.5$, $P < 0.05$) while 5 did not correlate as well. With more than 75% of the molecules validated by ELISA correlating to the SOMAscan, the use of SOMAscan for the detection of stool proteins can be further corroborated. SOMAscan's high sensitivity of protein detection can hinder applications of biomarkers discovered by the scan as such low abundance molecules can be difficult to detect with traditional assay techniques, but as most of the proteins that were detectable by ELISA in stool correlate well, the detection of stool biomarkers by SOMAscan has future possibility. Of proteins that did not correlate well between SOMAscan and ELISA (D-dimer, elastase, ferritin, LGBP3), D-dimer and elastase were detected at lower concentrations limiting the use of the dynamic range of the ELISA.

Correlation of antibody array validated proteins

For the 15 proteins validated from the antibody-based RayBiotech L1000 array, the relative fluorescent intensities of each sample were correlated to the ELISA validation concentrations as seen in Figure 45.

ELISA Validation of RayBiotech Molecules

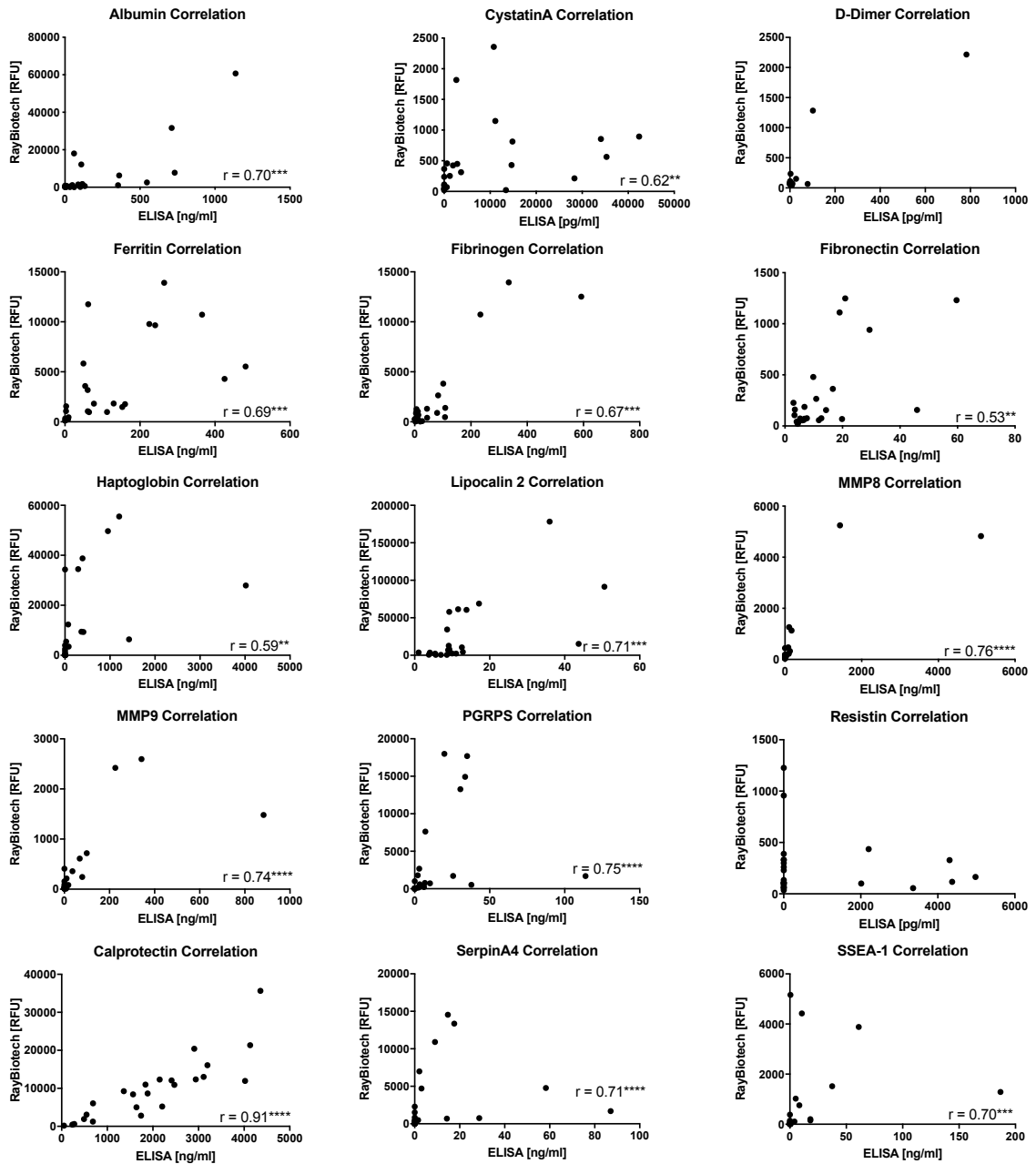


Figure 45: Of the 15 proteins validated by ELISA from the antibody array, 15 proteins had significant positive correlations between the two protein detection platforms (Spearman $r > 0.5$, $P < 0.05$).

13 of the 15 proteins had a strong positive correlation between their screening fluorescence intensity to their ELISA concentrations (Spearman $R > 0.5$, $P < 0.05$) while 2 did not correlate as well. More than 85% of the molecules validated by ELISA show correlation to the antibody array readings showing that the antibody

array can detect real, verifiable signal in stool samples. The two proteins that did not significantly correlate to the antibody array (D-dimer, resistin) were detectable at low concentrations in ELISA not taking advantage of the assay's full dynamic range. The ELISA used for resistin was manufactured by R&D Systems which may utilize different antibodies detecting different epitopes than RayBiotech's antibody array, causing increased variation in the data. resistin levels detected by ELISA correlated better to SOMAscan than the correlation to the antibody array.

Conclusion

Protein biomarker screening can be completed using multiple methodologies, but this research focuses on two technologies: the antibody array and aptamer-based screen. This work has utilized these two platforms to screen over 1000 human proteins for noninvasive stool biomarkers for two types of pediatric inflammatory bowel disease, Crohn's disease and ulcerative colitis.

The aptamer screen for protein biomarkers in IBD showed 48 proteins elevated in both Crohn's disease and ulcerative colitis patients' stool when compared to healthy controls, 20 proteins elevated in only ulcerative colitis and not Crohn's disease when compared to healthy controls, and 2 proteins elevated in only Crohn's disease and not ulcerative colitis when compared to healthy controls.

An analogous proteomic screen utilizing an antibody array has identified additional biomarkers for IBD as well an optimization of the commercial protocol to ensure the reliability of results for an unconventional sample type, stool. The antibody array as shown 71 proteins increased in the stool of pediatric IBD patients when compared to controls, 16 proteins increased in Crohn's disease patients' stool

when compared to healthy controls, and 104 proteins increased in ulcerative colitis patients' stool when compared to healthy controls. As stool was an unconventional sample type to be used for the antibody array, experimental variation was assessed by comparing the stool protein extraction protocol, sample processing through dialysis and biotinylation, and hybridization of the sample to the array for the same sample on different runs. The results showed that changing one of these three variables did not significantly change the distribution of proteins detected on the final scan, but more experimental variation in the processing did indeed cause more variation in the results.

These 23 biomarkers have further been validated by ELISA in a cohort of 30 patients and controls showing diagnostic capability in IBD as well as correlation with the initial aptamer screening. Nine proteins have been found to be elevated in both CD and UC versus HC, one has been elevated in CD vs HC, and nine have been elevated in UC vs HC stool. Of these, 10 proteins are elevated in the stools of UC patients versus CD. Thus far, these molecules have been validated in a small patient cohort of only 30 patients. By expansion of these patient numbers, the diagnostic ability of these markers can be better understood. With a larger sample size, machine-learning techniques can be applied to understand if combinations of these proteins will allow for better diagnostic ability than the proteins individually. These proteins have been currently assayed with cross-sectional samples or samples taken at one time-point. By looking at longitudinal samples over time, the biomarkers diagnostic ability to track and predict disease flares can be better understood.

These novel protein biomarkers have not only been validated across multiple proteomic platforms in stool, but gene microarray has shown these proteins to be elevated in the intestinal mucosa of pediatric inflammatory bowel disease patients and many hits have been implicated in inflammatory and other immune-related disease pathways. These novel protein biomarkers can not only be used in IBD diagnosis but can also help elucidate the mechanisms of this complicated disease.

Chapter 2: Alternate markers to creatinine for urine normalization

Introduction

The advent of personalized medicine and the development of large-scale OMICs technologies have accelerated the discovery of noninvasive biomarkers for diagnostic, prognostic, and therapeutic applications. For diseases affecting the urinary tract, urine represents a popularly tested body fluid that is potentially enriched for disease biomarkers.

Urine biomarkers are popular for countless diseases including bladder, prostate, and breast cancer [145]–[148], acute kidney injury [149], chronic kidney disease [150], and lupus nephritis [151]. To correctly interpret urine biomarker data, one needs to account for the hydration status of the patient, currently done by normalizing the biomarker level to urinary creatinine. Creatinine is currently the gold standard for urinary glomerular filtration rate normalization as this waste product of muscle metabolism that is neither secreted nor absorbed by the renal tubules [152]. Translation of creatinine normalization to point of care diagnostic devices depends on the type of assay employed. The most common assay used at the point of care is a sandwich lateral flow assay using antibodies to the target biomarker, best exemplified by the pregnancy test strip employing a sandwich assay for human chorionic gonadotropin (hCG).

Translating creatinine normalization to this sandwich lateral flow point of care assay has been challenging in that the small size of the metabolite makes it difficult to generate good antibodies to creatinine, limiting the translation of disease-specific urine protein biomarkers to antibody-based point of care

applications. To overcome this obstacle, an aptamer-based proteomic screen of 1129 human proteins was undertaken using diseased and healthy urine samples to identify urinary proteins that correlate with urinary creatinine and can be used for normalization of urine samples. Having such protein alternatives to urinary creatinine would greatly facilitate the design of point of care lateral flow tests for a variety of urinary biomarkers, spreading across a wide spectrum of diseases.

Methods

Human urine samples

For the initial aptamer-based screening, 23 human urine samples were obtained from University of Texas Southwestern Medical Center (UTSW) consisting of seven active lupus nephritis (LN), eight inactive SLE, and eight healthy controls (HC). Samples were obtained after informed consent at UTSW with Institutional Review Board approvals from UTSW and the University of Houston.

For the ELISA validation, 43 human urine samples were obtained from Johns Hopkins Medical Center (JHMC) and BioreclamationIVT consisting of 14 active LN, 13 inactive disease, and 16 healthy controls. Detailed clinical information of these subjects is provided in Table 9.

Table 9: Demographic and clinical characteristic of validation study cohort. Means are expressed with standard deviation.

Variable	Healthy Controls	Inactive SLE	Active LN
	n=16	n=13	n=14
Race			
Caucasian	7	7	7
African American	9	6	7
Age (yr)			
Mean	40 ± 10.7	48 ± 17.6	39 ± 12.5
Range	27–57	24–70	21–60
SLEDAI			
Mean	N/A	0 ± 0.6	11 ± 2.9
Range	N/A	0–2	8–18
rSLEDAI			
Mean	N/A	0 ± 0	9 ± 1.5
Range	N/A	0–0	8–12

SLE samples were obtained after informed consent at JHMC after Institutional Review Board approvals from both JHMC and the University of Houston. Active LN was defined as the renal component of SLEDAI > 8 (i.e. rSLEDAI > 8), while inactive disease was defined as the rSLEDAI = 0 and SLEDAI < 4. Inactive patients with SLICC (Systemic Lupus Collaborating Clinics) renal activity scores > 4 [153] were excluded from the study. SLEDAI was determined following the ACR disease guidelines [154]. Matched healthy controls were purchased from BioreclamationIVT (Westbury, NY).

Aptamer-based screen

An aptamer-based proteomic screen of 1129 proteins was conducted as described.[4] This SOMAscan assay has high sensitivity allowing for the detection of proteins up to the femtomolar range. The specificity of the assay is derived from the SOMAmer reagents consisting of modified DNA oligos [155]. Urine was diluted 20%

in dilution buffer and added to aptamer-coated beads. After incubation for 3.5 hours, the sample was removed and the beads were washed to remove unbound protein. Proteins in the sample that had bound to the aptamer coated beads were then biotinylated. The protein-aptamer complexes were photocleaved, collected, and immobilized on streptavidin-coated magnetic beads where a series of washes ensured specific binding of the aptamers to the proteins. The aptamers were uncoupled from the proteins using a high salt buffer, hybridized onto a DNA microarray, and the results were detected as relative fluorescence units.

Statistical analysis

The relative fluorescence unit readout from the hybridization array for each aptamer (corresponding to individual protein biomarkers) was normalized across the samples for the hybridization procedure using controls in the sample and probes on the slide. R Version 1.0.136 with the readxl [63], stats [64], and Hmisc [65] packages were used to carry out further data analysis. Mann-Whitney U-test and Student T-test were used to compare between groups to identify proteins that were significantly different between the subject groups. Pearson correlation was used to correlate the relative fluorescent units of each protein in the sample to the urinary creatinine of the subject (Cayman Chemical, Ann Arbor, MI, USA) to identify proteins that correlated well with creatinine.

ELISA validation

ELISA validation was carried out for five proteins: Herpesvirus entry mediator (HVEM), bone morphogenetic protein receptor type 2 (BMPRII), Dectin-1, Serine Peptidase Inhibitor Kunitz Type 2 (SPINT2), and Receptor Expressed In

Lymphoid Tissues (RELT). Kits were purchased for HVEM (Cat. No. EK1226, Boster Biological Technology, Pleasanton, CA, USA), BMPRII (Cat. No. ELH-BMPR2-1, RayBiotech, Inc., Norcross, GA, USA), Dectin-1 (Cat. No. ELH-DECTIN1-1, RayBiotech, Inc., Norcross, GA, USA), SPINT2 (Cat. No. DY1106, R&D Systems, Inc., Minneapolis, MN, USA), and RELT (Cat. No. SEK10530, Sino Biological Inc., Beijing, China). The samples were also assayed for ALCAM (Cat. No. DY656, R&D Systems, Inc., Minneapolis, MN, USA), a biomarker for lupus nephritis. Validation data was analyzed and graphed in GraphPad Version 6.05 using the Mann Whitney U-test, receiver operator curves (ROC), and area under the ROC curve (AUC).

Results

Screening results

23 human urine samples were screened for the levels of 1129 proteins using a comprehensive aptamer-based screen, the SOMAScan. Of the urine proteins interrogated, several were significantly elevated in the urine of patients with active LN [156]. As opposed to that study, the focus of this study was to ascertain which urine protein (out of the 1129 interrogated) correlated best with urine creatinine, and did not vary with disease status. Using Pearson correlation, we identified 62 urine proteins that were positively correlated with creatinine ($r > 0.5$, $P < 0.05$) as depicted in Figure 46.

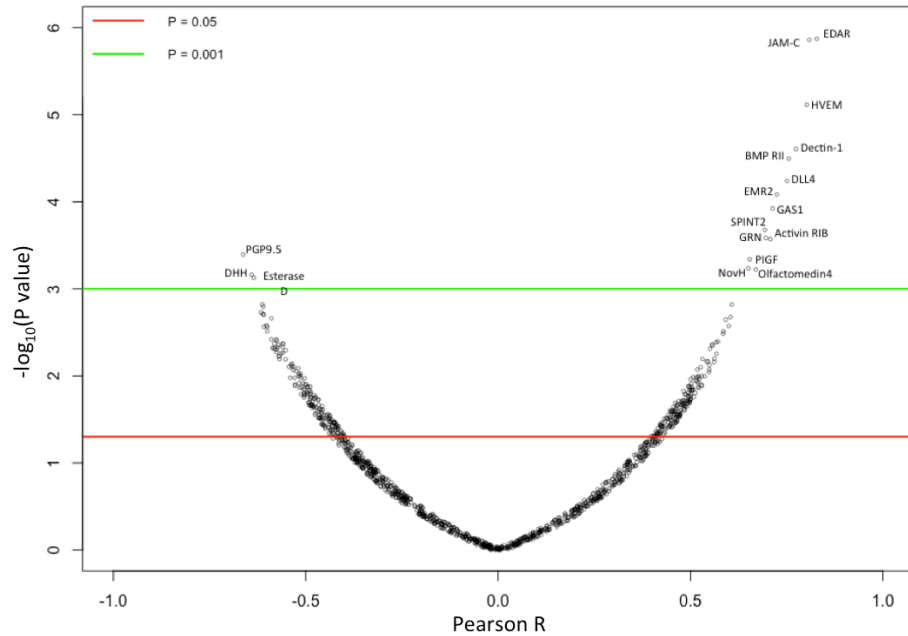


Figure 46: A volcano plot visualizing the Pearson correlation of 1129 proteins with creatinine in the human urine of 23 healthy and SLE subjects

Of these 62, 48 urine proteins were significantly different between at least two subject groups using Student t-test or Mann Whitney U-test at $P < 0.1$. Of the remaining 14 proteins, listed in Table 10, the top five proteins ranked based on Pearson correlation were HVEM, BMPRII, Dectin-1, SPINT2, and RELT.

Table 10: Proteins positively correlated to urinary creatinine that are not significantly different between patient groups.

Target	Pearson r
HVEM	0.79
BMP RII	0.76
Dectin-1	0.75
SPINT2	0.69
RELT	0.62
CLM6	0.60
JNK2	0.60
PAPP-A	0.58
HSP70 protein 8	0.56
PTN	0.54
Elafin	0.51
IL-1Rrp2	0.51
RASA1	0.50
APP	0.50

The correlation of these urine molecules with urine creatinine from the screening assay is summarized in Figure 47.

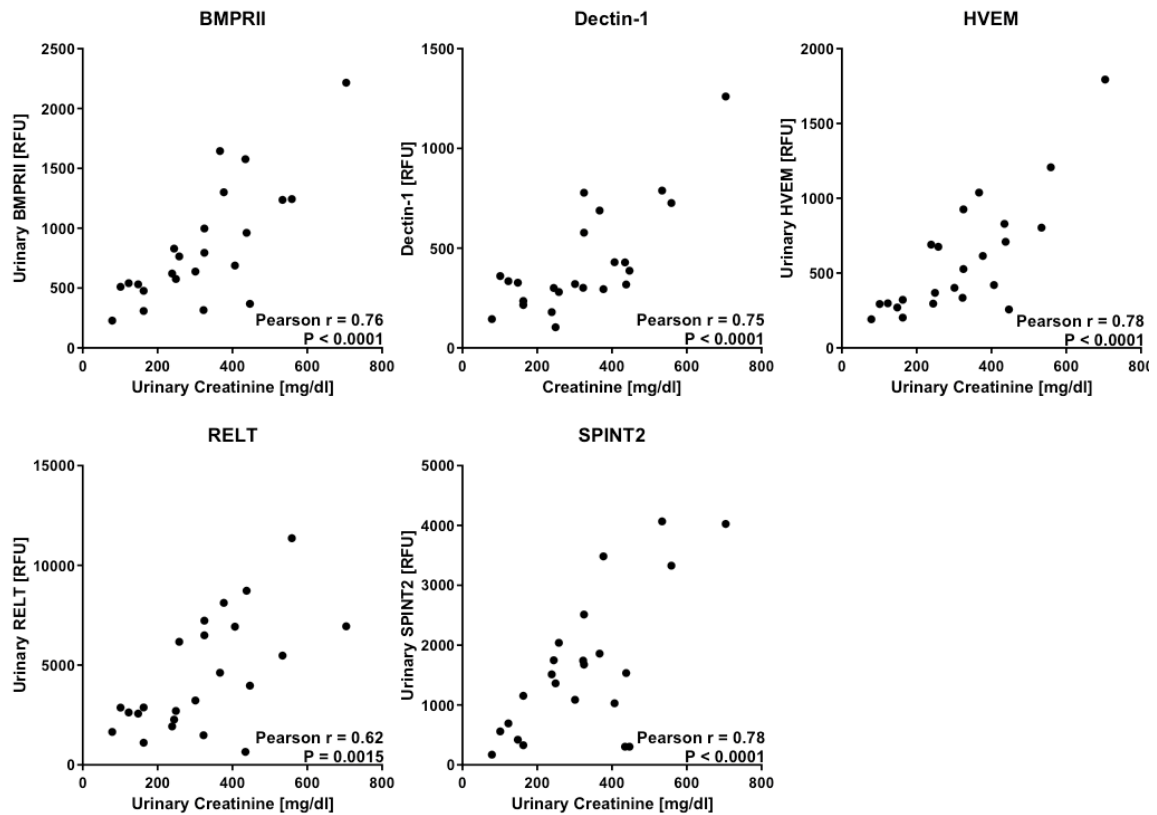


Figure 47: The screening identified five proteins that best positively correlate with creatinine and do not differ between subject groups.

These five proteins were chosen for ELISA validation in an independent cohort of samples.

ELISA validation results

An independent cohort of 43 urine samples was used for ELISA validation, comprised of 16 HC, 13 inactive SLE, and 14 active LN urine samples. ELISA kits for all five targets were tested for their detection sensitivity in urine. Urine BMPRII and SPINT2 were too low in concentration to be detected by ELISA. HVEM, Dectin-1, and RELT were validated further in a total of 43 urine samples. Once again, urinary HVEM and RELT were noted to have a significant positive correlation with urinary

creatinine (Pearson $r = 0.61$, $P < 0.0001$ and $r = 0.58$, $P < 0.0001$, respectively). In contrast, urinary Dectin-1 did not show a positive correlation with urinary creatinine in these samples (Pearson $r = 0.48$, $P = 0.0012$). A correlation of these molecules with urinary creatinine is shown in Figure 48.

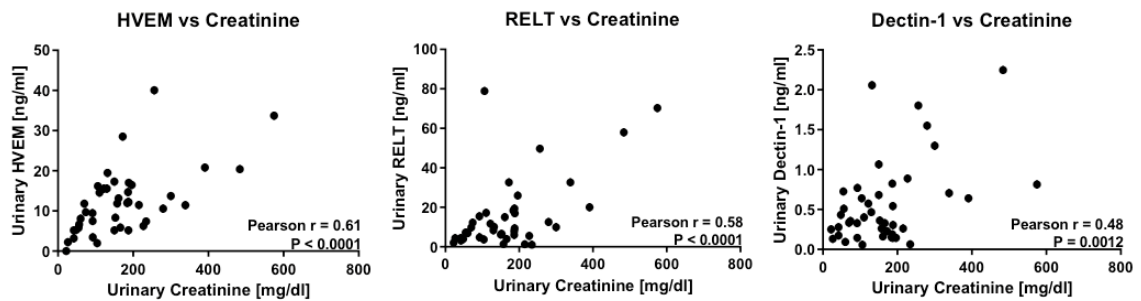


Figure 48: ELISA validation of the top five proteins in an independent cohort show positive correlation of HVEM and RELT to creatinine whereas Dectin-1 did not positively correlate in the validation set.

For the most promising of these proteins, HVEM, the impact of ethnicity was evaluated further. Urinary HVEM correlated with urinary creatinine in both Caucasian and African American subjects (Pearson $r = 0.70$, $P = 0.0004$ and $r = 0.58$, $P = 0.0047$, respectively) as shown in Figure 49.

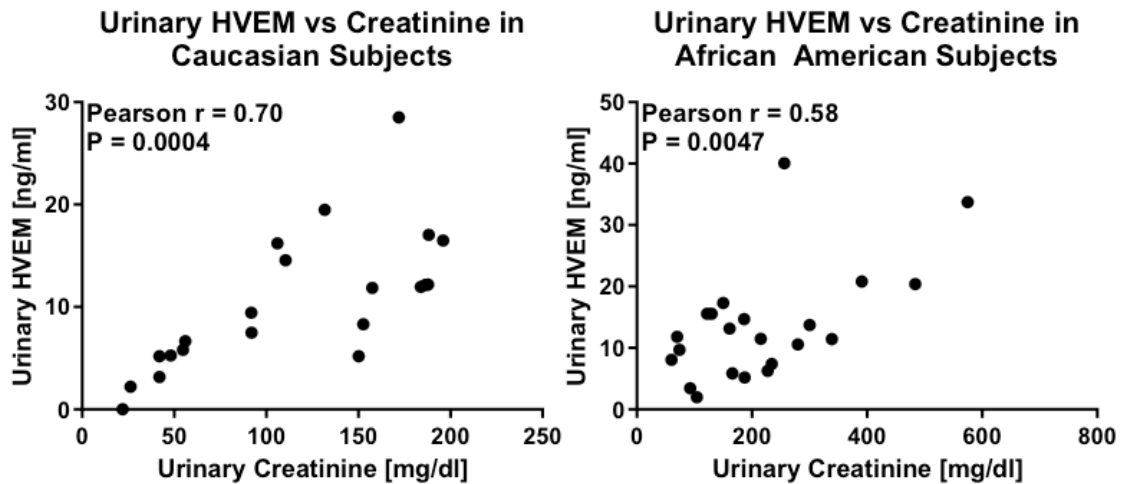


Figure 49: HVEM, the most promising biomarker for urine biomarker normalization, shows positive correlation in both Caucasian and African American subjects.

Testing the ability of urine HVEM to normalize urine biomarker levels

Given that urinary HVEM correlates consistently with urinary creatinine, we next assessed whether urinary HVEM can be used to normalize urine biomarker levels, just as urinary creatinine is currently used. The same validation cohort of 43 urine samples used above to assay urinary HVEM and creatinine were interrogated for the levels of urinary ALCAM, a biomarker candidate for LN [156]. Urine ALCAM normalized by creatinine, the current gold standard, showed a fold change of 4.06 (Mann Whitney U-Test P = 0.0040) between active and inactive lupus nephritis patients, while normalization of urine ALCAM with urine HVEM showed a similar fold change of 4.41 (Mann Whitney U-Test P = 0.0369) between active and inactive lupus nephritis, as shown in Figure 50.

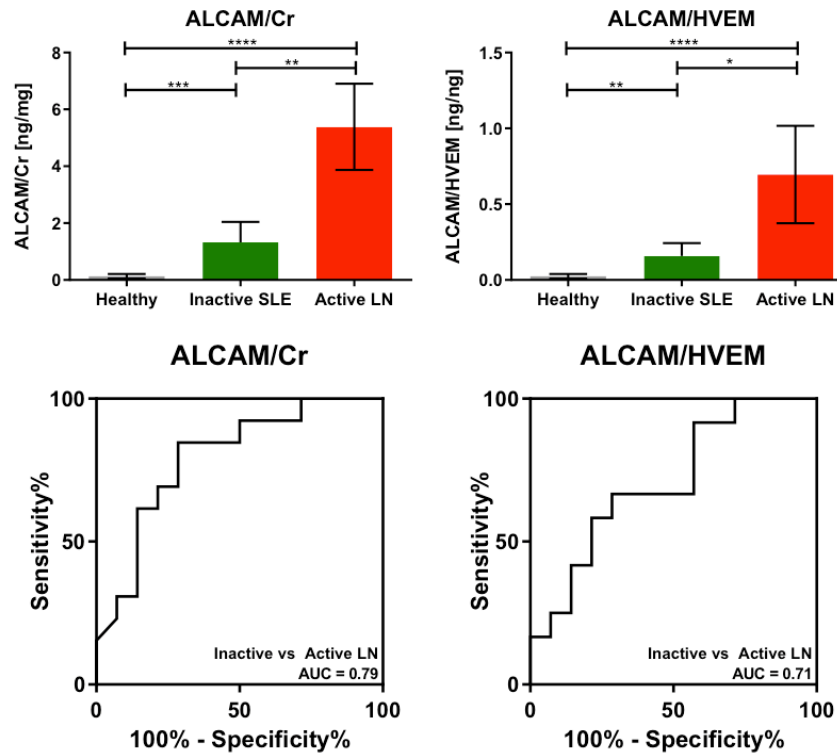


Figure 50: Normalization of ALCAM, a proposed biomarker for LN, with urinary creatinine and urinary HVEM shows comparable diagnostic ability. Bars show mean \pm SEM. One sample was removed from the plots, as the HVEM concentration was too low to be detected by ELISA.

ROC curves in Figure 5 illustrate the diagnostic ability of ALCAM for distinguishing active lupus nephritis using the two normalization methods (urine creatinine versus urine HVEM) showing a comparable performance with AUC = 0.79 and AUC = 0.71 respectively.

Discussion

This study is the first to screen over 1,100 human proteins for markers of glomerular filtration rate using a highly specific and sensitive targeted proteomic platform. By applying statistical criteria and identifying proteins that correlate to creatinine, but do not significantly vary with disease, we have identified 14 urine proteins that could potentially be used for urine biomarker normalization at the point of care. This is of practical importance because creatinine does not lend itself

for antibody-based diagnostics readily. Urine validation of these markers by ELISA further supports the need for easily detectable markers for normalization, as two of the five proteins chosen for validation were too low in concentration for ELISA to detect, making it even harder to detect these molecules at the point of care. Of the five chosen for validation, three, urinary HVEM, Dectin-1, and RELT, were detectable by ELISA, but urinary Dectin-1 did not correlate with urine creatinine in a larger independent cohort. At this point, urinary HVEM and urinary RELT emerged as promising urine protein candidates for normalization. In this study, urine concentrations of HVEM ranged from 5 ng/mL to 34 ng/mL in healthy subjects and 5 ng/mL to 41 ng/mL in patients with active LN. The urine concentrations of RELT ranged from 1 ng/mL to 71 ng/mL in healthy subjects and 4 ng/mL to 79 ng/mL in patients with active LN. In pursuing urine HVEM further, it shows good correlation with urine creatinine in both Caucasian and African American subjects. When using urinary HVEM as a normalization marker for the LN urinary biomarker candidate ALCAM, both HVEM and creatinine normalization exhibited comparable fold changes and ROC AUC values. Unlike creatinine, antibodies to HVEM are readily available, thus making it attractive for antibody-based point of care applications.

HVEM is a member of the tumor necrosis factor receptor superfamily and is a cell surface receptor that is used by the herpes simplex virus for cellular entry. It is also involved in the regulation of T-cell responses by inflammatory and inhibitory signaling pathways [157]. HVEM is widely expressed in the gallbladder, appendix, lymph nodes, tonsils, spleen, adrenal glands, stomach, rectum, kidney, bladder, and endometrium [158]. Expression of HVEM has been documented to be increased in

ovarian serous adenocarcinoma tissue [159], colorectal cancer epithelium [160], esophageal squamous cell carcinoma [161], and breast cancer [162]. Soluble HVEM has also been implicated in the serum of patients with hepatocellular carcinoma [163], gastric cancer [164], allergic asthma, atopic dermatitis and rheumatoid arthritis [165]. HVEM has also been implicated in innate mucosal defense against bacteria by promoting genes associated with immunity in the colon of a mouse model for *Escherichia coli* infection [166]. Interestingly, one report shows that active SLE patients had a significantly higher proportion of circulating HVEM-expressing CD4+T-cells than healthy individuals [167]. This study represents the first comprehensive proteomic screen for urine proteins that can be potentially be used as a substitute for urine creatinine, for normalizing urine biomarker levels. We find urine HVEM is not altered in patients with active LN and that urine HVEM correlates best with urine creatinine. As an example, urine HVEM is used to normalize urine ALCAM levels, a biomarker candidate for LN.

The utility of having such a normalizer protein for calibration extends beyond lupus nephritis. Urine biomarker testing is widely used for assessing cancers [145]–[148], multiple renal diseases [149]–[151], and other diseases[168] as well as for drug testing [169]. Urinary HVEM can certainly be used for normalization in all of the above scenarios, readily extending these tests to encompass point of care assays.

Further studies are warranted where urinary HVEM and urinary creatinine are compared head-to-head in larger, independent cohorts of lupus nephritis patient as well as in other diseases where urinary biomarkers are assessed. Renal

micropuncture studies are also warranted to detail how HVEM is handled in the nephron to assess if it is neither secreted nor absorbed. Studies are also warranted to assess if HVEM can be used to estimate glomerular filtration rate, just as creatinine is. Finally, some of the other urine protein candidates described in this work (e.g. BMPRII, SPINT2) also warrant further investigation, with comparisons to urinary creatinine and urinary HVEM.

Conclusion

To increase the sensitivity of urine biomarkers in diagnostics, most quantitative urine biomarkers are normalized to creatinine to account for GFR or urine production in the kidneys. As creatinine is a small metabolite and antibodies to creatinine are difficult to develop, applications of quantitative urine biomarkers to the point of care has been limited. To overcome this, an aptamer-based screen of 1000 proteins in urine was used to identify five proteins that correlate well to creatinine. Three of these proteins have been further validated in an independent patient cohort of 48 SLE patients and healthy controls identifying the best biomarker, herpes virus entry mediator (HVEM) for normalizing activated leukocyte cell adhesion molecule (ALCAM) and other urine biomarkers for lupus nephritis flares.

Chapter 3: Lateral Flow Assay for Active LN Diagnosis

Introduction

Systemic lupus erythematosus (SLE) is a chronic, systemic inflammatory autoimmune disorder affecting multiple organ systems including the skin, joints, and internal organs. One of the major causes of morbidity in SLE is lupus nephritis or inflammation of the kidneys due to lupus. Current diagnosis of lupus nephritis is done by a kidney biopsy, which can be painful and expensive for the patient. Kidney biopsies also cannot be routinely conducted, as the procedure is quite invasive calling for the importance of noninvasive biomarkers for lupus nephritis. Current research has shown urinary ALCAM to be a lupus nephritis biomarker [170] and the previous chapter has shown HVEM to be a promising marker for urine biomarker normalization. This study establishes and optimizes a point-of-care lateral flow assay for the sensitive and quantitative detection of urinary ALCAM, a lupus nephritis biomarker, and urinary HVEM, a urine biomarker normalizer, utilizing persistent luminescence nanophosphors.

Systemic lupus erythematosus

Like other autoimmune diseases, the cause of lupus is a combination of genetic, environmental, and immunologic factors with triggers such as sunlight, infections, and medications. SLE affects over 1.5 million Americans with greater prevalence among women, especially African-American and Hispanic, suggesting the importance of genes and hormones in the pathogenesis of SLE [171].

SLE manifests in both nonspecific symptoms including fatigue, fever, and a butterfly-shaped rash on the face but may include symptoms specific to organ

systems where the disease causes inflammation like skin lesions, shortness of breath, chest pain and joint pain, stiffness, and swelling. These initial symptoms may worsen with disease course causing secondary complications such as pleural effusions, heart problems, arthritis, and lupus nephritis [172].

The American College of Rheumatology has designed 11 classification criteria for the diagnosis of lupus including: the butterfly-shaped rash, discoid rash, photosensitivity, oral ulcers, joint inflammation, lung inflammation, kidney disorders, neurological disorders, blood disorders, immunologic disorders including anti-DNA, anti-Sm, or positive anti-phospholipid antibodies, and abnormal antinuclear antibodies [173]. By completing four of these criteria, a patient can be diagnosed with lupus with 95% specificity and 85% sensitivity [174].

Current treatment of SLE relies on hydroxychloroquine for the reduction of disease flares and glucocorticoids to treat other manifestations of lupus [174]. Although these treatments help suppress inflammation, when SLE gets out of hand, high morbidity diseases can come into play.

Lupus nephritis (LN), inflammation of the kidneys due to lupus, develops in up to 60% of adults and 80% of children with SLE. 10-30% of these patients progress to end-stage renal disease where the patient is put on dialysis or needs a kidney transplant [175]–[183]. Current diagnosis of LN is done by a kidney biopsy, but biopsies cannot be repeated to monitor LN progression or response to treatment. As a result, noninvasive biomarkers for LN are needed to diagnose kidney involvement earlier and to monitor and predict active disease flares for

subsequent treatment as an earlier treatment for LN can prevent morbidity and mortality [184]–[186].

Urine biomarkers for LN

Current laboratory measures of lupus nephritis include proteinuria, creatinine clearance, anti-dsDNA, and complement levels, but these measures have shown to be not as sensitive or specific for renal inflammation and damage [187]. Research for biomarkers for lupus nephritis has found leads in both serum and urine [151], [188], [189] An aptamer-based screen of 1129 proteins identified 12 biomarkers of active lupus nephritis [156], [190]–[193]. These molecules have been extensively validated in independent cohorts [194]–[202]. For this study, ALCAM was chosen as the initial biomarker for translation to the point of care. Along with ALCAM, HVEM was also chosen for translation to the point of care as a normalizing molecule in urine. Concentrations of ALCAM and HVEM as found in Chapter 2 of this work have found to be in the range of 0-32 ng/mL for ALCAM and 0-40 ng/mL for HVEM as illustrated in Figure 51.

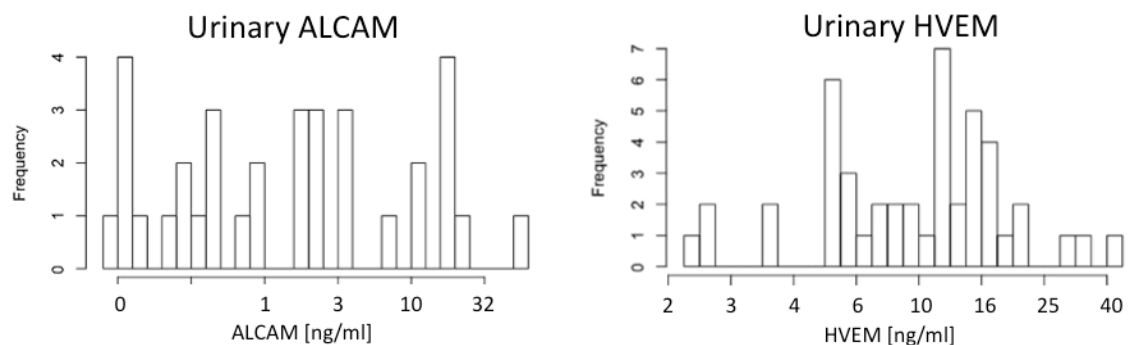


Figure 51: Histograms showing the concentrations of ALCAM and HVEM in human urine from subjects assayed in Chapter 2. ALCAM and HVEM have ranges of 0-32 ng/mL and 0-40 ng/mL, respectively in human urine.

As an early intervention to lupus nephritis and SLE flares is shown to decrease morbidity, an application of urinary biomarkers for active lupus nephritis to the

point of care is warranted. Because of the need for the sensitive detection between active and inactive lupus nephritis as well as the need for urine normalization, application of ALCAM and HVEM needs to be sensitive and quantitative.

Lateral flow assay

The lateral flow assay (LFA) is a point of care assay that allows for the detection of an analyte by the flow of sample across a paper-based membrane. This format is especially useful in a non-laboratory setting, such as the clinic or a patient's home, as the assay can be optimized to a dry format where the addition of sample can reconstitute the reagents allowing for a visualization of results within 20 minutes. The application of the lateral flow assay is common in many human diseases primarily infectious diseases [203]–[212], but the most common application of LFA is the pregnancy strip test detecting hCG (human chorionic gonadotropin). Although most assay formats are semi-quantitative with positive or negative test results, new advances in detection technologies have allowed for the quantitative detection of analytes opening the application of lateral flow assays to diseases that require more sensitive diagnostics [213].

The typical lateral flow assay employs an antibody sandwich based detection of an analyte in a sample. The lateral flow device itself is composed of a sample pad, conjugate pad, nitrocellulose membrane, and absorbent pad illustrated in Figure 52A.

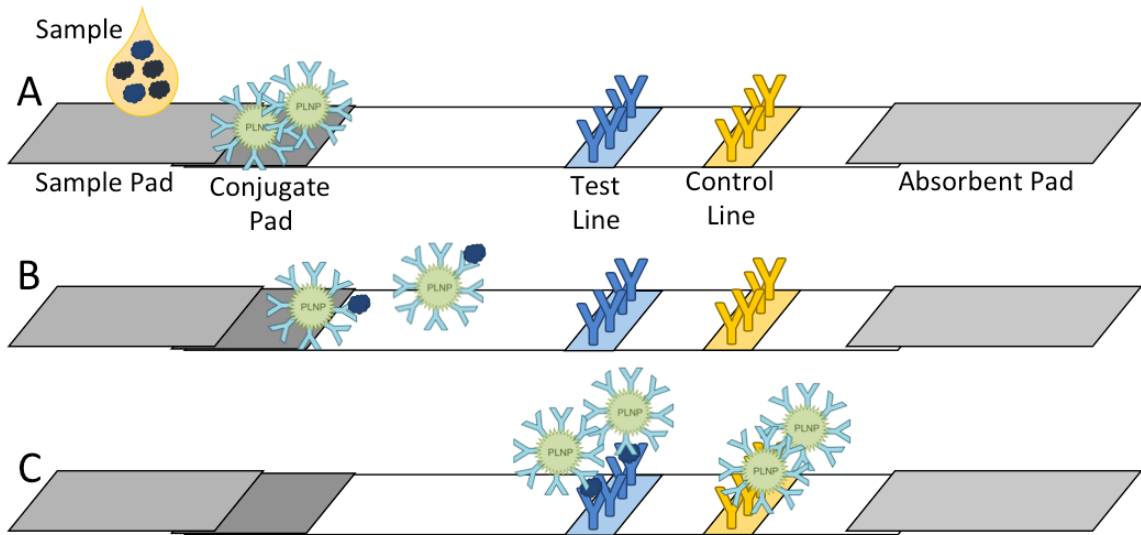


Figure 52: Illustration of the lateral flow assay format.

This paper stack is typically packaged and sold in a plastic cartridge. The sample pad allows for absorption of the sample matrix and controlled release of the sample to the conjugate pad. The conjugate pad houses dried detection reagents, typically detection antibodies conjugated to detection particles with latex, gold, and magnetic particles being used most often. The nitrocellulose membrane makes up the majority of the strip and is where the test and control lines are located. The capture antibody specific to the analyte is immobilized on a test line and a control antibody specific to the detection antibody is immobilized at the control line. The absorbent pad allowed for the collection of the excess sample. These paper membranes are sequentially positioned with a 2-3 mm overlap of each subsequent membrane. As a liquid sample is added to the sample pad, capillary force forces the flow of the sample through the membranes. After the sample pad, the sample will continue to flow to the conjugate pad where it will reconstitute the detection reagents (Figure 52B). These detection reagents will bind to the analyte of interest in the sample matrix as it flows across the nitrocellulose membrane. As the analyte-detection

molecule conjugate flows across the test line, the capture antibody on the nitrocellulose membrane will bind the analyte forming the detection sandwich. Excess detection molecule will continue to flow across the membrane to bind at the control line, and the excess sample will be collected on the absorbent pad. A positive test will have two positive signals: one at the test and one at the control line (Figure 52C). A negative test will have a single signal at the control line as no binding occurred at the test line. The absence of the control line will mean an indeterminate test, as the sample did not successfully flow across the membrane to reconstitute the detection molecule at the conjugate pad. Output quantitative signal is traditionally noted as the ratio of the test line to control line signal.

LFAs can be detected and quantified based on the detection molecule. Although latex and gold nanoparticles can be visualized with the naked eye for a semi-quantitative reading, image acquisition and analysis with a smartphone can greatly increase sensitivity and reproducibility to allow for a quantitative assay [214]–[220]. A disadvantage to latex and gold nanoparticles is the low sensitivity and quantitation of detection [213], [221]–[224] opening up the need for more sensitive detection molecules for diseases that require the quantitative detection of analytes.

Persistently luminescent nanophosphors

Persistently luminescent nanophosphors (PLNPs) made of strontium aluminate have recently been introduced as a sensitive detection molecule with the promise of an application towards a quantitative lateral flow assay. Neutravidin-labeled PLNPs have shown to have a limit of detection below 100 pg/mL, an order of

magnitude more sensitive than their gold nanoparticle equivalent [225]. The application of PLNPs to the point-of-care has been facilitated by the creation of a smartphone-based platform [215]. With the introduction of this smartphone adaptation, the camera's flash will allow for the excitation of the phosphors followed by the successive image capture of the LFA membrane. This controlled excitation and image capture has increased the sensitivity allowing for the limit of detection to reach a limit of detection to reach 45 pg/mL of hCG [215].

For the application to lupus nephritis diagnostics, this study has established and optimized the detection of ALCAM, a lupus nephritis biomarker, and HVEM, a urine biomarker normalizer using PLNPs as reporter molecules for the lateral flow assay. As the ideal format for the detection of ALCAM and HVEM would be a multiplexed LFA as illustrated in Figure 53, but for the purpose of optimization, two independent LFAs have been created for ALCAM and HVEM.

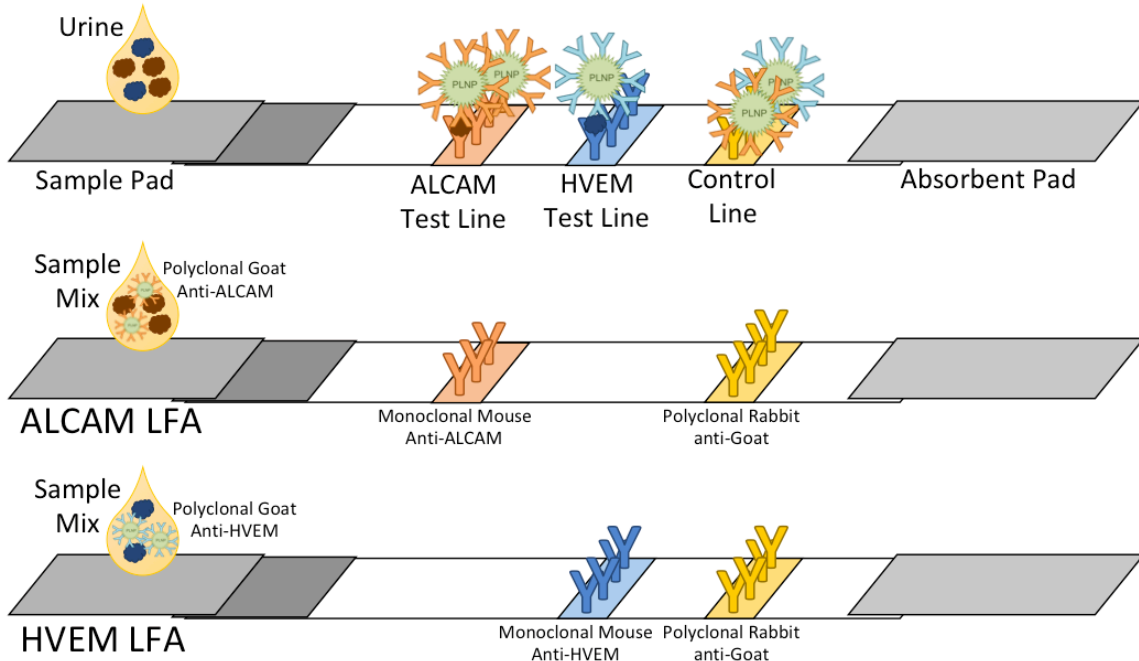


Figure 53: Lateral flow assay format for the detection of ALCAM and HVEM in urine using persistently luminescent nanophosphors.

As PLNPs have yet to be used for the detection of analytes human urine, urine feasibility studies have also been conducted to show the promise of quantitative detection of ALCAM and HVEM in human urine samples.

Methods

For the initial feasibility and optimization for lateral flow assays for the detection of ALCAM and HVEM, an antibody pair was chosen that is currently used for the commercial detection of ALCAM and HVEM by ELISA. R&D Systems' ELISA kit for ALCAM (R&D Systems, DY565) employs a monoclonal mouse IgG₁ anti-Human ALCAM antibody (R&D Systems, MAB6561-100) for the capture reagent and a biotinylated polyclonal goat anti-Human ALCAM antibody (R&D Systems, AF656) for its detection reagent. The standard for human ALCAM (R&D Systems, 656-AL-100) in the ELISA kit is derived from a mouse myeloma cell line. The HVEM ELISA (R&D Systems DY356) employs a monoclonal mouse anti-Human HVEM antibody

(R&D Systems, MAB356-100) for the capture reagent and a biotinylated polyclonal goat anti-Human HVEM antibody (R&D Systems, AF356) for its detection reagent. Standard for human HVEM (R&D Systems, 356-HV100) in the ELISA kit is also derived from a mouse myeloma cell line. For initial feasibility and testing, the polyclonal goat antibodies for ALCAM and HVEM have been conjugated to persistently luminescent nanophosphors and the monoclonal mouse capture antibodies have been immobilized to the nitrocellulose membrane.

Preparation of phosphor-labeled nanoparticles

Previously optimized methods for the preparation of persistently luminescent nanophosphors have been used for this study [225]. Strontium aluminate powder was wet-milled, size separated using centrifugal separation, silica-encapsulated, salinized, and bioconjugated with antibodies specific for ALCAM and HVEM.

Three to five grams of powdered strontium aluminate was added to 30-50 mL of ethyl acetate in a ceramic in a ceramic milling jar (U.S. Stoneware Roalox Alumina-Fortified Grinding Jar). Magnesia stabilized zirconia cylinders were used as grinding media for milling on a jar mill (U.S. Stoneware, Model 755RMV Unitized Jar Mill) at 60% power for 7–9 days followed by drying at room temperature to remove the ethyl acetate solvent. This milling created phosphor particles of various sizes and centrifugal separation was used to isolate 250 nm particles. For the centrifugal separation, 0.5 g of milled strontium aluminate powder was dispersed in 40 mL of ethanol in 50 mL tubes followed by a series of separations involving vortexing, sonication, and centrifugation for five minutes at 2400 RPM (Beckman Coulter

Avanti J-E centrifuge with a JS-5.3 rotor). Particles larger than 300 nm in collected in the pellet and particles smaller than 300 nm were dispersed in the supernatant. This initial separation was completed until 3 L of supernatant fraction was collected. A second separation of this collection separated particles larger than 200 nm collected in the pellet from particles smaller than 200 nm dispersed in the supernatant. This second separation was completed with centrifugation for 10 minutes at 2600 RPM. The supernatant of this collection was discarded while the pellet isolated particles between 200 and 300 nm in size. The yield of the separation procedure was approximated by drying a known volume of the product and weighing it on an analytical balance (Mettler Toledo XS64). The product yield was approximated to 3–4 mg of fractionated particles with an average predicted size of 250 nm.

To increase stability and allow for further conjugation, the 250 nm strontium aluminate nanoparticles were silica encapsulated with tetraethyl orthosilicate (TEOS). To 1 mL of isolated particles at a concentration of 1 – 2 mg/mL, 475 μ L of TEOS mastermix was added consisting of 221.6 μ L ethanol, 246.7 μ L H₂O, and 6.7 μ L TEOS. After vortexing to mix and sonication for 5 minutes, 25 μ L of 30% ammonium hydroxide was added to the solution followed by vortexing and sonication for 30 minutes. The mixture was then incubated on a rotator for 7.5 hours at room temperature to complete the silica encapsulation. The particles were washed with 1 mL of ethanol by centrifugation (Eppendorf Centrifuge 5418) at 5 minutes at 3,000 RCF to thoroughly remove excess encapsulation reagents. After three washes, silica encapsulated phosphors were stored in 1 mL of ethanol at room temperature.

To allow for further bioconjugation of the particles, the silica-encapsulated particles were functionalized with aldehydes by silanization using triethoxysilylbutyraldehyde (TESBA). To 1 mL of 1 mg/mL silica encapsulated phosphors, 10 μ L of TEOS/TESBA/ethanol master mix consisting of 155 μ L of TEOS, 5 μ L TESBA, and 1.393 μ L of H₂O was added followed by vortexing to mix. 205.8 μ L of ammonium hydroxide (8.1% NH₄OH in H₂O) was added to the mixture followed by sonication for 10 minutes and incubation at room temperature on a rotator for 12 hours. After incubation, the particles were washed with ethanol three times by centrifugation at 3000 RCF for 2.5 minutes, followed by a 5 minute-sonication, and 1-minute vortexing.

The silanized, silica encapsulated phosphors were immediately bioconjugated separately with polyclonal antibodies specific for ALCAM (R&D Systems, AF656) and HVEM (R&D Systems, AF356). Two aliquots of silanized, silica encapsulated phosphors were washed and resuspended with PBS pH 8.0. PBS, 50 μ g of antibody, and NaBH₃CN were added to the mixture to obtain a final concentration of 250 mM NaBH₃CN and a final volume of 1 mL. The mixture was sonicated for 5 minutes followed by incubation at room temperature on a rotator for 2 hours. Phosphors were washed once in PBS pH 7.4 to remove unbound antibody and resuspended in 200 μ L of PBS. To block unbound sites on the phosphors, particles were passivated with 750 μ L of 40 mg/mL of BSA in PBS and 50 μ L of 1M NaBH₃CN. The mixture was vortexed, sonicated for 5 minutes, and incubated at room temperature on a rotor for 3 hours. After passivation, phosphors were washed three times with PBS pH 7.4 followed by resuspension in 100 μ L of borate storage buffer

(10 mM sodium borate, pH 8.5, 150 mM NaCl, 0.1% BSA, 0.04% PVP-40, 0.025% Tween-20). Phosphor conjugated particles were stored in a low binding tube at 4C for future use.

Preparation of lateral flow membrane strips

Unless noted otherwise, lateral flow assay strips were assembled using FF80HP as the nitrocellulose membrane, Standard 14 as the sample pad, and CF5 as the absorbent pad. FF80HP (GE 13549206) was cut using a desktop paper cutter to 25 mm x 29.7 cm. Standard 14 (Whatman 81332250) and CF5 (Whatman 8115-2250) was cut to 30 cm lengths. All paper was assembled on a sticker backing (DCN) with a 2mm overlap of each membrane. The paper membrane sandwich was cut into 3mm strips.

To create the test line, 1ul of monoclonal anti-ALCAM (R&D Systems, MAB6561-100) or anti-HVEM (R&D Systems, MAB356-100) antibody was spotted at approximately at the middle of the nitrocellulose membrane at a concentration of 1mg/mL in PBS. Similarly, 1 uL of Rabbit anti-Goat polyclonal antibody (R&D Systems, R-401-C-ABS) was spotted between the test line and the absorbent pad at 1 mg/mL for the control line. Paper strips spotted with antibody were dried at 37°C for at least 2 hours and used immediately or stored in a centrifuge tube with desiccant for later use.

Other reagents and materials

For buffer components, the following reagents were used: PBS, HEPES, PVP40, NaCl, BSA, PEG 3350, Tween 20, non-fat dry milk, Tris-acid, Tris-base, TritonX100, sucrose, and SDS. For other membranes, the following components

were used: Fusion 5, HF90 (Millipore, HF090MC100), CN95 (Sartorius). Synthetic urine was purchased from Sigma-Aldrich (S-020-50ML).

Lateral flow assay, image acquisition, and analysis

Unless stated otherwise, antibody-conjugated nanophosphors were sonicated for 10 minutes, vortexed, and diluted to a working concentration of 1 mg/mL of nanophosphors with Buffer 2 (PBS pH 7.25, 2% Tween 20, 25mM NaCl, 0.5% non-fat dry milk). Diluted phosphors were added to a sample with known concentration of analyte and vortexed immediately. As phosphor yield differs between batches, phosphor dilution and loading requires optimization for each conjugated-phosphor batch. 40 uL of this sample mixture was added to the assembled lateral flow strip after which the strip was allowed to dry for at least 20 minutes. For replicates used in this study, twice the sample mixture was prepared and applied to two separate lateral flow strips.

Dried Strips were visualized using Alpha Innotech FluorChem SP gel documentation system adapted with a with a 370 nm Chauvet 18 in., 15 W UV light. Strips were imaged with an exposure time of 4-8 seconds and captured with a binning of 4. Images were analyzed using ImageJ Version 1.52a by drawing a line of width 8 pixels across the length of the strip. With the scale set to 1 pixel/unit ratio, an intensity profile was plotted and the peak area each test and control line was obtained. Peak areas were imported into Microsoft Excel where peak area ratios of the test line to the control line were calculated. When optimizing for maximum signal intensity, peak areas of the test and control line were used while when comparing analyte concentration to LFA signal, peak area ratios were used. Graphs

were plotted GraphPad Prism 8. The limit of blank and limit of detection was calculated according to previously published methods [7].

Results and Discussion

Buffer screen

For initial optimization of the lateral flow assay, a buffer screen of four running buffers containing additives commonly used in lateral flow assay was completed. The buffers consisted of Buffer 1: 10mM HEPES pH 7.95, 0.5% PVP40, 100mM NaCl, 1% BSA, 0.4% PEG, Buffer 2: PBS pH 7.25, 2% Tween 20, 25mM NaCl, 0.5% non-fat dry milk, Buffer 3: 50mM Tris pH 8.3, 0.55 Triton X 100, 50mM NaCl, 2% BSA, and Buffer 4: HEPES pH 7.4, 100mM NaCl, 0.1% Tween 20, 0.5% sucrose, 0.5% PEG, 0.1% SDS, 0.01% BSA. For each buffer, an approximate concentration of 9 ug of phosphors diluted in the buffer was added to 45 uL of the sample with a known concentration of the analyte in the buffer.

For the detection of ALCAM, an initial buffer screen consisting of Buffer 1, 2, and 3 yielded Buffer 1 to have the highest intensity on the test line for detecting 200 pg/mL of ALCAM as seen in Figure 54.

ALCAM LFA: Buffer Screening

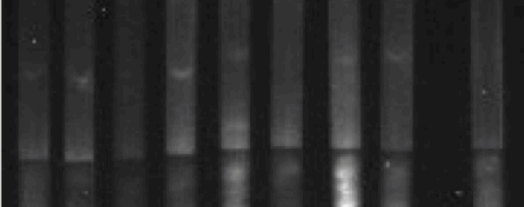
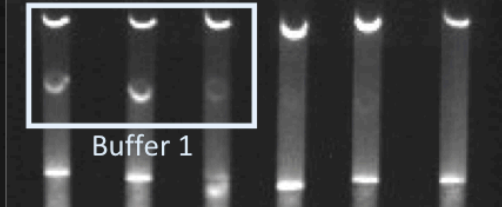
1	2	3	4	5	6	7	8	9	10	11	12	13	14	15	
B1	B1	B1	B2	B2	B2	B3	B3	B3	B1	B1	B1	B4	B4	B4	Buffer
200	200	0	200	200	0	200	200	0	1000	1000	0	1000	1000	0	ALCAM [pg/ml]
Sample Pad: Fusion 5, No control Line									Sample Pad: Standard 14						Notes
															Control
															Test

Figure 54: A buffer screen for the ALCAM lateral flow assay showed a buffer composed of 10mM HEPES pH 7.95, 0.5% PVP40, 100mM NaCl, 1% BSA, 0.4% PEG to have the strongest signal intensity.

Even though this initial buffer screen showed a low signal at the test line, Buffer 1 was seen to cause less background signal than Buffer 2 and 3 with a comparable signal at the test line. Fusion 5 was also used initially as the sample pad but quickly replaced with Standard 14 as this decreased aggregation of the PLNPs in the sample pad. This buffer screen was expanded in Figure 54 with the comparison of Buffer 1 with Buffer 4 in the detection of ALCAM at a higher concentration 1 ng/mL showing Buffer 1 to have a positive signal on the test line for the positive control and minimal signal at the test line for the no protein buffer blank. Buffer 4 showed a slight signal at the test line of the positive sample but was very close to the no protein buffer blank.

Similarly, for the detection of HVEM at 1 ng/mL, a buffer screen consisted of four buffers showed highest test line signal with the use of Buffer 2 as visualized in Figure 55.

HVEM LFA: Buffer Screening

1	2	3	4	5	6	7	8	9	10	11	12	
B2	B2	B2	B3	B3	B3	B1	B1	B1	B4	B4	B4	Buffer
1000	1000	0	1000	1000	0	1000	1000	0	1000	1000	0	HVEM [pg/ml]
Sample Pad: Standard 14												Notes
												Control
												Test

Figure 55: A buffer screen for the HVEM lateral flow assay showed a buffer composed of PBS pH 7.25, 2% Tween 20, 25mM NaCl, 0.5% non-fat dry milk to have the strongest signal intensity.

Buffer 1 and 3 did show positive signal on the test line positive samples and a minimal signal on the test line of the no protein buffer blanks for HVEM. Buffer 4 did not show a signal for the positive sample. Buffer 4 showed no signal for the positive controls on both ALCAM and HVEM LFAs. Looking at the components of the buffers, Buffer 4 includes the surfactant SDS, not included in the other buffers, which could be a factor in the absence of a positive signal.

Using this buffer screen, Buffer 1 consisting of 10mM HEPES pH 7.95, 0.5% PVP40, 100mM NaCl, 1% BSA, 0.4% PEG was used for the detection of ALCAM and Buffer 2 consisting of PBS pH 7.25, 2% Tween 20, 25mM NaCl, 0.5% non-fat dry milk was used for the detection of HVEM for the remaining optimization studies. As it was seen that Buffer 2 caused more aggregation than Buffer 1, Buffer 2 was used for the dilution of phosphors to the working concentration in the remaining optimization studies.

Membrane selection

To test for the optimal membrane for immobilization of the capture antibody and running of phosphors, a selection of nitrocellulose membranes of similar flow rates from different manufacturers were used. Each manufacturer uses different surfactants for the creation of their membranes that have the possibility to alter the process of antibody immobilization and flow of the antibody-conjugated phosphors across the membrane. After solubilization of the surfactants, the antibody-analyte binding kinetics at the test and control lines can also be changed depending on surfactant composition.

For each lateral flow strip, during the paper stack assembly GE FF80HP nitrocellulose membrane was replaced with Millipore HF09 and Sartorius CN95. The stack was cut and spotted with antibody as previously described. Each membrane was tested for binding of the analyte at high and low concentrations as well as a no protein buffer blank. Each sample mix contained 8 ug of phosphors and 40 uL of the sample mixture was applied to each lateral flow strip.

For the detection of ALCAM in

1	2	3	4	5	6	7	8	9	10	11	12	13	14	15	Membrane
GE FF80HP: 60-100 s/4 cm					Millipore HF090: 90 s/4 cm					Sartorius CN95: 90-135 s/4 cm					ID
+	+	LOD	LOD	-	+	+	LOD	LOD	-	+	+	LOD	LOD	-	
2000	2000	200	200	0	2000	2000	200	200	0	2000	2000	200	200	0	ALCAM [pg/ml]
															Control
															Test

Figure 56, GE FF80HP is seen to have the highest signal for high and mid-range concentrations of ALCAM.

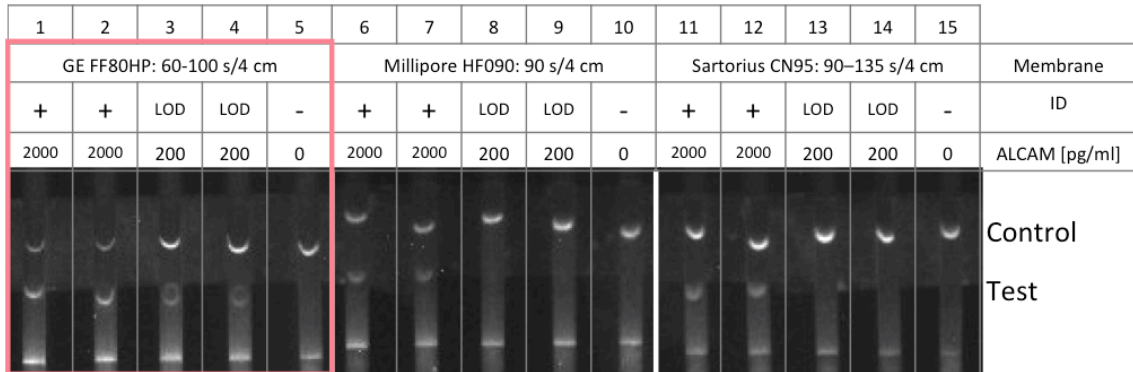


Figure 56: A nitrocellulose membrane screen for the ALCAM lateral flow assay showed GE FF80HP to have the strongest signal intensity.

Millipore HF09 and Sartorius CN95 did show intensity at the test line for high concentrations of ALCAM, but mid-range concentrations of ALCAM were not seen with these two membranes. None of the three membranes showed any background signal in the no-protein buffer blank.

Similarly, for HVEM in Figure 57 shows a positive signal for HVEM at high concentrations using GE FF80HP, while Millipore HF09 and Sartorius CN95 did now show a signal at the test line for a high concentration of HVEM.

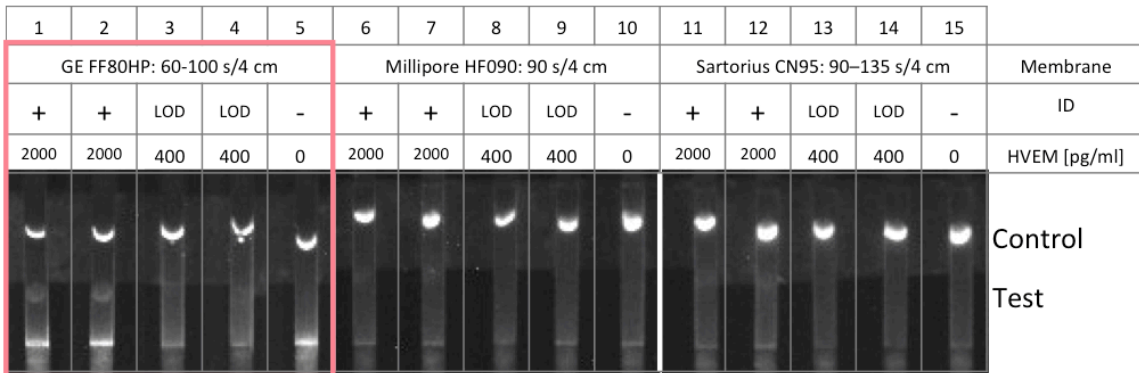


Figure 57: A nitrocellulose membrane screen for the HVEM lateral flow assay showed GE FF80HP to have the strongest signal intensity.

Mid-range concentrations of HVEM was not detectable on any of the three membranes screened. None of the three membranes showed any background signal in the no-protein buffer blank.

GE FF80HP was seen to be the most optimal nitrocellulose membrane for the detection of ALCAM and HVEM and was used to all the LFA optimizations. All membranes in this screen are manufactured for sample flow at similar flow rates. Further optimization of altering the flow rate by changing the pore size of the membrane can be completed in future studies. This is expected to change binding kinetics but is hypothesized to be negligible in comparison to the importance of nitrocellulose surfactant composition.

PLNP loading mass

The PLNP loading mass was further tested with a titration of antibody-conjugated phosphors detecting a high concentration of the analyte. As the yield for the antibody-conjugated phosphors differs with each batch, a titration of the phosphors is needed to understand the intensity behavior. For each analyte, PLNPs were diluted to a working concentration of 1 mg/mL and added to a sample mixture of analyte in the buffer so the final concentration of analyte was 5 ng/mL.

For ALCAM as seen in Figure 58, test and control line signal intensity was seen to increase with PLNP loading mass.

ALCAM LFA: Phosphor Loading

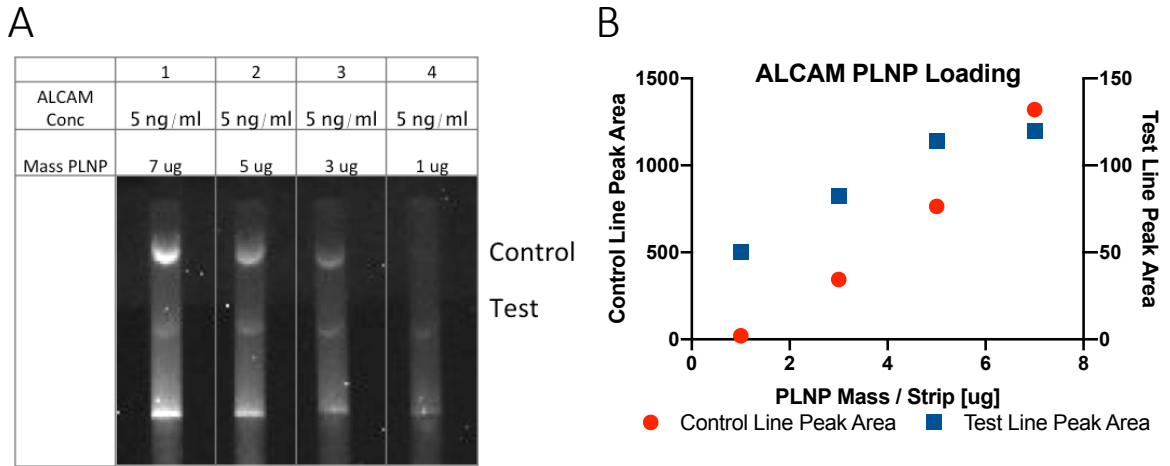


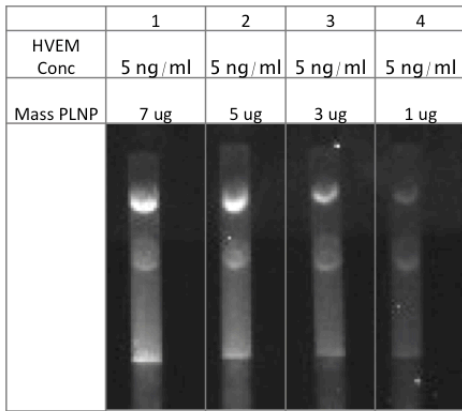
Figure 58: Phosphor loading testing for the ALCAM LFA showed 3 ug/strip was sufficient for a positive signal.

Although the control line signal intensity continued to increase proportionally with PLNP mass, test line signal with 5 ug/strip was seen to be comparable with 7 ug/strip. As the loading mass of 1ug/strip for ALCAM showed an absence of the control line, PLNP mass loading of at least 3 ug of PLNP per strip was seen to be sufficient for the assay.

Similarly, for HVEM in Figure 59, signal intensity was seen to increase with PLNP loading.

HVEM LFA: Phosphor Loading

A



B

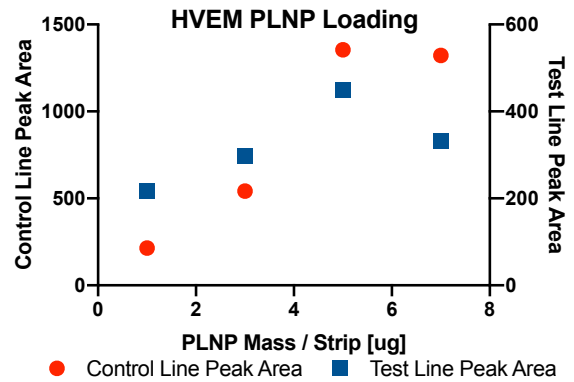


Figure 59: Phosphor loading testing for the HVEM LFA showed 1 ug/strip was sufficient for a positive signal.

Interestingly, 7 ug of PLNPs per strip was seen to have decreased test line intensity than loading of 5 ug of PLNPs per strip. For the HVEM PLNPs, 1 ug of PLNPs was sufficient for a low but quantitative test and control line signal.

With the addition of an excess of phosphors, a higher intensity was seen at the test and control line, with the disadvantage of a higher background. The background signal and aggregation of the PLNPs at the sample pad-membrane interface was seen to also increase with PLNP mass loading. With the current batch of phosphors used in this study, 3-5 ug of PLNP per strip was seen to be sufficient for a positive signal and minimal background.

Standard curve in buffer

Using the results from the optimization of buffer and membranes, a standard curve of each molecule in buffer was obtained for ALCAM and HVEM. For each molecule, 9 ug of phosphors were added to 45 uL of sample mixture of which 40 ul was added to the lateral flow strip.

0.2 with 90% of the detected concentrations with a standard deviation of less than 0.1. Reproducibility of the assay at 125 pg/mL was seen to have a standard deviation of 0.05. The limit of the blank (LoB) for the ALCAM assay was calculated using the 0.4 pg/mL sample and found to have a peak area ratio of 0.04817 and ALCAM concentration approximately 2 pg/mL. The limit of detection (LoD) of the ALCAM assay was using the standard deviation of 62.5 pg/mL sample and seen to have a peak area ratio of 0.1575 be near 125 pg/mL of ALCAM. There was good linearity at a concentration of ALCAM higher than 125 pg/mL limiting at 10 ng/mL in this study.

Similarly, for HVEM in Figure 61 concentrations were detected between 2000 pg/mL and 7.8 pg/mL in 4-fold dilutions.

HVEM LFA: Standard Curve in Buffer

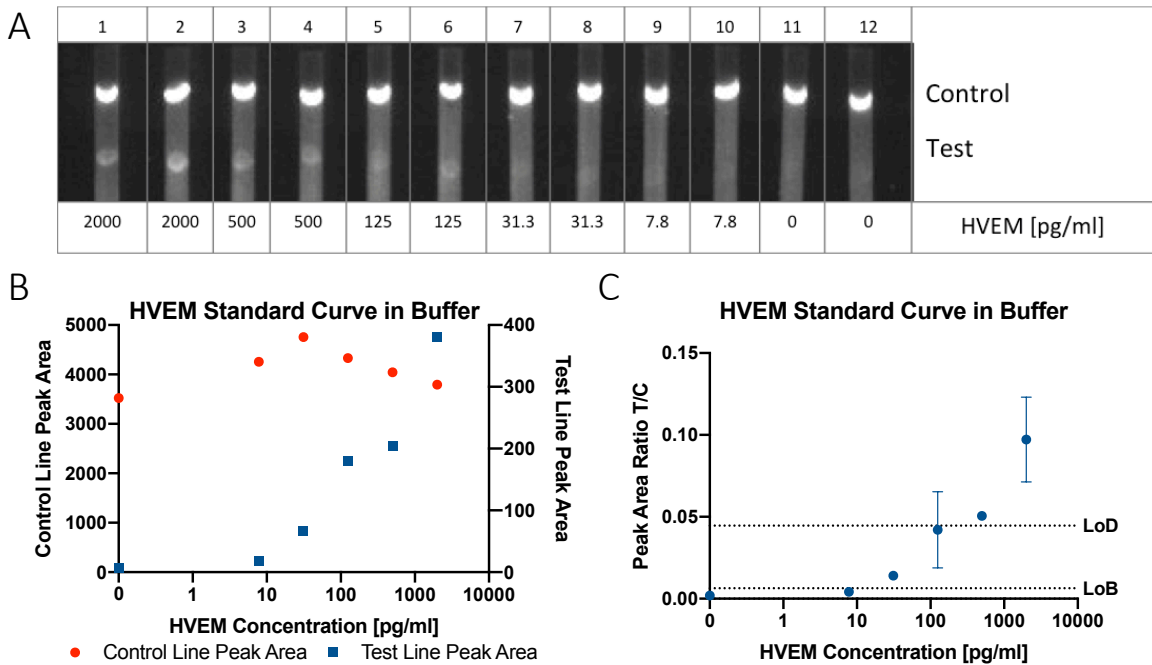


Figure 61: A standard curve for HVEM in buffer (A). For the test and control line peak areas (B), replicates are averaged together while for the standard curve (C) replicates are plotted with mean and standard deviation. Standard deviations smaller than the size of the point are not visualized.

As seen in Figure 61A and B, test line signal was seen to increase proportionately with increasing HVEM concentration. When looking at the peak area ratio of the test and control line in Figure 61C, a positive correlation of peak area ratio is seen to HVEM concentration. The standard deviations of the peak area ratio of the replicates range between 0.0010 and 0.02593. The limit of the blank (LoB) for the HVEM assay was calculated using the no-protein blank and found to have a peak area ratio of 0.006353 and HVEM concentration approximately 8 pg/mL. The limit of detection (LoD) of the HVEM assay was using the standard deviation of 125 pg/mL sample and seen to have a peak area ratio of 0.04458 be near 125 pg/mL of HVEM. There was good linearity at a concentration of HVEM higher than 125 pg/mL limiting at 20 ng/mL in this study.

Two independent LFAs for ALCAM and HVEM utilizing persistent luminescent nanophosphors were optimized and characterized in buffer. The two assays show comparable detection limits at 125 pg/ml as the initially published limit of detection for neutravidin-labeled nanophosphors of below 100 pg/mL [225]. Further optimization of the buffer system and perfecting the nanophosphors preparation process to improve yield can enhance the detection limits and enhance quantitation.

Human urine feasibility

To look at the application of PLNPs in urine, the buffer in the sample mixture was optimistically replaced with undiluted human urine with spiked concentrations of analyte. 7.5 ug of PLNPs were added to a 55 uL sample mixture containing buffer with 1 ng/mL of the analyte or human urine with the addition of 1 ng/mL of the analyte. 40 uL of this mixture was added to each strip. As seen in Figure 62 for both ALCAM and HVEM, the replacement of buffer with urine caused aggregation of phosphors in the sample pad and at the membrane-sample pad interface limiting the flow of phosphors across the strip.

ALCAM and HVEM LFA: Human Urine Dilution

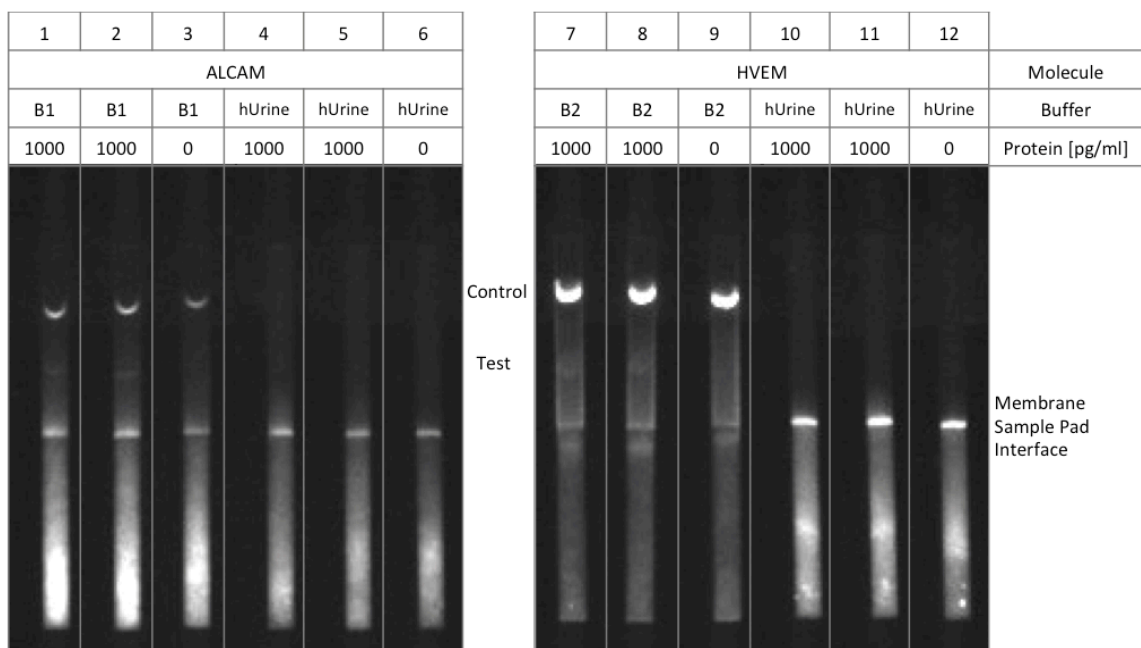


Figure 62: The buffer component of the ALCAM and HVEM lateral flow assays was replaced with undiluted human urine spiked with ALCAM and HVEM showing aggregation of PLNPs at the membrane sample pad interface and prevention of sample flow through the membrane.

Although test signal was significantly dimmer even in the buffer-analyte controls, the aggregation of phosphors in human urine at the sample pad would significantly hinder the application of PLNPs in urine further calling for the optimization of urine dilution.

Human urine dilution

To ascertain whether human urine inherently causes aggregation of PLNPs or if a buffer with additives is needed to prevent aggregation and support flow of phosphors across the membrane, the human urine was diluted with water and buffer at various ratios. 7.5 ug of phosphors was added to a sample mixture containing 2 ng/mL of analyte in a urine-water or urine-buffer mixture. A positive control of a sample mixture with 2 ng/mL of analyte in 100% buffer and a negative control of no protein buffer was also used.

For the ALCAM LFA in Figure 63, dilution of human urine with water shows aggregation while dilution of human urine with buffer reestablishes the flow of the sample mixture through the membrane.

ALCAM LFA: Human Urine Dilution with Buffer and Water

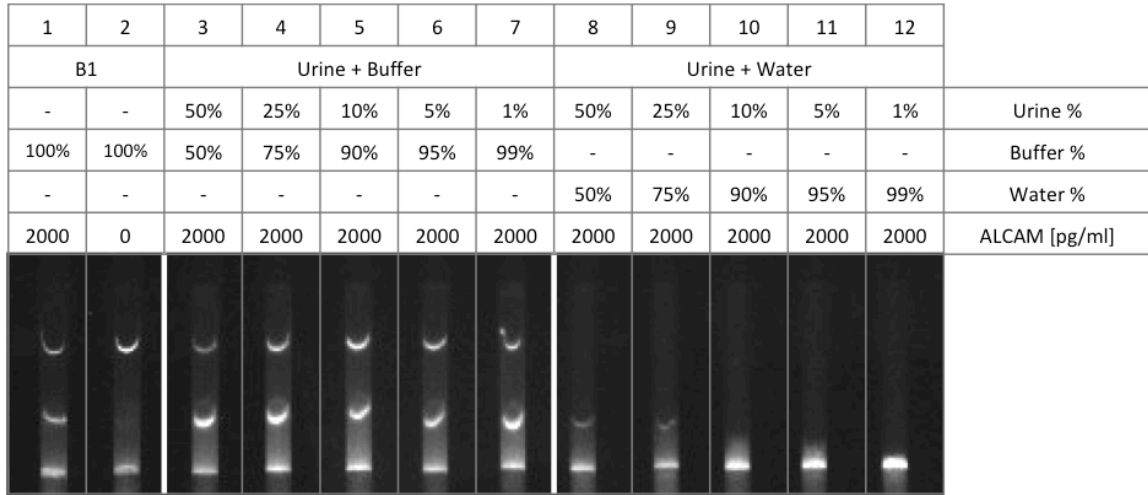


Figure 63: Human urine spiked with ALCAM was diluted with buffer and water to ascertain whether human urine inherently caused aggregation or if a buffer was required to facilitate sample flow and antigen binding.

While the addition of 50-75% water in the urine sample mixture for the ALCAM LFA does decrease aggregation enough for the flow of the phosphors to the test line, but the absence of the control line does not allow for adequate interpretation of results. Interestingly, with the increase of water percentage and the decrease of urine in the water-urine mixture, an increase in aggregation is seen at the sample pad-membrane interface alluding to the necessity of using a buffer to alleviate aggregation and facilitate the flow of the sample through the strip. When diluting the human urine with buffer, an addition of 50% buffer to the urine-buffer mixture in the ALCAM LFA prevents the aggregation and facilitates the flow of the sample mix allowing for binding at the test and control line.

For HVEM LFA in Figure 64, the dilution of human urine in water and buffer shows a similar trend of water causing aggregation while buffer reestablishes the flow of the sample mixture through the membrane.

HVEM LFA: Human Urine Dilution with Buffer and Water

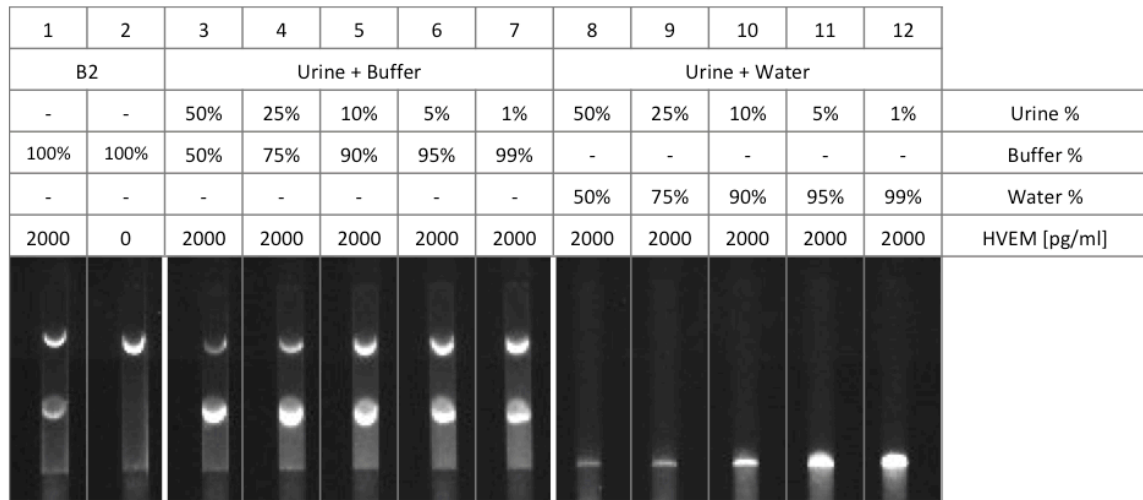


Figure 64: Human urine spiked with HVEM was diluted with buffer and water to ascertain whether human urine inherently caused aggregation or if a buffer was required to facilitate sample flow and antigen binding.

For the HVEM LFA, the addition of water to the urine mixture does not facilitate flow across the membrane and no test and control lines are seen. In the urine-buffer mixtures, high-intensity test and control lines are noted. With an increase of urine percentage in the urine-water sample mixture, a decrease in aggregation of the phosphors at the sample pad-membrane interface is seen alluding to components in urine that may prevent aggregation. Similar to ALCAM the addition of buffer in the urine-buffer mixture prevents aggregation and facilitates flow of the sample mixture through the membrane allowing for binding at the test and control line.

To understand the limiting amount of buffer needed to prevent aggregation and facilitate the flow of the sample through the membrane, the urine was diluted with buffer in decreasing proportions. 7.5 ug of phosphors was added to a sample

mixture containing 2 ng/mL of analyte in a urine-buffer mixture. A positive control of a sample mixture with 2 ng/mL of analyte in 100% buffer and a negative control of no protein buffer blank and 2 ng/mL of analyte in 100% urine was also used.

For ALCAM as seen in Figure 65, increasing urine percentage in the urine-buffer mixture decreases signal intensity at both the test and control line with aggregation and no sample slow at 100% urine as previously shown.

ALCAM LFA: Extended Human Urine Dilution with Buffer

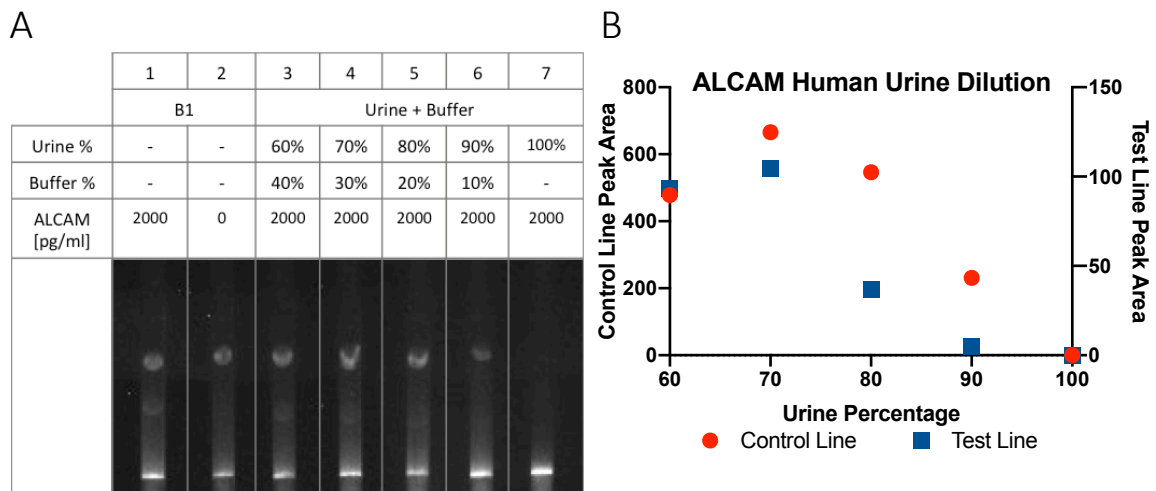


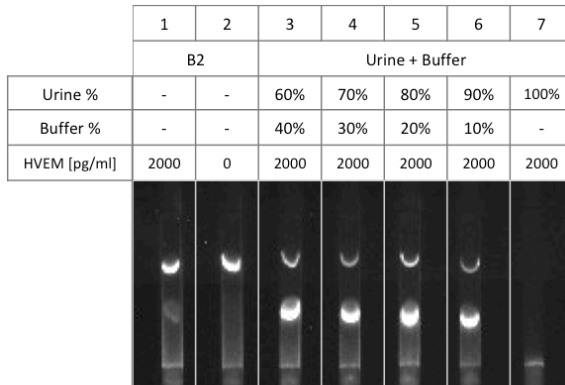
Figure 65: Human urine spiked with ALCAM was further diluted with buffer to see the minimal amount of buffer needed for sample flow and antigen binding.

In the ALCAM LFA, the dilution of 80% buffer and 20% urine allowed for the prevention of aggregation and sufficient binding at the test line, while maximum test and control line intensity was seen with a 20% buffer and 70% urine sample mixture. The urine-buffer dilutions showed comparable test line intensities as the positive control of 100% buffer. The negative control of 100% urine showed expected aggregation at the sample pad-membrane interface.

For HVEM as seen in Figure 66, high signal intensity is seen when human urine is diluted with at least 10% buffer.

HVEM LFA: Extended Human Urine Dilution with Buffer

A



B

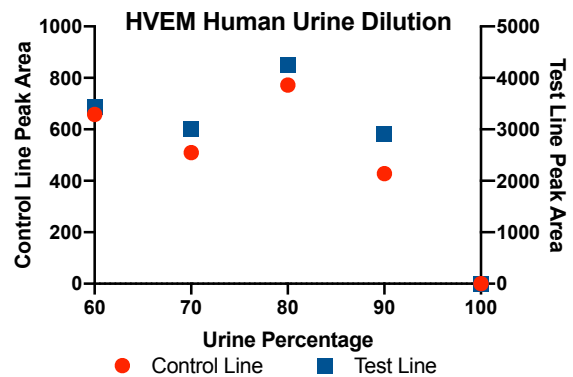


Figure 66: Human urine spiked with HVEM was further diluted with buffer To see the minimal amount of buffer needed for sample flow and antigen binding.

The dilution of at least 10% urine and 90% buffer showed no aggregation and an intense signal at the test and control lines. Increasing the buffer percentage does vary signal intensity but no trend is seen with the addition of more than 20% buffer. The urine-buffer dilutions showed higher signal than the buffer positive control as human urine with endogenous analyte was used in these dilutions. The negative control of 100% urine showed expected aggregation at the sample pad-membrane interface.

To ascertain the non-specific background signal for the ALCAM and HVEM lateral flow assays, the analytes were similarly diluted in a synthetic urine-buffer mixture of varying proportions. 5 ng/mL of ALCAM and HVEM were separately prepared in mixtures of 100%, 75%, 50%, and 0% synthetic urine with 0%, 25%, 50%, and 100% buffer. 3 ug of phosphors were added to 45 uL of each mixture and 40 uL of the sample mix was added to the strip.

For the ALCAM lateral flow assay in Figure 67, a decrease in test and control line signal intensity was seen with an increase in urine percentage in the urine-buffer mixture.

ALCAM LFA: Synthetic Urine Dilution with Buffer

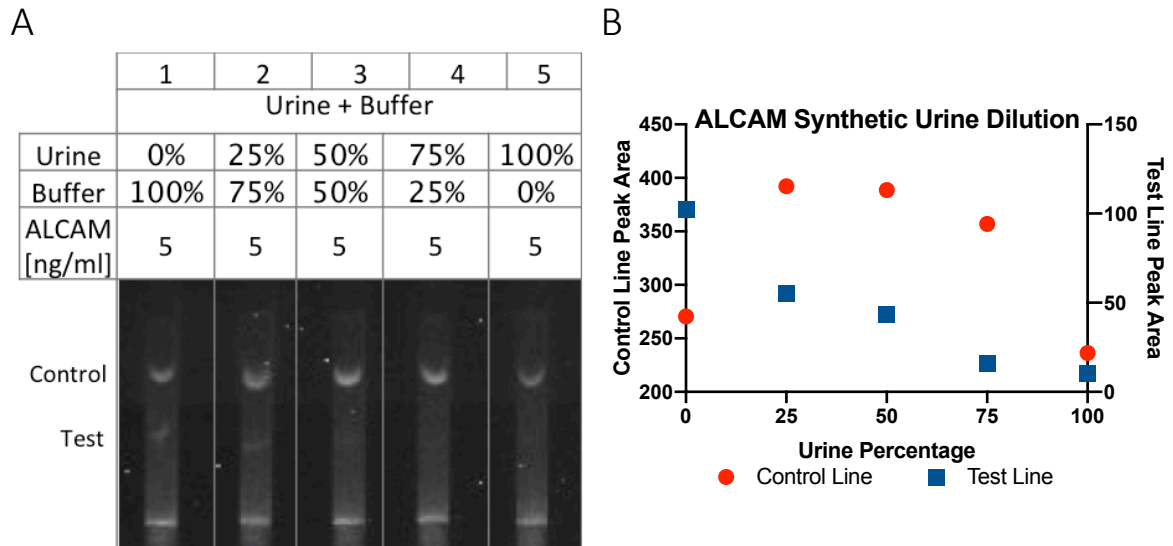


Figure 67: Synthetic urine spiked with ALCAM was diluted with buffer to see the minimal amount of buffer needed for sample flow and antigen binding and to quantitate non-specific background signal.

At least 75% buffer was needed for a positive signal at the test line. Decreasing the synthetic urine concentration did decrease the signal at the test line, showing that synthetic urine inhibits binding of ALCAM to the capture antibody. Aggregation was not seen with synthetic urine as was prominent in the human urine dilutions.

For the HVEM lateral flow assay in Figure 68, a positive test signal was seen with 100% synthetic urine without the use of a buffer.

HVEM LFA: Synthetic Urine Dilution with Buffer

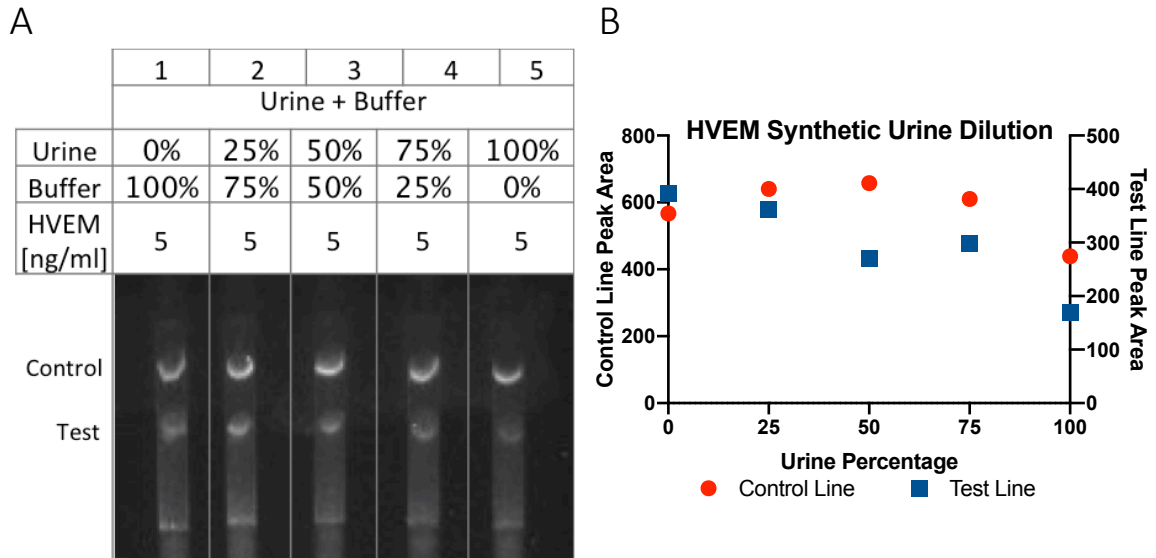


Figure 68: Synthetic urine spiked with HVEM was diluted with buffer to see the minimal amount of buffer needed for sample flow and antigen binding and to quantitate non-specific background signal.

This signal of HVEM in 100% synthetic urine shows a weaker but comparable signal to that of HVEM in 100% buffer showing that less buffer is needed to dilute the synthetic urine for the HVEM LFA when compared to the ALCAM LFA. Similar to ALCAM, almost no aggregation of PLNPs is seen at the sample pad-membrane interface.

Standard curve in synthetic urine

To determine the dynamic range of the ALCAM and HVEM lateral flow assays in synthetic urine, the analytes were diluted in synthetic urine at concentrations between 80 ng/mL and 5 ng/mL at 4-fold dilutions. This spiked synthetic urine was mixed with buffer at a 75% buffer:25% synthetic urine ratio. 3 ug of phosphors was added to 45 uL of the sample mix and 40 uL of the mixture was applied to the lateral flow strip.

As seen for the ALCAM synthetic urine standard curve in Figure 69, there is a positive correlation of signal intensity to ALCAM concentration.

ALCAM Standard Curve in Synthetic Urine

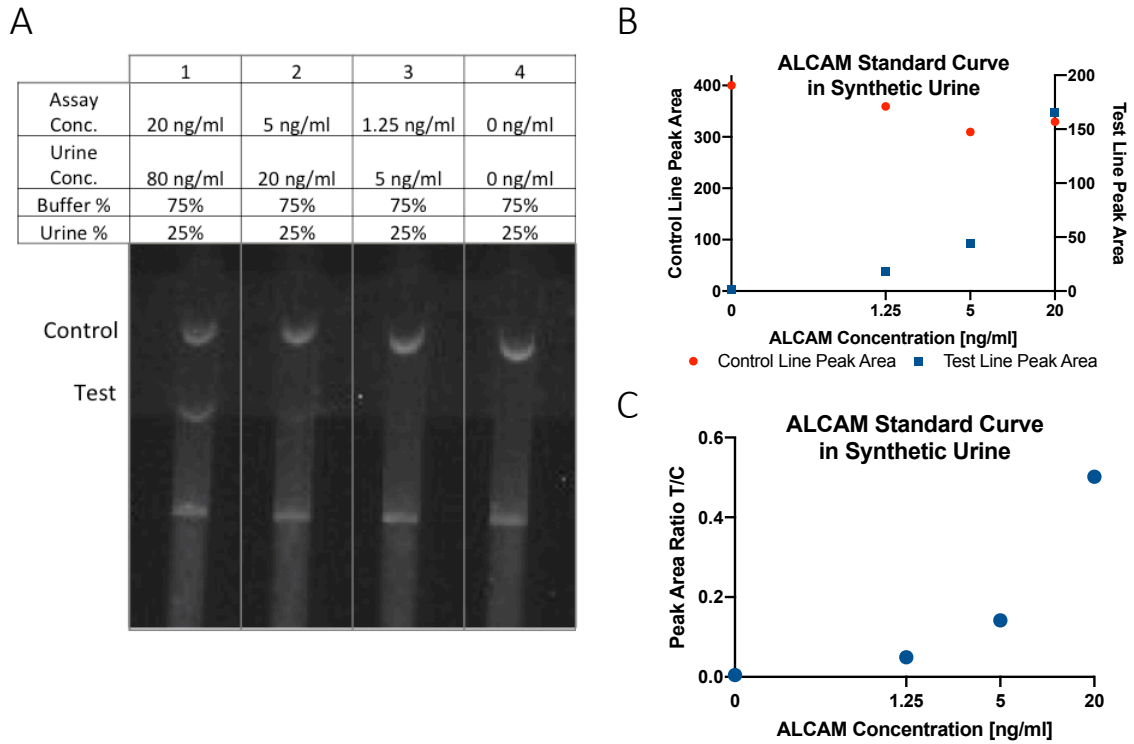


Figure 69: A standard curve of ALCAM spiked in synthetic urine showed a positive correlation of signal intensity with ALCAM concentration.

Almost no background signal is seen at a low concentration of ALCAM and the no protein buffer-synthetic urine negative control. Although the limit of detection of ALCAM cannot be empirically calculated, a positive signal is seen with at least 5 ng/mL ALCAM with a positive signal up to 20 ng/mL in this study.

Similarly, for the HVEM synthetic urine standard curve in Figure 70, a strong positive correlation of signal intensity is seen with HVEM concentration.

HVEM Standard Curve in Synthetic Urine

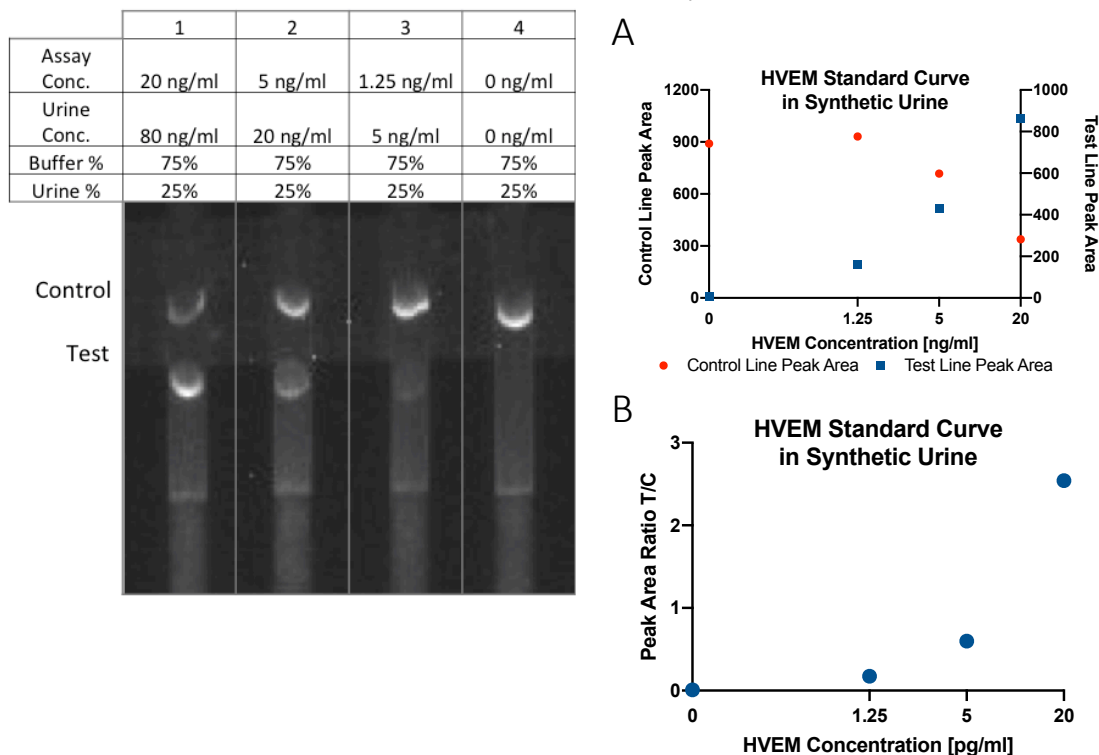


Figure 70: A standard curve of HVEM spiked in synthetic urine showed a positive correlation of signal intensity with HVEM concentration.

Again, no background signal is seen in the no-protein buffer-synthetic urine negative control. The limit of detection for HVEM is seen to be below that of the ALCAM lateral flow assay at below 5 ng/mL with a strong positive signal up to 20 ng/mL in this study.

Although the quantification of ALCAM and HVEM in synthetic urine and eventually human urine shows promise, the current limit of detection is not low enough for the detection of these molecules in clinical samples at the optimized dilution ratio. Concentrations of ALCAM and HVEM in urine range between 0-32 ng/mL and 0-40 ng/mL, respectively. With a 75% buffer:25% urine dilution, the LFAs will need to detect ALCAM and HVEM with dynamic ranges of 0-8 ng/ml and 0-10 ng/mL, respectively. With the current limit of detection at least 5 ng/mL for the

assays, further optimization of the buffer system and lateral flow assay components is warranted to increase sensitivity allowing for a quantitation of these analytes at lower concentrations. As the HVEM LFA is seen to have greater sensitivity than the ALCAM LFA, further optimization of the ALCAM LFA in terms of antibody and buffer selection may easily increase sensitivity and improve the assay.

Conclusion

This work has created and optimized a sensitive and quantitative phosphor-based lateral flow assays for the detection of ALCAM, a lupus nephritis biomarker, and HVEM, a GFR normalizing biomarker. Optimization of the buffer, membrane, and phosphor loading has shown for the assay to have a limit of detection of approximately than 125 pg/mL in buffer, far below the clinical range of ALCAM and HVEM in human urine samples. As this is the first application of these persistent luminescent nanophosphors in urine, the feasibility of the detection technology for use in urine has been evaluated and the components of the assay have been optimized for use in urine samples. Use of spiked human and synthetic urine in this optimization process has shown a 3:1 ratio of buffer to urine to be sufficient in producing a standard curve with spiked synthetic urine. Although this application in urine shows promise, current detection limits of the assay prevent the application of the LFAs in urine. Further optimization of nanophosphor stability and LFA components are expected to increase signals to values appropriate for the clinical ranges of urinary ALCAM and HVEM.

Summary of Work

Biomarkers of intricate and complicated human diseases are currently a hot topic of research due to their ability to give insight to disease that current medicine cannot visualize. Their value comes from their potential to be used in diagnostics as well as evaluating pathogenesis and understanding the disease process. This research portrays three aspects of the biomarker development pipeline: screening for stool biomarkers for pediatric inflammatory bowel disease, validation of urine normalizer proteins, and the translation of lupus nephritis urine biomarkers to point-of-care phosphor-based lateral flow assays.

Although I have gained thorough expertise in the screening of diagnostic biomarkers in many human diseases, this work has focused on the screening of pIBD biomarkers, as stool is an unconventional body fluid that deserves more attention in terms of diagnostic capability. This sample type can be very easy obtained, even from pediatric patients, and can give insight to the intestinal environment. Also of importance, but not focused on in this study, is the ability of stool to give a picture of the microbiome which continues to gain attention as an effector on an increasing number of human diseases. In this study, we have identified nine proteins have been found to be elevated in both CD and UC versus HC stool, one has been elevated in CD versus HC stool, and nine have been elevated in UC versus HC stool. Of these, ten proteins are elevated in the stools of UC patients versus CD. Some of these candidates have been already implicated in IBD literature but many molecules' relationship to IBD has yet to be investigated.

The validation of phase of the biomarker pipeline has been exemplified in the validation of pIBD biomarkers but also in the identification of HVEM as a urine normalization marker for urine biomarkers. HVEM, found to significantly correlate with creatinine across different races, pushes the application of sensitive biomarkers to clinical applications, especially to the point-of-care. Although both of these validation studies are relatively small, they exemplify the need for validation of screening technologies across different diseases and demographics.

Assay development of HVEM, urine normalizing marker, and ALCAM, a urinary active lupus nephritis biomarker, shows the potential of sensitive biomarkers at the point-of-care. With the optimization of ALCAM and HVEM lateral flow assays, the clinical utility of these biomarkers has been enhanced where a diagnostic lab and trained technician are no longer needed for the assessment of these molecules. The further optimization of persistent luminescent nanophosphors for application in urine has expanded the opportunity of these detection molecules in many other diseases.

In summary, this work has shown examples of the possibilities of biomarker research with examples in pediatric inflammatory bowel disease and lupus nephritis. Similarly, these methods can be applied to any human disease to not only improve diagnostics but also improve quality of life by reducing the need for invasive, costly procedures.

References

- [1] "Definition of biomarker - NCI Dictionary of Cancer Terms - National Cancer Institute." [Online]. Available: <https://www.cancer.gov/publications/dictionaries/cancer-terms/def/biomarker>. [Accessed: 16-Nov-2018].
- [2] A. A. Sinha, M. T. Lopez, and H. O. McDevitt, "Autoimmune diseases: the failure of self tolerance.," *Science*, vol. 248, no. 4961, pp. 1380–8, Jun. 1990.
- [3] F. Chowdhury, A. Williams, and P. Johnson, "Validation and comparison of two multiplex technologies, Luminex® and Mesoscale Discovery, for human cytokine profiling," *J. Immunol. Methods*, vol. 340, no. 1, pp. 55–64, Jan. 2009.
- [4] L. Gold, D. Ayers, J. Bertino, C. Bock, A. Bock, E. N. Brody, J. Carter, A. B. Dalby, B. E. Eaton, T. Fitzwater, D. Flather, A. Forbes, T. Foreman, C. Fowler, B. Gawande, M. Goss, M. Gunn, S. Gupta, D. Halladay, J. Heil, J. Heilig, B. Hicke, G. Husar, N. Janjic, T. Jarvis, S. Jennings, E. Katilius, T. R. Keeney, N. Kim, T. H. Koch, S. Kraemer, L. Kroiss, N. Le, D. Levine, W. Lindsey, B. Lollo, W. Mayfield, M. Mehan, R. Mehler, S. K. Nelson, M. Nelson, D. Nieuwlandt, M. Nikrad, U. Ochsner, R. M. Ostroff, M. Otis, T. Parker, S. Pietrasiewicz, D. I. Resnicow, J. Rohloff, G. Sanders, S. Sattin, D. Schneider, B. Singer, M. Stanton, A. Sterkel, A. Stewart, S. Stratford, J. D. Vaught, M. Vrkljan, J. J. Walker, M. Watrobka, S. Waugh, A. Weiss, S. K. Wilcox, A. Wolfson, S. K. Wolk, C. Zhang, and D. Zichi, "Aptamer-Based Multiplexed Proteomic Technology for Biomarker Discovery," *PLoS One*, vol. 5, no. 12, p. e15004, Dec. 2010.
- [5] R. R.-P. R. F. Huang, W. Jiang, J. Yang, Y. Q. Mao, Y. Zhang, W. Yang, D. Yang, B.

- Burkholder, R. R.-P. R. F. Huang, and R. R.-P. R. F. Huang, "A biotin label-based antibody array for high-content profiling of protein expression.," *Cancer Genomics Proteomics*, vol. 7, no. 3, pp. 129–41, May 2010.
- [6] D. J. Hunter, E. Losina, A. Guerhazi, D. Burstein, M. N. Lassere, and V. Kraus, "A pathway and approach to biomarker validation and qualification for osteoarthritis clinical trials.," *Curr. Drug Targets*, vol. 11, no. 5, pp. 536–45, May 2010.
- [7] D. A. Armbruster and T. Pry, "Limit of blank, limit of detection and limit of quantitation.," *Clin. Biochem. Rev.*, vol. 29 Suppl 1, no. Suppl 1, pp. S49-52, Aug. 2008.
- [8] N. Goossens, S. Nakagawa, X. Sun, and Y. Hoshida, "Cancer biomarker discovery and validation.," *Transl. Cancer Res.*, vol. 4, no. 3, pp. 256–269, Jun. 2015.
- [9] "Inflammatory Bowel Disease | Children's Hospital of Philadelphia." [Online]. Available: <https://www.chop.edu/conditions-diseases/inflammatory-bowel-disease>. [Accessed: 17-Nov-2018].
- [10] M. Dubinsky, "Special issues in pediatric inflammatory bowel disease.," *World J. Gastroenterol.*, vol. 14, no. 3, pp. 413–20, Jan. 2008.
- [11] "Inflammatory Bowel Disease | iCons in Medicine." [Online]. Available: <https://iconsinmedicine.wordpress.com/2011/02/28/inflammatory-bowel-disease/>. [Accessed: 20-Nov-2018].
- [12] C. Cuffari, "Diagnostic Considerations in Pediatric Inflammatory Bowel Disease Management," *Gastroenterol. Hepatol. (N. Y.)*, vol. 5, no. 11, p. 775,

2009.

- [13] S. B. Menees, C. Powell, J. Kurlander, A. Goel, and W. D. Chey, "A Meta-Analysis of the Utility of C-Reactive Protein, Erythrocyte Sedimentation Rate, Fecal Calprotectin and Fecal Lactoferrin to Exclude Inflammatory Bowel Disease in Adults With IBS," *Am. J. Gastroenterol.*, vol. 110, no. 3, pp. 444–454, Mar. 2015.
- [14] R. Palmon, S. J. Brown, and M. T. Abreu, "What is the role and significance of serum and stool biomarkers in the diagnosis of IBD?," *Inflamm. Bowel Dis.*, vol. 14, no. suppl_2, pp. S187–S189, Oct. 2008.
- [15] D. Foell, H. Wittkowski, and J. Roth, "Monitoring disease activity by stool analyses: from occult blood to molecular markers of intestinal inflammation and damage.," *Gut*, vol. 58, no. 6, pp. 859–68, Jun. 2009.
- [16] E. K. Wright, P. De Cruz, R. Gearry, A. S. Day, and M. A. Kamm, "Fecal Biomarkers in the Diagnosis and Monitoring of Crohn's Disease," *Inflamm. Bowel Dis.*, vol. 20, no. 9, pp. 1668–1677, Sep. 2014.
- [17] A. D. Sutherland, R. B. Gearry, and F. A. Frizelle, "Review of Fecal Biomarkers in Inflammatory Bowel Disease," *Dis. Colon Rectum*, vol. 51, no. 8, pp. 1283–1291, Aug. 2008.
- [18] M. Di Ruscio, F. Vernia, A. Ciccone, G. Frieri, and G. Latella, "Surrogate Fecal Biomarkers in Inflammatory Bowel Disease: Rivals or Complementary Tools of Fecal Calprotectin?," *Inflamm. Bowel Dis.*, vol. 24, no. 1, pp. 78–92, Jan. 2018.
- [19] F. S. Lehmann, E. Burri, and C. Beglinger, "The role and utility of faecal markers in inflammatory bowel disease.," *Therap. Adv. Gastroenterol.*, vol. 8, no. 1, pp. 23–36, Jan. 2015.

- [20] A. C. von Roon, L. Karamountzos, S. Purkayastha, G. E. Reese, A. W. Darzi, J. P. Teare, P. Paraskeva, and P. P. Tekkis, "Diagnostic Precision of Fecal Calprotectin for Inflammatory Bowel Disease and Colorectal Malignancy," *Am. J. Gastroenterol.*, vol. 102, no. 4, pp. 803–813, Apr. 2007.
- [21] A. M. Schoepfer, C. Beglinger, A. Straumann, M. Trummler, S. R. Vavricka, L. E. Bruegger, and F. Seibold, "Fecal Calprotectin Correlates More Closely With the Simple Endoscopic Score for Crohn's Disease (SES-CD) than CRP, Blood Leukocytes and the CDAI," *Am. J. Gastroenterol.*, vol. 105, no. 1, pp. 162–169, Jan. 2010.
- [22] U. L. Fagerberg, L. Löf, R. D. Merzoug, L.-O. Hansson, and Y. Finkel, "Fecal calprotectin levels in healthy children studied with an improved assay.," *J. Pediatr. Gastroenterol. Nutr.*, vol. 37, no. 4, pp. 468–72, Oct. 2003.
- [23] S. K. Bunn, W. M. Bisset, M. J. Main, and B. E. Golden, "Fecal calprotectin as a measure of disease activity in childhood inflammatory bowel disease.," *J. Pediatr. Gastroenterol. Nutr.*, vol. 32, no. 2, pp. 171–7, Feb. 2001.
- [24] N. E. Walsham and R. A. Sherwood, "Fecal calprotectin in inflammatory bowel disease.," *Clin. Exp. Gastroenterol.*, vol. 9, pp. 21–9, 2016.
- [25] M. R. Konikoff and L. A. Denson, "Role of fecal calprotectin as a biomarker of intestinal inflammation in inflammatory bowel disease," *Inflamm. Bowel Dis.*, vol. 12, no. 6, pp. 524–534, Jun. 2006.
- [26] A. G. Røseth, E. Aadland, and K. Grzyb, "Normalization of faecal calprotectin: a predictor of mucosal healing in patients with inflammatory bowel disease," *Scand. J. Gastroenterol.*, vol. 39, no. 10, pp. 1017–1020, Jan. 2004.

- [27] F. Costa, M. G. Mumolo, L. Ceccarelli, M. Bellini, M. R. Romano, C. Sterpi, A. Ricchiuti, S. Marchi, and M. Bottai, "Calprotectin is a stronger predictive marker of relapse in ulcerative colitis than in Crohn's disease," *Gut*, vol. 54, no. 3, pp. 364–368, Mar. 2005.
- [28] F. Costa, M. . Mumolo, M. Bellini, M. . Romano, L. Ceccarelli, P. Arpe, C. Sterpi, S. Marchi, and G. Maltinti, "Role of faecal calprotectin as non-invasive marker of intestinal inflammation," *Dig. Liver Dis.*, vol. 35, no. 9, pp. 642–647, Sep. 2003.
- [29] X. Ye, J. Huai, and J. Ding, "Diagnostic accuracy of fecal calprotectin for screening patients with colorectal cancer: A meta-analysis," 2018.
- [30] S. V. Kane, W. J. Sandborn, P. A. Rufo, A. Zholudev, J. Boone, D. Lyerly, M. Camilleri, and S. B. Hanauer, "Fecal lactoferrin is a sensitive and specific marker in identifying intestinal inflammation," *Am. J. Gastroenterol.*, vol. 98, no. 6, pp. 1309–1314, Jun. 2003.
- [31] T. Sipponen, C.-G. A. Björkesten, M. Färkkilä, H. Nuutinen, E. Savilahti, and K.-L. Kolho, "Faecal calprotectin and lactoferrin are reliable surrogate markers of endoscopic response during Crohn's disease treatment," *Scand. J. Gastroenterol.*, vol. 45, no. 3, pp. 325–331, Mar. 2010.
- [32] S. Vermeire, G. Van Assche, and P. Rutgeerts, "Laboratory markers in IBD: useful, magic, or unnecessary toys?," *Gut*, vol. 55, no. 3, pp. 426–31, Mar. 2006.
- [33] E. Mooiweer, H. H. Fidder, P. D. Siersema, R. J. F. Laheij, and B. Oldenburg, "Fecal Hemoglobin and Calprotectin Are Equally Effective in Identifying Patients with Inflammatory Bowel Disease with Active Endoscopic Inflammation," *Inflamm. Bowel Dis.*, vol. 20, no. 2, pp. 307–314, Feb. 2014.

- [34] A. Annaházi, T. Molnár, K. Farkas, A. Rosztóczy, F. Izbéki, K. Gecse, O. Inczeffi, F. Nagy, I. Földesi, M. Szűcs, M. Dabek, L. Ferrier, V. Theodorou, L. Bueno, T. Wittmann, and R. Róka, "Fecal MMP-9," *Inflamm. Bowel Dis.*, vol. 19, no. 2, pp. 316–320, Feb. 2013.
- [35] K.-L. Kolho, T. Sipponen, E. Valtonen, and E. Savilahti, "Fecal calprotectin, MMP-9, and human beta-defensin-2 levels in pediatric inflammatory bowel disease," *Int. J. Colorectal Dis.*, vol. 29, no. 1, pp. 43–50, Jan. 2014.
- [36] K. Farkas, Z. Sarodi, A. Balint, I. Foldesi, L. Tiszlavicz, M. Sz cs, T. Nyari, J. Tajti, F. Nagy, Z. Szepes, R. Bor, A. Annahazi, R. Roka, and T. Molnar, "The Diagnostic Value of a New Fecal Marker, Matrix Metalloprotease-9, in Different Types of Inflammatory Bowel Diseases," *J. Crohn's Colitis*, vol. 9, no. 3, pp. 231–237, Mar. 2015.
- [37] T. SAIKI, "Myeloperoxidase Concentrations in the Stool as a New Parameter of Inflammatory Bowel Disease.," *Kurume Med. J.*, vol. 45, no. 1, pp. 69–73, Apr. 1998.
- [38] B. Chassaing, G. Srinivasan, M. A. Delgado, A. N. Young, A. T. Gewirtz, and M. Vijay-Kumar, "Fecal Lipocalin 2, a Sensitive and Broadly Dynamic Non-Invasive Biomarker for Intestinal Inflammation," *PLoS One*, 2012.
- [39] O. H. Nielsen, P. Gionchetti, M. Ainsworth, B. Vainer, M. Campieri, N. Borregaard, and L. Kjeldsen, "Rectal dialysate and fecal concentrations of neutrophil gelatinase-associated lipocalin, interleukin-8, and tumor necrosis factor- α in ulcerative colitis," *Am. J. Gastroenterol.*, vol. 94, no. 10, pp. 2923–2928, Oct. 1999.

- [40] F. Sjöberg, D. K. Malipatlolla, P. Patel, U. Wilderäng, M. Kalm, G. Steineck, and C. Bull, "Elastase as a potential biomarker for radiation-induced gut wall injury of the distal bowel in an experimental mouse model," *Acta Oncol. (Madr)*, vol. 57, no. 8, pp. 1025–1030, Aug. 2018.
- [41] H. Silberer, B. Küppers, O. Mickisch, W. Baniewicz, M. Drescher, L. Traber, A. Kempf, and H. Schmidt-Gayk, "Fecal leukocyte proteins in inflammatory bowel disease and irritable bowel syndrome," *Clin. Lab.*, vol. 51, no. 3–4, pp. 117–26, 2005.
- [42] J. Langhorst, S. Elsenbruch, J. Koelzer, A. Rueffer, A. Michalsen, and G. J. Dobos, "Noninvasive Markers in the Assessment of Intestinal Inflammation in Inflammatory Bowel Diseases: Performance of Fecal Lactoferrin, Calprotectin, and PMN-Elastase, CRP, and Clinical Indices," *Am. J. Gastroenterol.*, vol. 103, no. 1, pp. 162–169, Jan. 2008.
- [43] M. Sattlecker, S. J. Kiddle, S. Newhouse, P. Proitsi, S. Nelson, S. Williams, C. Johnston, R. Killick, A. Simmons, E. Westman, A. Hodges, H. Soininen, I. Kłoszewska, P. Mecocci, M. Tsolaki, B. Vellas, S. Lovestone, R. J. B. Dobson, and R. J. B. Dobson, "Alzheimer's disease biomarker discovery using SOMAscan multiplexed protein technology," *Alzheimer's Dement.*, vol. 10, no. 6, pp. 724–734, Nov. 2014.
- [44] S. J. Kiddle, M. Sattlecker, P. Proitsi, A. Simmons, E. Westman, C. Bazenet, S. K. Nelson, S. Williams, A. Hodges, C. Johnston, H. Soininen, I. Kłoszewska, P. Mecocci, M. Tsolaki, B. Vellas, S. Newhouse, S. Lovestone, and R. J. B. Dobson, "Candidate Blood Proteome Markers of Alzheimer's Disease Onset and

- Progression: A Systematic Review and Replication Study,” *J. Alzheimer’s Dis.*, vol. 38, no. 3, pp. 515–531, Nov. 2013.
- [45] M. A. De Groote, P. Nahid, L. Jarlsberg, J. L. Johnson, M. Weiner, G. Muzanyi, N. Janjic, D. G. Sterling, and U. A. Ochsner, “Elucidating Novel Serum Biomarkers Associated with Pulmonary Tuberculosis Treatment,” *PLoS One*, vol. 8, no. 4, p. e61002, Apr. 2013.
- [46] P. Nahid, E. Bliven-Sizemore, L. G. Jarlsberg, M. A. De Groote, J. L. Johnson, G. Muzanyi, M. Engle, M. Weiner, N. Janjic, D. G. Sterling, and U. A. Ochsner, “Aptamer-based proteomic signature of intensive phase treatment response in pulmonary tuberculosis,” *Tuberculosis*, vol. 94, no. 3, pp. 187–196, May 2014.
- [47] Y. Hathout, E. Brody, P. R. Clemens, L. Cripe, R. K. DeLisle, P. Furlong, H. Gordish-Dressman, L. Hache, E. Henricson, E. P. Hoffman, Y. M. Kobayashi, A. Lorts, J. K. Mah, C. McDonald, B. Mehler, S. Nelson, M. Nikrad, B. Singer, F. Steele, D. Sterling, H. L. Sweeney, S. Williams, and L. Gold, “Large-scale serum protein biomarker discovery in Duchenne muscular dystrophy,” *Proc. Natl. Acad. Sci.*, vol. 112, no. 23, pp. 7153–7158, Jun. 2015.
- [48] R. M. Ostroff, W. L. Bigbee, W. Franklin, L. Gold, M. Mehan, Y. E. Miller, H. I. Pass, W. N. Rom, J. M. Siegfried, A. Stewart, J. J. Walker, J. L. Weissfeld, S. Williams, D. Zichi, and E. N. Brody, “Unlocking Biomarker Discovery: Large Scale Application of Aptamer Proteomic Technology for Early Detection of Lung Cancer,” *PLoS One*, vol. 5, no. 12, p. e15003, Dec. 2010.
- [49] M. R. Mehan, S. A. Williams, J. M. Siegfried, W. L. Bigbee, J. L. Weissfeld, D. O.

- Wilson, H. I. Pass, W. N. Rom, T. Muley, M. Meister, W. Franklin, Y. E. Miller, E. N. Brody, and R. M. Ostroff, "Validation of a blood protein signature for non-small cell lung cancer," *Clin. Proteomics*, vol. 11, no. 1, p. 32, 2014.
- [50] R. M. Ostroff, M. R. Mehan, A. Stewart, D. Ayers, E. N. Brody, S. A. Williams, S. Levin, B. Black, M. Harbut, M. Carbone, C. Goparaju, and H. I. Pass, "Early Detection of Malignant Pleural Mesothelioma in Asbestos-Exposed Individuals with a Noninvasive Proteomics-Based Surveillance Tool," *PLoS One*, vol. 7, no. 10, p. e46091, Oct. 2012.
- [51] P. Ganz, B. Heidecker, K. Hveem, C. Jonasson, S. Kato, M. R. Segal, D. G. Sterling, and S. A. Williams, "Development and Validation of a Protein-Based Risk Score for Cardiovascular Outcomes Among Patients With Stable Coronary Heart Disease," *JAMA*, vol. 315, no. 23, p. 2532, Jun. 2016.
- [52] T. Liu, R. Xue, L. Dong, H. Wu, D. Zhang, and X. Shen, "Rapid determination of serological cytokine biomarkers for hepatitis B virus-related hepatocellular carcinoma using antibody microarrays," *Acta Biochim. Biophys. Sin. (Shanghai)*, vol. 43, no. 1, pp. 45–51, Jan. 2011.
- [53] H. C. Toh, W.-W. Wang, W. K. Chia, P. Kvistborg, L. Sun, K. Teo, Y. P. Phoon, Y. Soe, S. H. Tan, S. W. Hee, K. F. Foo, S. Ong, W. H. Koo, M.-B. Zocca, and M. H. Claesson, "Clinical Benefit of Allogeneic Melanoma Cell Lysate-Pulsed Autologous Dendritic Cell Vaccine in MAGE-Positive Colorectal Cancer Patients," *Clin. Cancer Res.*, vol. 15, no. 24, pp. 7726–7736, Dec. 2009.
- [54] U. R. Chowdhury, B. J. Madden, M. C. Charlesworth, and M. P. Fautsch, "Proteome Analysis of Human Aqueous Humor," *Investig. Ophthalmology Vis.*

Sci., vol. 51, no. 10, p. 4921, Oct. 2010.

- [55] C. Torres, A. Linares, M. J. Alejandre, R. J. Palomino-Morales, O. Caba, J. Prados, A. Aránega, J. R. Delgado, A. Irigoyen, J. Martínez-Galán, F. M. Ortuño, I. Rojas, and S. Perales, "Prognosis Relevance of Serum Cytokines in Pancreatic Cancer," *Biomed Res. Int.*, vol. 2015, pp. 1–12, Aug. 2015.
- [56] H. Jiang, L. Zhang, Y. Yu, M. Liu, X. Jin, P. Zhang, P. Yu, S. Zhang, H. Zhu, R. Chen, Y. Zou, and J. Ge, "A pilot study of angiogenin in heart failure with preserved ejection fraction: a novel potential biomarker for diagnosis and prognosis?," *J. Cell. Mol. Med.*, vol. 18, no. 11, pp. 2189–2197, Nov. 2014.
- [57] H. Chen, Y. Wang, C. Bai, and X. Wang, "Alterations of plasma inflammatory biomarkers in the healthy and chronic obstructive pulmonary disease patients with or without acute exacerbation," *J. Proteomics*, vol. 75, no. 10, pp. 2835–2843, Jun. 2012.
- [58] S. Meltzer, E. Kalanxhi, H. H. Hektoen, S. Dueland, K. Flatmark, K. R. Redalen, and A. H. Ree, "Systemic release of osteoprotegerin during oxaliplatin-containing induction chemotherapy and favorable systemic outcome of sequential radiotherapy in rectal cancer," *Oncotarget*, vol. 7, no. 23, pp. 34907–17, Jun. 2016.
- [59] L. E. Edsberg, J. T. Wyffels, M. S. Brogan, and K. M. Fries, "Analysis of the proteomic profile of chronic pressure ulcers," *Wound Repair Regen.*, vol. 20, no. 3, pp. 378–401, May 2012.
- [60] P. Lu, D.-C. Zheng, C. Fang, J.-M. Huang, W.-J. Ke, L.-Y. Wang, W.-Y. Zeng, H.-P. Zheng, and B. Yang, "Cytokines in cerebrospinal fluid of neurosyphilis

- patients: Identification of Urokinase plasminogen activator using antibody microarrays," *J. Neuroimmunol.*, vol. 293, pp. 39–44, Apr. 2016.
- [61] A. J. Onderdijk, A. S. Ijpma, S. P. Menting, E. M. Baerveldt, and E. P. Prens, "Potential serum biomarkers of treatment response to ustekinumab in patients with psoriasis: a pilot study," *Br. J. Dermatol.*, vol. 173, no. 6, pp. 1536–1539, Dec. 2015.
- [62] H.-P. Wang, Y.-Y. Wang, J. Pan, R. Cen, and Y.-K. Cai, "Evaluation of specific fecal protein biochips for the diagnosis of colorectal cancer.," *World J. Gastroenterol.*, vol. 20, no. 5, pp. 1332–9, Feb. 2014.
- [63] H. Wickham, "readxl: Read Excel Files." 2016.
- [64] R Core Team, "R: A language and environment for statistical computing." Vienna, Austria, 2016.
- [65] F. E. J. Harrell, "Hmisc: Harrell Miscellaneous." 2016.
- [66] N. A. O’Leary, M. W. Wright, J. R. Brister, S. Ciufu, D. Haddad, R. McVeigh, B. Rajput, B. Robbertse, B. Smith-White, D. Ako-Adjei, A. Astashyn, A. Badretdin, Y. Bao, O. Blinkova, V. Brover, V. Chetvernin, J. Choi, E. Cox, O. Ermolaeva, C. M. Farrell, T. Goldfarb, T. Gupta, D. Haft, E. Hatcher, W. Hlavina, V. S. Joardar, V. K. Kodali, W. Li, D. Maglott, P. Masterson, K. M. McGarvey, M. R. Murphy, K. O’Neill, S. Pujar, S. H. Rangwala, D. Rausch, L. D. Riddick, C. Schoch, A. Shkeda, S. S. Storz, H. Sun, F. Thibaud-Nissen, I. Tolstoy, R. E. Tully, A. R. Vatsan, C. Wallin, D. Webb, W. Wu, M. J. Landrum, A. Kimchi, T. Tatusova, M. DiCuccio, P. Kitts, T. D. Murphy, and K. D. Pruitt, "Reference sequence (RefSeq) database at NCBI: current status, taxonomic expansion, and functional annotation,"

Nucleic Acids Res., vol. 44, no. D1, pp. D733–D745, Jan. 2016.

- [67] I. C. Lawrance, C. Fiocchi, and S. Chakravarti, "Ulcerative colitis and Crohn's disease: distinctive gene expression profiles and novel susceptibility candidate genes," *Hum. Mol. Genet.*, vol. 10, no. 5, pp. 445–456, Mar. 2001.
- [68] A. M. Bowcock, W. Shannon, F. Du, J. Duncan, K. Cao, K. Aftergut, J. Catier, M. A. Fernandez-Vina, and A. Menter, "Insights into psoriasis and other inflammatory diseases from large-scale gene expression studies," *Hum. Mol. Genet.*, vol. 10, no. 17, pp. 1793–1805, Aug. 2001.
- [69] M. Järvinen, A. Rinne, and V. K. Hopsu-Havu, "Human cystatins in normal and diseased tissues — a review," *Acta Histochem.*, vol. 82, no. 1, pp. 5–18, Jan. 1987.
- [70] F. Rieder, G. Paul, E. Schnoy, S. Schleder, A. Wolf, F. Kamm, A. Dirmeier, U. Strauch, F. Obermeier, R. Lopez, J.-P. Achkar, G. Rogler, and F. Klebl, "Hemoglobin and Hematocrit Levels in the Prediction of Complicated Crohn's Disease Behavior – A Cohort Study," *PLoS One*, vol. 9, no. 8, p. e104706, Aug. 2014.
- [71] A. Stadnicki, U. Mazurek, D. Plewka, and T. Wilczok, "Intestinal tissue kallikrein–kallistatin profile in inflammatory bowel disease," *Int. Immunopharmacol.*, vol. 3, no. 7, pp. 939–944, Jul. 2003.
- [72] M. DEVANI, M. VECCHI, S. FERRERO, E. AVESANI, C. ARIZZI, L. CHAO, R. COLMAN, and M. CUGNO, "Kallikrein–kinin system in inflammatory bowel diseases: Intestinal involvement and correlation with the degree of tissue inflammation," *Dig. Liver Dis.*, vol. 37, no. 9, pp. 665–673, Sep. 2005.

- [73] S. O'Sullivan, J. F. Gilmer, and C. Medina, "Matrix metalloproteinases in inflammatory bowel disease: An update," *Mediators of Inflammation*. 2015.
- [74] B. Eksteen, E. Liaskou, and D. H. Adams, "Lymphocyte homing and its role in the pathogenesis of IBD," *Inflamm. Bowel Dis.*, vol. 14, no. 9, pp. 1298–1312, Sep. 2008.
- [75] K. O. Arseneau and F. Cominelli, "Targeting leukocyte trafficking for the treatment of inflammatory bowel disease," *Clin. Pharmacol. Ther.*, vol. 97, no. 1, pp. 22–8, Jan. 2015.
- [76] G. Bamias, D. J. Clark, and J. Rivera-Nieves, "Leukocyte traffic blockade as a therapeutic strategy in inflammatory bowel disease," *Curr. Drug Targets*, vol. 14, no. 12, pp. 1490–500, Nov. 2013.
- [77] A. M. Manicone and J. K. McGuire, "Matrix metalloproteinases as modulators of inflammation," *Semin. Cell Dev. Biol.*, vol. 19, no. 1, pp. 34–41, Feb. 2008.
- [78] X. Wang, Y. Y. Yu, S. Lieu, F. Yang, J. Lang, C. Lu, Z. Werb, D. Hu, T. Mclau, R. Marcucio, and C. Colnot, "MMP9 regulates the cellular response to inflammation after skeletal injury," *Bone*, vol. 52, no. 1, pp. 111–9, Jan. 2013.
- [79] M. Corbel, C. Belleguic, E. Boichot, and V. Lagente, "Involvement of gelatinases (MMP-2 and MMP-9) in the development of airway inflammation and pulmonary fibrosis," *Cell Biol. Toxicol.*, vol. 18, no. 1, pp. 51–61, 2002.
- [80] G. V. Halade, Y.-F. Jin, and M. L. Lindsey, "Matrix metalloproteinase (MMP)-9: A proximal biomarker for cardiac remodeling and a distal biomarker for inflammation," *Pharmacol. Ther.*, vol. 139, no. 1, pp. 32–40, Jul. 2013.
- [81] R. L. Warner, N. Bhagavathula, K. C. Nerusu, H. Lateef, E. Younkin, K. J. Johnson,

- and J. Varani, "Matrix metalloproteinases in acute inflammation: induction of MMP-3 and MMP-9 in fibroblasts and epithelial cells following exposure to pro-inflammatory mediators in vitro," *Exp. Mol. Pathol.*, vol. 76, no. 3, pp. 189–195, Jun. 2004.
- [82] M. Russell, N. Prokoph, N. Henderson, S. Eketjäll, C. A. Balendran, E. Michaëlsson, M. Fidock, and G. Hughes, "Determining myeloperoxidase activity and protein concentration in a single assay: Utility in biomarker and therapeutic studies," *J. Immunol. Methods*, vol. 449, pp. 76–79, Oct. 2017.
- [83] J. Broekroelofs, A. H. L. Mulder, G. F. Nelis, B. D. Westerveld, J. W. Cohen Tervaert, and C. G. M. Kallenberg, "Anti-Neutrophil Cytoplasmic Antibodies (ANCA) in Sera from Patients with Inflammatory Bowel Disease (IBD) Relation to Disease Pattern and Disease Activity," 1994.
- [84] J. J. Kim, M. S. Shajib, M. M. Manocha, and W. I. Khan, "Investigating intestinal inflammation in DSS-induced model of IBD.," *J. Vis. Exp.*, no. 60, Feb. 2012.
- [85] J. Royet, D. Gupta, and R. Dziarski, "Peptidoglycan recognition proteins: modulators of the microbiome and inflammation," *Nat. Rev. Immunol.*, vol. 11, no. 12, pp. 837–851, Dec. 2011.
- [86] F. Zulfiqar, I. Hozo, S. Rangarajan, R. A. Mariuzza, R. Dziarski, and D. Gupta, "Genetic Association of Peptidoglycan Recognition Protein Variants with Inflammatory Bowel Disease," *PLoS One*, 2013.
- [87] E. Dukhanina, T. Lukyanova, E. Romanova, V. Guerriero, N. Gnuchev, G. Georgiev, D. Yashin, and L. Sashchenko, "A new role for PGRP-S (Tag7) in immune defense: lymphocyte migration is induced by a chemoattractant

- complex of Tag7 with Mts1," *Cell Cycle*, vol. 14, no. 22, pp. 3635–3643, Nov. 2015.
- [88] H. Liu, Y. Liu, Y. Li, Z. Liu, L. Li, S. Ding, Y. Wang, T. Zhang, L. Li, Z. Shao, and R. Fu, "Proteinase 3 expression on the neutrophils of patients with paroxysmal nocturnal hemoglobinuria," *Exp. Ther. Med.*, vol. 15, no. 3, pp. 2525–2532, Mar. 2018.
- [89] J. A. Rump, J. Schölmerich, V. Gross, M. Roth, R. Helfesrieder, A. Rautmann, J. Lüdemann, W. L. Gross, and H. H. Peter, "A New Type of Perinuclear Anti-Neutrophil Cytoplasmic Antibody (p-ANCA) in Active Ulcerative Colitis but not in Crohn's Disease," *Immunobiology*, vol. 181, no. 4–5, pp. 406–413, Nov. 1990.
- [90] A. Carroccio, G. Vitale, L. Di Prima, N. Chifari, S. Napoli, C. La Russa, G. Gulotta, M. R. Averna, G. Montalto, S. Mansueto, A. Notarbartolo, and M. R. Averna, "Comparison of anti-transglutaminase ELISAs and an anti-endomysial antibody assay in the diagnosis of celiac disease: a prospective study," *Clin. Chem.*, vol. 48, no. 9, pp. 1546–50, Sep. 2002.
- [91] D. Walkiewicz, S. L. Werlin, D. Fish, M. Scanlon, P. Hanaway, and S. Kugathasan, "Fecal calprotectin is useful in predicting disease relapse in pediatric inflammatory bowel disease," *Inflamm. Bowel Dis.*, vol. 14, no. 5, pp. 669–673, May 2008.
- [92] D. Benet, B. Dhas, B. V. Bhat, and D. B. Gane, "Role of Calprotectin in Infection and Inflammation," *Curr Pediatr Res*, vol. 16, no. 2, pp. 83–94, 2012.
- [93] M. Ichikawa, R. Williams, L. Wang, T. Vogl, and G. Srikrishna, "S100A8/A9

- activate key genes and pathways in colon tumor progression.," *Mol. Cancer Res.*, vol. 9, no. 2, pp. 133–48, Feb. 2011.
- [94] D. Xi, T. Luo, H. Xiong, J. Liu, H. Lu, M. Li, Y. Hou, and Z. Guo, "SAP: structure, function, and its roles in immune-related diseases," *Int. J. Cardiol.*, vol. 187, pp. 20–26, May 2015.
- [95] A. L. Wester, M. H. Vatn, and O. Fausa, "Secondary Amyloidosis in Inflammatory Bowel Disease: A Study of 18 Patients Admitted to Rikshospitalet University Hospital, Oslo, from 1962 to 1998," *Inflamm. Bowel Dis.*, vol. 7, no. 4, pp. 295–300, Nov. 2001.
- [96] M. J. Gitkind and S. C. Wright, "Amyloidosis Complicating Inflammatory Bowel Disease A Case Report and Review of the Literature," 1990.
- [97] I. Serra, B. Oller, M. Mañosa, J. E. Naves, Y. Zabana, E. Cabré, and E. Domènech, "Systemic amyloidosis in inflammatory bowel disease: Retrospective study on its prevalence, clinical presentation, and outcome," *J. Crohn's Colitis*, vol. 4, no. 3, pp. 269–274, Sep. 2010.
- [98] A. J. Greenstein, D. B. Sachar, A. K. Panday, S. H. Dikman, S. Meyers, T. Heimann, V. Gumaste, J. L. Werther, and H. D. Janowitz, "Amyloidosis and inflammatory bowel disease. A 50-year experience with 25 patients.," *Medicine (Baltimore)*, vol. 71, no. 5, pp. 261–70, Sep. 1992.
- [99] Y. K. Park, D. S. Han, and C. S. Eun, "Systemic amyloidosis with Crohn's disease treated with infliximab," *Inflamm. Bowel Dis.*, vol. 14, no. 3, pp. 431–432, Mar. 2008.
- [100] F. Sánchez de Medina, O. Martínez-Augustin, R. González, I. Ballester, A. Nieto,

- J. Gálvez, and A. Zarzuelo, "Induction of alkaline phosphatase in the inflamed intestine: a novel pharmacological target for inflammatory bowel disease," *Biochem. Pharmacol.*, vol. 68, no. 12, pp. 2317–2326, Dec. 2004.
- [101] R. López-Posadas, R. González, I. Ballester, P. Martínez-Moya, I. Romero-Calvo, M. D. Suárez, A. Zarzuelo, O. Martínez-Augustin, and F. Sánchez de Medina, "Tissue-nonspecific alkaline phosphatase is activated in enterocytes by oxidative stress via changes in glycosylation," *Inflamm. Bowel Dis.*, vol. 17, no. 2, pp. 543–556, Feb. 2011.
- [102] J. Fawley and D. M. Gourlay, "Intestinal alkaline phosphatase: a summary of its role in clinical disease," *J. Surg. Res.*, vol. 202, no. 1, pp. 225–234, May 2016.
- [103] K. Molnár, Á. Vannay, B. Szebeni, N. F. Bánki, E. Sziksz, Á. Cseh, H. Gyorffy, P. L. Lakatos, M. Papp, A. Arató, and G. Veres, "Intestinal alkaline phosphatase in the colonic mucosa of children with inflammatory bowel disease," *World J. Gastroenterol.*, 2012.
- [104] A. Tuin, K. Poelstra, A. de Jager-Krikken, L. Bok, W. Raaben, M. P. Velders, and G. Dijkstra, "Role of alkaline phosphatase in colitis in man and rats," *Gut*, vol. 58, no. 3, pp. 379–387, Mar. 2009.
- [105] S. Ramasamy, D. D. Nguyen, M. A. Eston, S. Nasrin Alam, A. K. Moss, F. Ebrahimi, B. Biswas, G. Mostafa, K. T. Chen, K. Kaliannan, H. Yammine, S. Narisawa, J. L. Millán, S. H. Warren, E. L. Hohmann, E. Mizoguchi, H.-C. Reinecker, A. K. Bhan, S. B. Snapper, M. S. Malo, and R. A. Hodin, "Intestinal alkaline phosphatase has beneficial effects in mouse models of chronic colitis," *Inflamm. Bowel Dis.*, vol. 17, no. 2, pp. 532–542, Feb. 2011.

- [106] M. Lukas, P. Drastich, M. Konecny, P. Gionchetti, O. Urban, F. Cantoni, M. Bortlik, D. Duricova, and M. Bulitta, "Exogenous alkaline phosphatase for the treatment of patients with moderate to severe ulcerative colitis," *Inflamm. Bowel Dis.*, vol. 16, no. 7, pp. 1180–1186, Jul. 2010.
- [107] L. Biancone, F. Scopinaro, M. Maletta, G. Monteleone, F. Luzzza, M. Banci, P. Mercantini, T. Renda, and F. Pallone, "Circulating D dimer in inflammatory bowel disease," *Ital. J. Gastroenterol.*, vol. 26, no. 3, pp. 116–20, Apr. 1994.
- [108] J. C. Souto, E. Martínez, M. Roca, J. Mateo, J. Pujol, D. González, and J. Fontcuberta, "Prothrombotic state and signs of endothelial lesion in plasma of patients with inflammatory bowel disease," *Dig. Dis. Sci.*, vol. 40, no. 9, pp. 1883–1889, Sep. 1995.
- [109] A. Canero, D. Parmeggiani, N. Avenia, P. F. Atelli, L. Goffredi, R. Peltrini, I. Madonna, P. Ambrosino, S. Apperti, and M. Apperti, "Thromboembolic tendency (TE) in IBD (Inflammatory bowel disease) patients.," *Ann. Ital. Chir.*, vol. 83, no. 4, pp. 313–7.
- [110] R. W. TALBOT, J. HEPPELL, R. R. DOZOIS, and R. W. BEART, "Vascular Complications of Inflammatory Bowel Disease," *Mayo Clin. Proc.*, 1986.
- [111] C. Dolapcioglu, A. Soyly, T. Kendir, A. T. Ince, H. Dolapcioglu, S. Purisa, C. Bolukbas, H. M. Sokmen, R. Dalay, and O. Ovunc, "Coagulation parameters in inflammatory bowel disease," *Int. J. Clin. Exp. Med.*, 2014.
- [112] P. Miranda-García, M. Chaparro, and J. P. Gisbert, "P103 Correlation between serological biomarkers and clinical activity in patients with inflammatory bowel disease (IBD)," *J. Crohn's Colitis*, vol. 6, no. Supplement_1, p. S51, Feb.

2012.

- [113] R. Pankov and K. M. Yamada, "Fibronectin at a glance," *J. Cell Sci.*, vol. 115, no. Pt 20, pp. 3861–3, Oct. 2002.
- [114] J. Brenmoehl, W. Falk, M. Göke, J. Schölmerich, and G. Rogler, "Inflammation modulates fibronectin isoform expression in colonic lamina propria fibroblasts (CLPF)," *Int. J. Colorectal Dis.*, vol. 23, no. 10, pp. 947–955, Oct. 2008.
- [115] J. Dammeier, M. Brauchle, W. Falk, G. R. Grotendorst, and S. Werner, "Connective tissue growth factor: a novel regulator of mucosal repair and fibrosis in inflammatory bowel disease?," *Int. J. Biochem. Cell Biol.*, vol. 30, no. 8, pp. 909–22, Aug. 1998.
- [116] A. C. Petrey and C. A. de la Motte, "The extracellular matrix in IBD," *Curr. Opin. Gastroenterol.*, vol. 33, no. 4, pp. 234–238, Jul. 2017.
- [117] T. Vanuytsel, S. Vermeire, and I. Cleynen, "The role of Haptoglobin and its related protein, Zonulin, in inflammatory bowel disease," *Tissue Barriers*. 2013.
- [118] M. Papp, P. L. Lakatos, K. Palatka, I. Foldi, M. Udvardy, J. Harsfalvi, I. Tornai, Z. Vitalis, T. Dinya, A. Kovacs, T. Molnar, P. Demeter, J. Papp, L. Lakatos, I. Altorjay, P. Fuszek, H. C. Horvath, P. Vargha, S. Fischer, J. Osztoivits, L. Bene, F. Nagy, J. Lonovics, L. Balint, F. Huoranszky, I. Dobo, Z. Tulassay, L. Herszenyi, P. Miheller, A. Nemeth, G. Szekely, Z. Erdelyi, G. Mester, C. Molnar, and T. Pandur, "Haptoglobin polymorphisms are associated with Crohn's disease, disease behavior, and extraintestinal manifestations in hungarian patients," *Dig. Dis.*

Sci., 2007.

- [119] I. Maza, R. Miller-Lotan, A. P. Levy, S. Nesher, A. Karban, and R. Eliakim, "The association of Haptoglobin polymorphism with Crohn's disease in Israel," *J. Crohn's Colitis*, vol. 2, no. 3, pp. 214–218, Sep. 2008.
- [120] L. Marquez, I. Cleynen, K. Machiels, S. Organe, M. Ferrante, L. Henckaerts, V. Ballet, P. J. Rutgeerts, and S. Vermeire, "W1237 Haptoglobin Polymorphisms are Associated With Ulcerative Colitis and Crohn's Disease," *Gastroenterology*, vol. 138, no. 5, p. S-680-S-681, May 2010.
- [121] J. Yang, D. Goetz, J.-Y. Li, W. Wang, K. Mori, D. Setlik, T. Du, H. Erdjument-Bromage, P. Tempst, R. Strong, and J. Barasch, "An Iron Delivery Pathway Mediated by a Lipocalin," *Mol. Cell*, vol. 10, no. 5, pp. 1045–1056, Nov. 2002.
- [122] K. A. Oikonomou, A. N. Kapsoritakis, A. I. Kapsoritaki, A. C. Manolakis, E. K. Tiaka, F. D. Tsiopoulos, I. A. Tsiompanidis, and S. P. Potamianos, "Angiogenin, angiopoietin-1, angiopoietin-2, and endostatin serum levels in inflammatory bowel disease," *Inflamm. Bowel Dis.*, 2011.
- [123] K. A. Oikonomou, A. N. Kapsoritakis, C. Theodoridou, D. Karangelis, A. Germanis, I. Stefanidis, and S. P. Potamianos, "Neutrophil gelatinase-associated lipocalin (NGAL) in inflammatory bowel disease: association with pathophysiology of inflammation, established markers, and disease activity," *J. Gastroenterol.*, vol. 47, no. 5, pp. 519–530, May 2012.
- [124] J. Stallhofer, M. Friedrich, A. Konrad-Zerna, M. Wetzke, P. Lohse, J. Glas, C. Tillack-Schreiber, F. Schnitzler, F. Beigel, and S. Brand, "Lipocalin-2 Is a Disease Activity Marker in Inflammatory Bowel Disease Regulated by IL-17A,

IL-22, and TNF- α and Modulated by IL23R Genotype Status," *Inflamm. Bowel Dis.*, 2015.

- [125] E. Pirilä, N. S. Ramamurthy, T. Sorsa, T. Salo, J. Hietanen, and P. Maisi, "Gelatinase A (MMP-2), Collagenase-2 (MMP-8), and Laminin-5 γ 2-Chain Expression in Murine Inflammatory Bowel Disease (Ulcerative Colitis)," *Dig. Dis. Sci.*, vol. 48, no. 1, pp. 93–98, 2003.
- [126] P. J. Koelink, S. A. Overbeek, S. Braber, M. E. Morgan, P. A. J. Henricks, M. A. Roda, H. W. Verspaget, S. C. Wolfkamp, A. A. Te Velde, C. W. Jones, P. L. Jackson, J. E. Blalock, R. W. Sparidans, J. A. W. Kruijtzter, J. Garssen, G. Folkerts, and A. D. Kraneveld, "Collagen degradation and neutrophilic infiltration: A vicious circle in inflammatory bowel disease," *Gut*, 2014.
- [127] L. Mäkitalo, H. Rintamäki, T. Tervahartiala, T. Sorsa, and K.-L. Kolho, "Serum MMPs 7–9 and their inhibitors during glucocorticoid and anti-TNF- α therapy in pediatric inflammatory bowel disease," *Scand. J. Gastroenterol.*, vol. 47, no. 7, pp. 785–794, Jul. 2012.
- [128] A. R. Morgan, D. Y. Han, W. J. Lam, C. M. Triggs, A. G. Fraser, M. Barclay, R. B. Geary, S. Meisner, P. Stokkers, G. E. Boeckxstaens, and L. R. Ferguson, "Genetic variations in matrix metalloproteinases may be associated with increased risk of ulcerative colitis," *Hum. Immunol.*, 2011.
- [129] U. Jain, Q. Cao, N. A. Thomas, T. M. Woodruff, W. J. Schwaeble, C. M. Stover, and A. W. Stadnyk, "Properdin provides protection from *Citrobacter rodentium*-induced intestinal inflammation in a C5a/IL-6-dependent manner," *J. Immunol.*, vol. 194, no. 7, pp. 3414–21, Apr. 2015.

- [130] U. Jain, C. A. Midgen, W. J. Schwaeble, C. M. Stover, and A. W. Stadnyk, "Properdin Regulation of Complement Activation Affects Colitis in Interleukin 10 Gene-Deficient Mice," *Inflamm. Bowel Dis.*, vol. 21, no. 7, pp. 1519–1528, Jul. 2015.
- [131] A. M. Lake, A. E. Stitzel, J. R. Urmson, W. A. Walker, and R. E. Spitzer, "Complement alterations in inflammatory bowel disease," *Gastroenterology*, vol. 76, no. 6, pp. 1374–1379, Jun. 1979.
- [132] C. M. Steppan and M. A. Lazar, "Resistin and obesity-associated insulin resistance," *Trends Endocrinol. Metab.*, vol. 13, no. 1, pp. 18–23, Jan. 2002.
- [133] C. M. Steppan, S. T. Bailey, S. Bhat, E. J. Brown, R. R. Banerjee, C. M. Wright, H. R. Patel, R. S. Ahima, and M. A. Lazar, "The hormone resistin links obesity to diabetes," *Nature*, vol. 409, no. 6818, pp. 307–312, Jan. 2001.
- [134] C. McTernan, P. McTernan, A. Harte, P. Levick, A. Barnett, and S. Kumar, "Resistin, central obesity, and type 2 diabetes," *Lancet*, vol. 359, no. 9300, pp. 46–47, Jan. 2002.
- [135] A. Konrad, M. Lehrke, V. Schachinger, F. Seibold, R. Stark, T. Ochsenkühn, K. G. Parhofer, B. Göke, and U. C. Broedl, "Resistin is an inflammatory marker of inflammatory bowel disease in humans," *Eur. J. Gastroenterol. Hepatol.*, vol. 19, no. 12, pp. 1070–1074, Dec. 2007.
- [136] K. Karmiris, I. E. Koutroubakis, C. Xidakis, M. Polychronaki, T. Voudouri, and E. A. Kouroumalis, "Circulating levels of leptin, adiponectin, resistin, and ghrelin in inflammatory bowel disease," *Inflamm. Bowel Dis.*, vol. 12, no. 2, pp. 100–105, Feb. 2006.

- [137] N. A. Abdel Kader, F. A. Ali El-Din, E. A. A. Khatab, and N. E. ELAbd, "Does plasma resistin level have a role in predicting inflammatory bowel disease activity?," *Indian J. Gastroenterol.*, vol. 29, no. 3, pp. 126–127, May 2010.
- [138] K. Karmiris, I. E. Koutroubakis, C. Xidakis, M. Polychronaki, and E. A. Kouroumalis, "The effect of infliximab on circulating levels of leptin, adiponectin and resistin in patients with inflammatory bowel disease," *Eur. J. Gastroenterol. Hepatol.*, vol. 19, no. 9, pp. 789–794, Sep. 2007.
- [139] Y. L. Miao, Y. L. Xiao, Y. Du, and L. P. Duan, "Gene expression profiles in peripheral blood mononuclear cells of ulcerative colitis patients," *World J. Gastroenterol.*, 2013.
- [140] M. E. Burczynski, R. L. Peterson, N. C. Twine, K. A. Zuberek, B. J. Brodeur, L. Casciotti, V. Maganti, P. S. Reddy, A. Strahs, F. Immermann, W. Spinelli, U. Schwertschlag, A. M. Slager, M. M. Cotreau, and A. J. Dorner, "Molecular classification of Crohn's disease and ulcerative colitis patients using transcriptional profiles in peripheral blood mononuclear cells.," *J. Mol. Diagn.*, vol. 8, no. 1, pp. 51–61, Feb. 2006.
- [141] S.-Y. Park, S.-H. Lee, N. Kawasaki, S. Itoh, K. Kang, S. Hee Ryu, N. Hashii, J.-M. Kim, J.-Y. Kim, and J. Hoe Kim, " α 1-3/4 fucosylation at Asn 241 of β -haptoglobin is a novel marker for colon cancer: A combinatorial approach for development of glycan biomarkers," *Int. J. Cancer*, vol. 130, no. 10, pp. 2366–2376, May 2012.
- [142] N. Khan, D. Patel, Y. Shah, C. Trivedi, and Y.-X. Yang, "Albumin as a prognostic marker for ulcerative colitis.," *World J. Gastroenterol.*, vol. 23, no. 45, pp.

8008–8016, Dec. 2017.

- [143] M. L. Mackenzie, M. R. Warren, and L. J. Wykes, “Colitis Increases Albumin Synthesis at the Expense of Muscle Protein Synthesis in Macronutrient-Restricted Piglets,” *J. Nutr.*, vol. 133, no. 6, pp. 1875–1881, Jun. 2003.
- [144] U. Bartels, N. S. Pedersen, and S. Jarnum, “Iron Absorption and Serum Ferritin in Chronic Inflammatory Bowel Disease,” *Scand. J. Gastroenterol.*, vol. 13, no. 6, pp. 649–656, Sep. 1978.
- [145] H. Zhang, Y. Fan, L. Xia, C. Gao, X. Tong, H. Wang, L. Sun, T. Ji, M. Jin, B. Gu, and B. Fan, “The impact of advanced proteomics in the search for markers and therapeutic targets of bladder cancer,” *Tumor Biol.*, vol. 39, no. 3, p. 101042831769118, Mar. 2017.
- [146] D. Rodrigues, C. Jerónimo, R. Henrique, L. Belo, M. de Lourdes Bastos, P. G. de Pinho, and M. Carvalho, “Biomarkers in bladder cancer: A metabolomic approach using *in vitro* and *ex vivo* model systems,” *Int. J. Cancer*, vol. 139, no. 2, pp. 256–268, Jul. 2016.
- [147] N. W. Gaikwad, L. Yang, S. Pruthi, J. N. Ingle, N. Sandhu, E. G. Rogan, and E. L. Cavalieri, “Urine Biomarkers of Risk in the Molecular Etiology of Breast Cancer,” *Breast Cancer Basic Clin. Res.*, vol. 3, p. BCBCR.S2112, Jan. 2009.
- [148] G. Ploussard and A. de la Taille, “Urine biomarkers in prostate cancer,” *Nat. Rev. Urol.*, vol. 7, no. 2, pp. 101–109, Feb. 2010.
- [149] E. V. Schrezenmeier, J. Barasch, K. Budde, T. Westhoff, and K. M. Schmidt-Ott, “Biomarkers in acute kidney injury - pathophysiological basis and clinical performance,” *Acta Physiol.*, vol. 219, no. 3, pp. 556–574, Mar. 2017.

- [150] V. L'Imperio, A. Smith, C. Chinello, F. Pagni, and F. Magni, "Proteomics and glomerulonephritis: A complementary approach in renal pathology for the identification of chronic kidney disease related markers," *PROTEOMICS - Clin. Appl.*, vol. 10, no. 4, pp. 371–383, Apr. 2016.
- [151] S. Soliman and C. Mohan, "Lupus nephritis biomarkers," *Clin. Immunol.*, vol. 185, pp. 10–20, Dec. 2017.
- [152] K. W. A. Tang, Q. C. Toh, and B. W. Teo, "Normalisation of urinary biomarkers to creatinine for clinical practice and research--when and why.," *Singapore Med. J.*, vol. 56, no. 1, pp. 7–10, Jan. 2015.
- [153] M. Petri, A.-M. Orbai, G. S. Alarcón, C. Gordon, J. T. Merrill, P. R. Fortin, I. N. Bruce, D. Isenberg, D. J. Wallace, O. Nived, G. Sturfelt, R. Ramsey-Goldman, S.-C. Bae, J. G. Hanly, J. Sánchez-Guerrero, A. Clarke, C. Aranow, S. Manzi, M. Urowitz, D. Gladman, K. Kalunian, M. Costner, V. P. Werth, A. Zoma, S. Bernatsky, G. Ruiz-Irastorza, M. A. Khamashta, S. Jacobsen, J. P. Buyon, P. Maddison, M. A. Dooley, R. F. van Vollenhoven, E. Ginzler, T. Stoll, C. Peschken, J. L. Jorizzo, J. P. Callen, S. S. Lim, B. J. Fessler, M. Inanc, D. L. Kamen, A. Rahman, K. Steinsson, A. G. Franks, L. Sigler, S. Hameed, H. Fang, N. Pham, R. Brey, M. H. Weisman, G. McGwin, L. S. Magder, Jr., and L. S. Magder, "Derivation and validation of the Systemic Lupus International Collaborating Clinics classification criteria for systemic lupus erythematosus.," *Arthritis Rheum.*, vol. 64, no. 8, pp. 2677–86, Aug. 2012.
- [154] M. C. Hochberg, "Updating the American College of Rheumatology revised criteria for the classification of systemic lupus erythematosus.," *Arthritis*

Rheum., vol. 40, no. 9, p. 1725, Sep. 1997.

- [155] J. C. Rohloff, A. D. Gelinas, T. C. Jarvis, U. A. Ochsner, D. J. Schneider, L. Gold, and N. Janjic, "Nucleic Acid Ligands With Protein-like Side Chains: Modified Aptamers and Their Use as Diagnostic and Therapeutic Agents.," *Mol. Ther. Nucleic Acids*, vol. 3, no. 10, p. e201, Oct. 2014.
- [156] S. Stanley, H. Ding, C. Pedroza, R. Saxena, M. Petri, and C. Mohan, "Comprehensive Aptamer-Based Screening of 1129 Proteins Reveals Novel Urinary Biomarkers of Lupus Nephritis," in *2016 ACR/ARHP Annual Meeting*, 2016.
- [157] M. W. Steinberg, T. C. Cheung, and C. F. Ware, "The signaling networks of the herpesvirus entry mediator (TNFRSF14) in immune regulation," *Immunol. Rev.*, vol. 244, no. 1, pp. 169–187, Nov. 2011.
- [158] M. Uhlén, L. Fagerberg, B. M. Hallström, C. Lindskog, P. Oksvold, A. Mardinoglu, Å. Sivertsson, C. Kampf, E. Sjöstedt, A. Asplund, I. Olsson, K. Edlund, E. Lundberg, S. Navani, C. A.-K. Szigyarito, J. Odeberg, D. Djureinovic, J. O. Takanen, S. Hober, T. Alm, P.-H. Edqvist, H. Berling, H. Tegel, J. Mulder, J. Rockberg, P. Nilsson, J. M. Schwenk, M. Hamsten, K. von Feilitzen, M. Forsberg, L. Persson, F. Johansson, M. Zwahlen, G. von Heijne, J. Nielsen, and F. Pontén, "Proteomics. Tissue-based map of the human proteome.," *Science*, vol. 347, no. 6220, p. 1260419, Jan. 2015.
- [159] Y. Fang, L. Ye, T. Zhang, Q.-Z. He, and J.-L. Zhu, "High expression of herpesvirus entry mediator (HVEM) in ovarian serous adenocarcinoma tissue.," *J. BUON.*, vol. 22, no. 1, pp. 80–86.

- [160] T. Inoue, M. Sho, S. Yasuda, S. Nishiwada, S. Nakamura, T. Ueda, N. Nishigori, K. Kawasaki, S. Obara, T. Nakamoto, F. Koyama, H. Fujii, and Y. Nakajima, "HVEM expression contributes to tumor progression and prognosis in human colorectal cancer.," *Anticancer Res.*, vol. 35, no. 3, pp. 1361–7, Mar. 2015.
- [161] K. Migita, M. Sho, K. Shimada, S. Yasuda, I. Yamato, T. Takayama, S. Matsumoto, K. Wakatsuki, K. Hotta, T. Tanaka, M. Ito, N. Konishi, and Y. Nakajima, "Significant involvement of herpesvirus entry mediator in human esophageal squamous cell carcinoma," *Cancer*, vol. 120, no. 6, pp. 808–817, Mar. 2014.
- [162] J. Y. S. Tsang, K.-W. Chan, Y.-B. Ni, T. Hlaing, J. Hu, S.-K. Chan, S.-Y. Cheung, and G. M. Tse, "Expression and Clinical Significance of Herpes Virus Entry Mediator (HVEM) in Breast Cancer," *Ann. Surg. Oncol.*, vol. 24, no. 13, pp. 4042–4050, Dec. 2017.
- [163] Q. Zhao, G. Zhang, X. Zhu, D. Su, Z.-L. Huang, Z. Hu, and L. Peng, "The paradoxical changes of membrane and soluble herpes virus entry mediator in hepatocellular carcinoma patients," *J. Gastroenterol. Hepatol.*, vol. 32, no. 8, pp. 1520–1524, Aug. 2017.
- [164] S.-K. Heo, S.-A. Ju, G. Y. Kim, S.-M. Park, S. H. Back, N.-H. Park, Y. J. Min, W. G. An, T.-H. T. Nguyen, S.-M. Kim, and B.-S. Kim, "The presence of high level soluble herpes virus entry mediator in sera of gastric cancer patients," *Exp. Mol. Med.*, vol. 44, no. 2, p. 149, Feb. 2012.
- [165] H. W. Jung, S. J. La, J. Y. Kim, S. K. Heo, J. Y. Kim, S. Wang, K. K. Kim, K. M. Lee, H. R. Cho, H. W. Lee, B. Kwon, B. S. Kim, and B. S. Kwon, "High levels of soluble herpes virus entry mediator in sera of patients with allergic and autoimmune

- diseases," *Exp. Mol. Med.*, vol. 35, no. 6, pp. 501–508, Dec. 2003.
- [166] J.-W. Shui, A. Larange, G. Kim, J. L. Vela, S. Zahner, H. Cheroutre, and M. Kronenberg, "HVEM signalling at mucosal barriers provides host defence against pathogenic bacteria," *Nature*, vol. 488, no. 7410, pp. 222–225, Aug. 2012.
- [167] A. Seretis, A. Zampoulaki, C. Choulaki, I. Gergianaki, P. Sidiropoulos, D. Boumpas, and G. Bertsias, "A6.34 The role of the costimulatory receptor herpes virus entry mediator (HVEM) in B-cell activation and differentiation. implications for SLE pathogenesis," *Ann. Rheum. Dis.*, vol. 74, no. Suppl 1, p. A69.3-A70, Mar. 2015.
- [168] S. Y. Kong, T. V. Stabler, L. G. Criscione, A. L. Elliott, J. M. Jordan, and V. B. Kraus, "Diurnal variation of serum and urine biomarkers in patients with radiographic knee osteoarthritis," *Arthritis Rheum.*, vol. 54, no. 8, pp. 2496–2504, Aug. 2006.
- [169] R. Dams, C. M. Murphy, W. E. Lambert, and M. A. Huestis, "Urine drug testing for opioids, cocaine, and metabolites by direct injection liquid chromatography/tandem mass spectrometry," *Rapid Commun. Mass Spectrom.*, vol. 17, no. 14, pp. 1665–1670, Jul. 2003.
- [170] I. G. and C. M. Deena Habazi, Kamala Vanarsa, Samantha Stanley, Sirisha Gokaraju, Huihua Ding, Ioannis Parodis, "ALCAM and VCAM-1 as potential urinary biomarkers in Caucasian lupus patients," *J. Immunol.*, vol. 200, no. 1 Supplement, p. 175.17-175.17, May 1950.
- [171] "Lupus - Symptoms and causes - Mayo Clinic." [Online]. Available:

<https://www.mayoclinic.org/diseases-conditions/lupus/symptoms-causes/syc-20365789>. [Accessed: 17-Nov-2018].

- [172] A. M. HARVEY, L. E. SHULMAN, P. A. TUMULTY, C. L. CONLEY, and E. H. SCHOENRICH, "Systemic lupus erythematosus: review of the literature and clinical analysis of 138 cases.," *Medicine (Baltimore)*, vol. 33, no. 4, pp. 291–437, Dec. 1954.
- [173] Y. Sherer, A. Gorstein, M. J. Fritzler, and Y. Shoenfeld, "Autoantibody explosion in systemic lupus erythematosus: More than 100 different antibodies found in SLE patients," *Semin. Arthritis Rheum.*, vol. 34, no. 2, pp. 501–537, Oct. 2004.
- [174] N.-C. V. American Academy of Family Physicians., M. V. Ghetu, and M. L. Bieniek, *American family physician.*, vol. 94, no. 4. American Academy of Family Physicians, 1970.
- [175] L. B. Tucker, S. Menon, J. G. Schaller, and D. A. Isenberg, "Adult- and childhood-onset systemic lupus erythematosus: a comparison of onset, clinical features, serology, and outcome.," *Br. J. Rheumatol.*, vol. 34, no. 9, pp. 866–72, Sep. 1995.
- [176] M. Adler, S. Chambers, C. Edwards, G. Neild, and D. Isenberg, "An assessment of renal failure in an SLE cohort with special reference to ethnicity, over a 25-year period," *Rheumatology*, vol. 45, no. 9, pp. 1144–1147, Sep. 2006.
- [177] L. Carreño, F. J. López-Longo, I. Monteagudo, M. Rodríguez-Mahou, M. Bascones, C. M. González, C. Saint-Cyr, and N. Lapointe, "Immunological and clinical differences between juvenile and adult onset of systemic lupus erythematosus," *Lupus*, vol. 8, no. 4, pp. 287–292, May 1999.
- [178] C. H. Feldman, L. T. Hiraki, J. Liu, M. A. Fischer, D. H. Solomon, G. S. Alarcón, W.

C. Winkelmayer, and K. H. Costenbader, "Epidemiology and sociodemographics of systemic lupus erythematosus and lupus nephritis among US adults with Medicaid coverage, 2000-2004.," *Arthritis Rheum.*, vol. 65, no. 3, pp. 753–63, Mar. 2013.

[179] J. G. Hanly, A. G. O’Keeffe, L. Su, M. B. Urowitz, J. Romero-Diaz, C. Gordon, S.-C. Bae, S. Bernatsky, A. E. Clarke, D. J. Wallace, J. T. Merrill, D. A. Isenberg, A. Rahman, E. M. Ginzler, P. Fortin, D. D. Gladman, J. Sanchez-Guerrero, M. Petri, I. N. Bruce, M. A. Dooley, R. Ramsey-Goldman, C. Aranow, G. S. Alarcón, B. J. Fessler, K. Steinsson, O. Nived, G. K. Sturfelt, S. Manzi, M. A. Khamashta, R. F. van Vollenhoven, A. A. Zoma, M. Ramos-Casals, G. Ruiz-Irastorza, S. S. Lim, T. Stoll, M. Inanc, K. C. Kalunian, D. L. Kamen, P. Maddison, C. A. Peschken, S. Jacobsen, A. Askanase, C. Theriault, K. Thompson, and V. Farewell, "The frequency and outcome of lupus nephritis: results from an international inception cohort study.," *Rheumatology (Oxford)*, vol. 55, no. 2, pp. 252–62, Feb. 2016.

[180] C. Mohan and C. Putterman, "Genetics and pathogenesis of systemic lupus erythematosus and lupus nephritis," *Nat. Rev. Nephrol.*, vol. 11, no. 6, pp. 329–341, Jun. 2015.

[181] L. T. Hiraki, C. H. Feldman, J. Liu, G. S. Alarcón, M. A. Fischer, W. C. Winkelmayer, and K. H. Costenbader, "Prevalence, incidence, and demographics of systemic lupus erythematosus and lupus nephritis from 2000 to 2004 among children in the US medicaid beneficiary population," *Arthritis Rheum.*, vol. 64, no. 8, pp. 2669–2676, Aug. 2012.

- [182] D. L. Huong, T. Papo, H. Beaufils, B. Wechsler, O. Blétry, A. Baumelou, P. Godeau, and J. C. Piette, "Renal involvement in systemic lupus erythematosus. A study of 180 patients from a single center.," *Medicine (Baltimore)*, vol. 78, no. 3, pp. 148–66, May 1999.
- [183] K. H. Costenbader, A. Desai, G. S. Alarcón, L. T. Hiraki, T. Shaykevich, M. A. Brookhart, E. Massarotti, B. Lu, D. H. Solomon, and W. C. Winkelmayr, "Trends in the incidence, demographics, and outcomes of end-stage renal disease due to lupus nephritis in the US from 1995 to 2006," *Arthritis Rheum.*, vol. 63, no. 6, pp. 1681–1688, Jun. 2011.
- [184] J. M. Esdaile, L. Joseph, T. MacKenzie, M. Kashgarian, and J. P. Hayslett, "The benefit of early treatment with immunosuppressive agents in lupus nephritis.," *J. Rheumatol.*, vol. 21, no. 11, pp. 2046–51, Nov. 1994.
- [185] M. M. WARD, "Changes in the Incidence of Endstage Renal Disease Due to Lupus Nephritis in the United States, 1996–2004," *J. Rheumatol.*, vol. 36, no. 1, pp. 63–67, Jan. 2009.
- [186] C. Fiehn, Y. Hajjar, K. Mueller, R. Waldherr, A. D. Ho, and K. Andrassy, "Improved clinical outcome of lupus nephritis during the past decade: importance of early diagnosis and treatment.," *Ann. Rheum. Dis.*, vol. 62, no. 5, pp. 435–9, May 2003.
- [187] C. C. Mok, "Biomarkers for lupus nephritis: a critical appraisal.," *J. Biomed. Biotechnol.*, vol. 2010, p. 638413, Apr. 2010.
- [188] C.-C. Liu, A. H. Kao, S. Manzi, and J. M. Ahearn, "Biomarkers in systemic lupus erythematosus: challenges and prospects for the future," *Ther. Adv.*

- Musculoskelet. Dis.*, vol. 5, no. 4, pp. 210–233, Aug. 2013.
- [189] R. Misra and R. Gupta, “Biomarkers in lupus nephritis,” *Int. J. Rheum. Dis.*, vol. 18, no. 2, pp. 219–232, Feb. 2015.
- [190] T. Wu, H. Ding, J. Han, C. Arriens, C. Wei, W. Han, C. Pedroza, S. Jiang, J. Anolik, M. Petri, I. Sanz, R. Saxena, and C. Mohan, “Antibody-Array-Based Proteomic Screening of Serum Markers in Systemic Lupus Erythematosus: A Discovery Study,” *J. Proteome Res.*, vol. 15, no. 7, pp. 2102–2114, Jul. 2016.
- [191] T. Wu, C. Xie, J. Han, Y. Ye, J. Weiel, Q. Li, I. Blanco, C. Ahn, N. Olsen, C. Putterman, R. Saxena, and C. Mohan, “Metabolic disturbances associated with systemic lupus erythematosus,” *PLoS One*, vol. 7, no. 6, p. e37210, 2012.
- [192] T. Wu, Y. Du, J. Han, S. Singh, C. Xie, Y. Guo, X. J. Zhou, C. Ahn, R. Saxena, and C. Mohan, “Urinary Angiostatin - A Novel Putative Marker of Renal Pathology Chronicity in Lupus Nephritis,” *Mol. Cell. Proteomics*, vol. 12, no. 5, pp. 1170–1179, May 2013.
- [193] T. Wu, Y. Fu, D. Brekken, M. Yan, X. J. Zhou, K. Vanarsa, N. Deljavan, C. Ahn, C. Putterman, and C. Mohan, “Urine proteome scans uncover total urinary protease, prostaglandin D synthase, serum amyloid P, and superoxide dismutase as potential markers of lupus nephritis,” *J. Immunol.*, vol. 184, no. 4, pp. 2183–93, Feb. 2010.
- [194] C. C. Mok, H. H. Ding, M. Kharboutli, and C. Mohan, “Axl, Ferritin, Insulin-Like Growth Factor Binding Protein 2, and Tumor Necrosis Factor Receptor Type II as Biomarkers in Systemic Lupus Erythematosus,” *Arthritis Care Res. (Hoboken)*, vol. 68, no. 9, pp. 1303–9, 2016.

- [195] I. Parodis, H. Ding, A. Zickert, L. Arnaud, C. Mohan, and I. Gunnarsson, "AB0458 Serum Ferritin as A Biomarker of Clinical and Histopathological Response To Treatment in Lupus Nephritis," *Ann. Rheum. Dis.*, vol. 75, no. Suppl 2, p. 1063.1-1063, Jun. 2016.
- [196] K. Vanarsa, Y. Ye, J. Han, C. Xie, C. Mohan, and T. Wu, "Inflammation associated anemia and ferritin as disease markers in SLE," *Arthritis Res. Ther.*, vol. 14, no. 4, p. R182, Aug. 2012.
- [197] T. Wu, C. Xie, J. Han, Y. Ye, S. Singh, J. Zhou, Y. Li, H. Ding, Q. Li, X. Zhou, C. Putterman, R. Saxena, and C. Mohan, "Insulin-Like Growth Factor Binding Protein-4 as a Marker of Chronic Lupus Nephritis," *PLoS One*, vol. 11, no. 3, p. e0151491, Mar. 2016.
- [198] J. Hutcheson, Y. Ye, J. Han, C. Arriens, R. Saxena, Q.-Z. Li, C. Mohan, and T. Wu, "Resistin as a potential marker of renal disease in lupus nephritis," *Clin. Exp. Immunol.*, vol. 179, no. 3, pp. 435–443, Mar. 2015.
- [199] I. G. Ioannis Parodis, Huihua Ding, Agneta Zickert, Chandra Mohan, "Serum Ferritin and Insulin-like Growth Factor-Binding Protein 2 As Biomarkers of Clinical and Histopathological Treatment Response in Lupus Nephritis - ACR Meeting Abstracts," *Arthritis Rheumatol.*, vol. 67, no. suppl 10, 2015.
- [200] I. Parodis, H. Ding, A. Zickert, L. Arnaud, A. Larsson, E. Svenungsson, C. Mohan, and I. Gunnarsson, "Serum soluble tumour necrosis factor receptor-2 (sTNFR2) as a biomarker of kidney tissue damage and long-term renal outcome in lupus nephritis," *Scand. J. Rheumatol.*, vol. 46, no. 4, pp. 263–272, Jul. 2017.

- [201] A. N. Kiani, T. Wu, H. Fang, X. J. Zhou, C. W. Ahn, L. S. Magder, C. Mohan, and M. Petri, "Urinary vascular cell adhesion molecule, but not neutrophil gelatinase-associated lipocalin, is associated with lupus nephritis," *J. Rheumatol.*, vol. 39, no. 6, pp. 1231–7, Jun. 2012.
- [202] S. Singh, T. Wu, C. Xie, K. Vanarsa, J. Han, T. Mahajan, H. Oei, C. Ahn, X. J. Zhou, C. Putterman, R. Saxena, and C. Mohan, "Urine VCAM-1 as a marker of renal pathology activity index in lupus nephritis," *Arthritis Res. Ther.*, vol. 14, no. 4, p. R164, Jul. 2012.
- [203] Y. C. Manabe, B. A. S. Nonyane, L. Nakiyingi, O. Mbabazi, G. Lubega, M. Shah, L. H. Moulton, M. Joloba, J. Ellner, and S. E. Dorman, "Point-of-care lateral flow assays for tuberculosis and cryptococcal antigenuria predict death in HIV infected adults in Uganda," *PLoS One*, vol. 9, no. 7, p. e101459, 2014.
- [204] E. I. Laderman, E. Whitworth, E. Dumauual, M. Jones, A. Hudak, W. Hogrefe, J. Carney, and J. Groen, "Rapid, sensitive, and specific lateral-flow immunochromatographic point-of-care device for detection of herpes simplex virus type 2-specific immunoglobulin G antibodies in serum and whole blood," *Clin. Vaccine Immunol.*, vol. 15, no. 1, pp. 159–63, Jan. 2008.
- [205] L.-W. Song, Y.-B. Wang, L.-L. Fang, Y. Wu, L. Yang, J.-Y. Chen, S.-X. Ge, J. Zhang, Y.-Z. Xiong, X.-M. Deng, X.-P. Min, J. Zhang, P.-J. Chen, Q. Yuan, and N.-S. Xia, "Rapid Fluorescent Lateral-Flow Immunoassay for Hepatitis B Virus Genotyping," *Anal. Chem.*, vol. 87, no. 10, pp. 5173–5180, May 2015.
- [206] J. H. Ryu, M. Kwon, J.-D. Moon, M.-W. Hwang, J.-M. Lee, K.-H. Park, S. J. Yun, H. J. Bae, A. Choi, H. Lee, B. Jung, J. Jeong, K. Han, Y. Kim, E.-J. Oh, B.S., A. Choi, B.S.,

- H. Lee, B.S., B. Jung, Ph.D., J. Jeong, M.S., K. Han, M.D., Ph.D., Y. Kim, M.D., Ph.D., and E.-J. Oh, M.D., and Ph.D., "Development of a Rapid Automated Fluorescent Lateral Flow Immunoassay to Detect Hepatitis B Surface Antigen (HBsAg), Antibody to HBsAg, and Antibody to Hepatitis C," *Ann. Lab. Med.*, vol. 38, no. 6, p. 578, Nov. 2018.
- [207] D. S. Kim, Y. T. Kim, S. B. Hong, J. Kim, N. S. Huh, M.-K. Lee, S. J. Lee, B. Il Kim, I. S. Kim, Y. S. Huh, and B. G. Choi, "Development of Lateral Flow Assay Based on Size-Controlled Gold Nanoparticles for Detection of Hepatitis B Surface Antigen.," *Sensors (Basel)*, vol. 16, no. 12, Dec. 2016.
- [208] S. Gwyn, A. Mitchell, D. Dean, H. Mkocho, S. Handali, and D. L. Martin, "Lateral flow-based antibody testing for *Chlamydia trachomatis*," *J. Immunol. Methods*, vol. 435, pp. 27–31, Aug. 2016.
- [209] B. A. Rohrman, V. Leautaud, E. Molyneux, and R. R. Richards-Kortum, "A Lateral Flow Assay for Quantitative Detection of Amplified HIV-1 RNA," *PLoS One*, vol. 7, no. 9, p. e45611, Sep. 2012.
- [210] T. T. Le, P. Chang, D. J. Benton, J. W. McCauley, M. Iqbal, and A. E. G. Cass, "Dual Recognition Element Lateral Flow Assay Toward Multiplex Strain Specific Influenza Virus Detection.," *Anal. Chem.*, vol. 89, no. 12, pp. 6781–6786, Jun. 2017.
- [211] L. Chen, H. Wang, T. Guo, C. Xiao, L. Liu, X. Zhang, B. Liu, P. Li, A. Liu, B. Li, B. Li, and Y. Mao, "A rapid point-of-care test for dengue virus-1 based on a lateral flow assay with a near-infrared fluorescent dye," *J. Immunol. Methods*, vol. 456, pp. 23–27, May 2018.

- [212] F. D. Krampa, Y. Aniweh, G. A. Awandare, and P. Kanyong, "Recent Progress in the Development of Diagnostic Tests for Malaria," *Diagnostics (Basel, Switzerland)*, vol. 7, no. 3, Sep. 2017.
- [213] G. A. Posthuma-Trumpie, J. Korf, and A. van Amerongen, "Lateral flow (immuno)assay: its strengths, weaknesses, opportunities and threats. A literature survey," *Anal. Bioanal. Chem.*, vol. 393, no. 2, pp. 569–582, Jan. 2009.
- [214] D. Erickson, D. O'Dell, L. Jiang, V. Oncescu, A. Gumus, S. Lee, M. Mancuso, and S. Mehta, "Smartphone technology can be transformative to the deployment of lab-on-chip diagnostics," *Lab Chip*, vol. 14, no. 17, pp. 3159–64, Sep. 2014.
- [215] A. S. Paterson, B. Raja, V. Mandadi, B. Townsend, M. Lee, A. Buell, B. Vu, J. Brgoch, and R. C. Willson, "A low-cost smartphone-based platform for highly sensitive point-of-care testing with persistent luminescent phosphors," *Lab Chip*, vol. 17, no. 6, pp. 1051–1059, 2017.
- [216] S. Lee, D. O'Dell, J. Hohenstein, S. Colt, S. Mehta, and D. Erickson, "NutriPhone: a mobile platform for low-cost point-of-care quantification of vitamin B12 concentrations," *Sci. Rep.*, vol. 6, no. 1, p. 28237, Sep. 2016.
- [217] S. Lee, B. Srinivasan, S. Vemulapati, S. Mehta, and D. Erickson, "Personalized nutrition diagnostics at the point-of-need," *Lab Chip*, vol. 16, no. 13, pp. 2408–17, 2016.
- [218] J. X. H. Wong, X. Li, F. S. F. Liu, and H.-Z. Yu, "Direct Reading of Bona Fide Barcode Assays for Diagnostics with Smartphone Apps," *Sci. Rep.*, vol. 5, no. 1, p. 11727, Dec. 2015.
- [219] A. Carrio, C. Sampedro, J. Sanchez-Lopez, M. Pimienta, and P. Campoy,

- “Automated Low-Cost Smartphone-Based Lateral Flow Saliva Test Reader for Drugs-of-Abuse Detection,” *Sensors*, vol. 15, no. 11, pp. 29569–29593, Nov. 2015.
- [220] S.-J. Yeo, K. Choi, B. T. Cuc, N. N. Hong, D. T. Bao, N. M. Ngoc, M. Q. Le, N. L. K. Hang, N. C. Thach, S. K. Mallik, H. S. Kim, C.-K. Chong, H. S. Choi, H. W. Sung, K. Yu, and H. Park, “Smartphone-Based Fluorescent Diagnostic System for Highly Pathogenic H5N1 Viruses,” *Theranostics*, vol. 6, no. 2, pp. 231–242, 2016.
- [221] D. Wild, *The immunoassay handbook : theory and applications of ligand binding, ELISA and related techniques*. .
- [222] B. O’Farrell, “Evolution in Lateral Flow–Based Immunoassay Systems,” in *Lateral Flow Immunoassay*, Totowa, NJ: Humana Press, 2009, pp. 1–33.
- [223] M. D. Borysiak, M. J. Thompson, and J. D. Posner, “Translating diagnostic assays from the laboratory to the clinic: analytical and clinical metrics for device development and evaluation,” *Lab Chip*, vol. 16, no. 8, pp. 1293–1313, Apr. 2016.
- [224] P. Chun, “Colloidal Gold and Other Labels for Lateral Flow Immunoassays,” in *Lateral Flow Immunoassay*, Totowa, NJ: Humana Press, 2009, pp. 1–19.
- [225] A. S. Paterson, B. Raja, G. Garvey, A. Kolhatkar, A. E. V. Hagström, K. Kourentzi, T. R. Lee, and R. C. Willson, “Persistent Luminescence Strontium Aluminate Nanoparticles as Reporters in Lateral Flow Assays,” *Anal. Chem.*, vol. 86, no. 19, pp. 9481–9488, Oct. 2014.

Appendix A: Normalization and Descriptive Statistics of ELISA Validation of Stool Biomarkers

Descriptive statistics of the raw concentrations of the 23 candidate biomarkers for IBD validated by ELISA are listed in Table 11.

Table 11: Descriptive statistics of ELISA validation of stool biomarkers for IBD. Concentrations have been normalized by the ratio of stool weight to volume of protein extract. Concentrations are in pg/ml unless otherwise noted: †[mg/mg], ▽ [ng/mg], § [ug/mg], ‡ [nIU/mg]

Protein	Mean ± StdError (Median)				Fold Change			
	Healthy	IBD	CD	UC	IBDvsHC	CDvsHC	UCvsHC	UCvsCD
Albumin	805.1 ± 1 (570.9)	1174.9 ± 1.7 (264.1)	699.2 ± 1.7 (164.7)	2601.9 ± 1.3 (580.2)	1.46	0.87	3.23	3.72
Alkaline Phosphatase	63.5 ± 1.4 (34.5)‡	180.3 ± 0.7 (157.3)‡	194.5 ± 0.7 (166.4)‡	137.5 ± 0.9 (148.3)‡	2.84	3.06	2.17	0.71
Calprotectin	4159.5 ± 1 (2639.8)	13174.6 ± 0.5 (12260.7)	11199 ± 0.5 (10542.2)	19101.6 ± 0.4 (16271.7)	3.17	2.69	4.59	1.71
Cystatin A	362.3 ± 2.6 (0)	2582.9 ± 0.9 (2198.9)	1978.7 ± 0.9 (2157.9)	4395.3 ± 0.7 (5240)	7.13	5.46	12.13	2.22
D-Dimer	0 ± 1.7 (0)	0.4 ± 3 (0)	0.1 ± 2.6 (0)	1.1 ± 1.9 (0)	18.95	5.99	57.85	9.66
Elastase	21.2 ± 1.2 (12)	63.1 ± 2.6 (18)	26.9 ± 1.2 (17.8)	171.4 ± 1.9 (38.3)	2.98	1.27	8.10	6.37
Ferritin	364.7 ± 1.3 (159.6)	722.9 ± 1 (468.8)	607.9 ± 0.9 (482.6)	1067.9 ± 1.1 (345.6)	1.98	1.67	2.93	1.76
Fibrinogen	94.6 ± 1.2 (39.7)	569.2 ± 1.6 (297.8)	236.7 ± 1 (208)	1566.5 ± 0.9 (1308.5)	6.01	2.50	16.55	6.62
Fibronectin	43.7 ± 0.7 (28.4)	90.2 ± 1 (63.6)	65.8 ± 0.8 (54.4)	163.3 ± 0.9 (125.7)	2.06	1.50	3.74	2.48
Galectin-3BP	49.2 ± 2 (20.6)	80.9 ± 1.4 (33.9)	62.9 ± 1.6 (29.9)	135.2 ± 1.1 (44)	1.65	1.28	2.75	2.15
Haptoglobin	204.5 ± 2.8 (26.9)	2817.6 ± 2.1 (399.2)	1241.6 ± 1.9 (114.3)	7545.5 ± 1.4 (2530.4)	13.78	6.07	36.89	6.08
Hemoglobin	0.3 ± 1.4 (0.1)§	3.4 ± 1.5 (1.1)§	1.7 ± 1.7 (1)§	8.6 ± 0.8 (9.8)§	12.35	6.13	31.00	5.06
Lipocalin 2	35.3 ± 0.2 (36)	85.5 ± 1 (55.3)	50.9 ± 0.6 (43)	189.4 ± 0.6 (201.5)	2.42	1.44	5.37	3.72
MMP 8	112.6 ± 2.1 (0)	2316.7 ± 3.3 (0)	151.3 ± 2.6 (0)	8813 ± 1.6 (857)	20.57	1.34	78.25	58.26
MMP-9	10.9 ± 2.3 (0)	549.4 ± 2.3 (66.2)	100.7 ± 1.4 (46.9)	1895.5 ± 1.2 (1489.2)	50.46	9.25	174.10	18.82
MPO	3.4 ± 2.2 (0.7)†	58.3 ± 0.7 (46.3)†	50.3 ± 0.8 (42.2)†	82.5 ± 0.5 (97.5)†	16.95	14.61	23.98	1.64
PGRPS	4.4 ± 2.5 (0)	120.4 ± 1.4 (71)	77.8 ± 1 (45.8)	248.2 ± 1.1 (168)	27.51	17.78	56.70	3.19
Properdin	1.7 ± 1.9 (0)	56 ± 2.8 (10)	11.1 ± 1.7 (2.8)	190.7 ± 1.5 (75.9)	33.48	6.62	114.08	17.24
Proteinase 3	5.3 ± 1 (2.9)▽	36.3 ± 1 (23.2)▽	29.8 ± 1.1 (19.9)▽	56.1 ± 0.8 (54.5)▽	6.87	5.63	10.61	1.88
Resistin	0 ± 0 (0)	6.8 ± 1.5 (0)	2.7 ± 2.1 (0)	19.1 ± 0.7 (21.9)	>>	>>	>>	7.05
SAP	375.7 ± 1.3 (228.6)	3428.3 ± 0.7 (3864)	3162.9 ± 0.8 (3452.5)	4224.5 ± 0.6 (4295.5)	9.13	8.42	11.25	1.34
SerpinA4	0.8 ± 3.2 (0)	78.8 ± 1.7 (14.2)	65.5 ± 2 (13.3)	118.5 ± 1.3 (88.6)	104.82	87.20	157.68	1.81
SSEA-1	4.7 ± 2.8 (0)	108.4 ± 2.6 (1.8)	16.8 ± 1.7 (0)	382.9 ± 1.3 (243.4)	23.24	3.61	82.12	22.75

To minimize the effect of the stool extraction process, raw protein concentrations for the stool samples were normalized by the stool weight to protein extract volume for each sample. Descriptive statistics of these molecules are summarized in Table 12. To note, D-dimer was found to be statistically elevated only after stool normalization.

Table 12: Descriptive statistics of ELISA validation of stool biomarkers for IBD in protein extract.
Concentrations are in ng/ml unless otherwise noted: ‡[mIU/ml], ▽ [pg/ml], §[ug/ml].

Protein	Mean ± StdError (Median)				Fold Change			
	Healthy	IBD	CD	UC	IBDvsHC	CDvsHC	UCvsHC	UCvsCD
Albumin	160 ± 1 (109.1)	198 ± 1.6 (50.1)	128.4 ± 1.7 (32.9)	406.9 ± 1.2 (116)	1.24	0.80	2.54	3.17
Alkaline Phosphatase	12.5 ± 1.4 (6.9)‡	33.8 ± 0.8 (30.9)‡	36.6 ± 0.7 (32.2)‡	25.4 ± 0.9 (24.7)‡	2.69	2.92	2.02	0.69
Calprotectin	941.3 ± 1 (587.7)	2466.8 ± 0.4 (2415.8)	2222.1 ± 0.4 (2187.3)	3201.1 ± 0.3 (2905.7)	2.62	2.36	3.40	1.44
Cystatin A	1.8 ± 2.6 (0)	14.4 ± 0.9 (12)	10.7 ± 0.9 (10.8)	25.3 ± 0.7 (34.1)	7.92	5.91	13.97	2.37
D-Dimer	4.7 ± 1.8 (2)▽	62.2 ± 2.9 (2)▽	23.3 ± 2.6 (1.2)▽	179 ± 1.9 (6)▽	13.18	4.93	37.93	7.69
Elastase	4.6 ± 1.1 (2.9)	11 ± 2.4 (4)	5.5 ± 1.2 (3.2)	27.4 ± 1.9 (7)	2.38	1.19	5.95	5.00
Ferritin	87.8 ± 1.3 (31.5)	139.5 ± 0.9 (89.6)	126.4 ± 0.9 (91.7)	178.7 ± 1 (61.7)	1.59	1.44	2.04	1.41
Fibrinogen	20 ± 1.2 (9.4)	99.1 ± 1.4 (53.6)	46.3 ± 1 (40.2)	257.5 ± 0.9 (233.7)	4.95	2.31	12.88	5.56
Fibronectin	8.7 ± 0.7 (5.4)	15.9 ± 0.9 (12.2)	12.4 ± 0.8 (10.9)	26.4 ± 0.8 (20.9)	1.83	1.43	3.04	2.12
Galectin-3BP	9.7 ± 2 (4.1)	13.7 ± 1.3 (6.8)	11.2 ± 1.5 (6.2)	21.3 ± 1.1 (8.8)	1.40	1.14	2.19	1.91
Haptoglobin	40.9 ± 2.8 (5.4)	468.1 ± 2 (76.3)	225.8 ± 1.9 (25.4)	1195.1 ± 1.4 (389.3)	11.45	5.53	29.24	5.29
Hemoglobin	55.3 ± 1.4 (20.9)§	576.8 ± 1.4 (219.9)§	308.9 ± 1.6 (195.6)§	1380.3 ± 0.7 (1627.8)§	10.42	5.58	24.95	4.47
Lipocalin 2	8 ± 0.2 (8.7)	15.4 ± 0.9 (12.1)	10.2 ± 0.5 (10)	31.2 ± 0.6 (36)	1.92	1.26	3.88	3.08
MMP 8	22.5 ± 2.1 (0)	361.3 ± 3.2 (0)	26.6 ± 2.5 (0)	1365.4 ± 1.6 (171.4)	16.04	1.18	60.62	51.37
MMP-9	2.5 ± 2.3 (0)	91.8 ± 2.2 (14.1)	19.1 ± 1.3 (9.8)	309.9 ± 1.1 (225.6)	36.18	7.51	122.18	16.26
MPO	0.7 ± 2.2 (0.1)§	10.8 ± 0.7 (8.4)§	9.6 ± 0.8 (8.4)§	14.1 ± 0.5 (16.2)§	15.66	14.03	20.56	1.47
PGRPS	0.9 ± 2.5 (0)	21 ± 1.2 (14)	14.6 ± 0.9 (10.2)	40.1 ± 1.1 (30.5)	23.94	16.63	45.84	2.76
Properdin	0.3 ± 1.9 (0)	9 ± 2.7 (1.7)	2 ± 1.5 (0.6)	30.1 ± 1.5 (11.7)	27.07	6.08	90.06	14.81
Proteinase 3	982.5 ± 1 (567.3)	7009 ± 1.1 (4301.3)	5890.9 ± 1.2 (4189.9)	10363.3 ± 0.8 (9088.6)	7.13	6.00	10.55	1.76
Resistin	0 ± 0 (0)	1.2 ± 1.5 (0)	0.5 ± 2 (0)	3.2 ± 0.6 (4.3)	>>	>>	>>	6.49
SAP	79.7 ± 1.3 (47)	664.7 ± 0.7 (791.6)	634 ± 0.7 (816.2)	756.9 ± 0.6 (767.1)	8.34	7.96	9.50	1.19
SerpinA4	0.2 ± 3.2 (0)	13.4 ± 1.7 (3)	11.7 ± 1.9 (3)	18.6 ± 1.3 (14.8)	89.32	77.94	123.45	1.58
SSEA-1	0.9 ± 2.8 (0)	17.5 ± 2.4 (0.3)	3.1 ± 1.7 (0)	60.7 ± 1.2 (37.5)	18.78	3.35	65.08	19.41

